Late-Stage Fluorination with \(^{18}F\)

Professor Tobias Ritter Adam Seth Kamlet

LATE-STAGE FLUORINATION WITH ^{18}F

Abstract

Positron emission tomography (PET) is a powerful, non-invasive *in vivo* imaging technique used for diagnostics and drug development. The synthesis of ^{18}F-PET tracers is challenging due to the short half-life of the unnatural isotope that necessitates late-stage fluorination, and the limited reactivity of nucleophilic fluoride, the preferred and widely accessible form of ^{18}F. This thesis describes the development of an electrophilic fluorination reagent derived from fluoride. The reagent can be employed in a late-stage fluorination reaction of palladium aryl complexes to give access to small molecule aryl fluorides. The reagent can be made from [^{18}F]fluoride and used to synthesize radiolabeled small molecules for PET imaging experiments. Two small molecules known to interact with the serotonergic system were synthesized, radiolabeled, and imaged in rats and non-human primates and evaluated for use as PET tracers.

Table of Contents

Acknowledgements

The translational research described in this thesis could not have been accomplished without the guidance of my two advisers, Professors Tobias Ritter and David Liu. Both advisers have allowed me to pursue challenging scientific problems, providing opportunity, patience, and freedom. Though my interactions with the two labs, I have been fortunate enough to learn a wide breadth of science and leadership skills. Specifically, I thank Tobias for teaching me how to identify worthwhile research problems, and I thank David for teaching me experimental design.

The radiochemistry and imaging experiments were only done through the generosity of Professor Jacob Hooker. He has provided his expertise, time, and laboratory space and equipment to help us reach our goals. He has been a tremendous collaborator.

I appreciate the efforts of my current and former Ph.D. committee members, Professors Eric Jacobsen, Ted Betley, and Alan Saghatelian, to guide my research and to give me perspective whenever asked. Their commitment to graduate student education motivates me.

The Ritter and Liu Laboratories have been wonderful environments to conduct research. I thank my labmates for their support and friendship. My success is shared with the many post-docs, graduate students, undergraduate students, and technicians that I have been fortunate to discuss, design, execute, and analyze experiments with. They include Dr. David Gorin, Dr. Yiyun Chen, Dr. Eunsung Lee, Dr. Nicky Stephenson, Dr. Takeru Furuya, Dr. David Powers, Constanze Neumann, Greg Boursalian, Dr. Jimbo Cronican, Jonathan Steinman, Dan Choi, Steve Carlin, and Christian Moseley. Multidisciplinary research is a team effort, and I was a member of a great team.

List of Abbreviations

5-HT: 5-hydroxytryptamine
18-cr-6: 18-crown-6; 1,4,7,10,13,16-hexaoxacyclooctadecane
Ac: acetyl
Ar: aryl
BINAP: 1,1'-binaphthalene
Bn: benzyl
Boc: *tert*-butoxycarbonyl
bp: base pair
Bu: butyl
calcd: calculated
CAN: ceric ammonium nitrate
CNS: central nervous system
C_T: threshold cycle
Cy: cyanine
DAM: bis(4-methoxyphenyl)methyl
DBU: 1,8-diazabicyclo[5.4.0]undec-7-ene
DCC: dicyclohexylcarbodiimide
DCE: 1,2-dichloroethane
DIAD: diisopropyl azodicarboxylate
DIBAL-H: diisobutylaluminum hydride
DIPEA: diisopropylethylamine
DME: dimethoxyethane
DMF: *N*, *N*-dimethylformamide
DMSO: dimethylsulfoxide
DMT-MM: 4-(4,6-dimethoxy-1,3,5-triazin-2-yl)-4-methylmorpholinium chloride
DNA: deoxyribonucleic acid
dppf: 1,1'-bis(diphenylphosphino)ferrocene
DTT: DL-dithiothreitol
EDC: ethyldimethylaninopropylcarbodiimide
ee: enantiomeric excess
equiv: equivalent
Et: ethyl
EWG: electron-withdrawing group
FDG: 2-fluoro-2-deoxy-D-glucose
FMOC: 9-fluorenylmethoxycarbonyl
GMP: good manufacturing practice

h: hour
HATU: *O*-(7-azabenzotriazol-1-yl)-*N,N,N',N'*-tetramethyluronium hexfluorophosphate
HEPES: 4-(2-hydroxyethyl)-1-piperazineethanesulfonic acid
HMPA: hexamethylphosphoramide
HPLC: high-performance liquid chromatography
HRMS: high resolution mass spectroscopy
ICP: inductively coupled plasma
i-Pr: *iso*-propyl
LC: liquid chromatography
LG: leaving group
LUMO: lowest unoccupied molecular orbital
Me: methyl
MES: 2-(*N*-morpholino)ethanesulfonic acid
min: minute
MOM: methoxymethyl
MOPS: 3-(*N*-morpholino)propanesulfonic acid
Ms: methanesulfonyl
MS: mass spectroscopy
NHS: *N*-hydroxysuccinimide
NMP: *N*-methylpyrrolidine
NMR: nuclear magnetic resonance
OMP: oligonucleotide modeling program
PAGE: polyacrylamide gel electrophoresis
PCR: polymerase chain reaction
PET: positron emission tomography
Ph: phenyl
PMP: 4-methoxyphenyl
ppb: parts per billion
RCY: radiochemical yield
RDPCR: reactivity dependent polymerase chain reaction
RTLC: radio thin layer chromatography
pin: pinacolato
PMHS: polymethylhydrosiloxane
RNA: ribonucleic acid
Pr: propyl
py: pyridine
qPCR: quantitative real-time polymerase chain reaction
S_N: nucleophilic substitution

SSRI: selective serotonin reuptake inhibitor
t-Bu: *tert*-butyl
TEDA: N-chloromethyl-N-fluorotriethylenediammonium bis(tetrafluoroborate)
Tf: trifluoromethanesulfonyl
TFA: trifluoroacetic Acid
THF: tetrahydrofuran
TLC: thin layer chromatography
T_M: melting temperature
TMS: trimethylsilyl
Tris: 2-Amino-2-hydroxymethyl-propane-1,3-diol
Tol: *para*-tolyl
Tp: tetrapyrazole borate
Ts: *para*-toluenesulfonyl
UPLC: ultra high-performance liquid chromatography
v: volume

Portions of this thesis have been published in peer-reviewed journals in the following publications:

1. Lee, E.*; Kamlet, A. S.*; Powers, D. C.; Neumann, C. N.; Boursalian G. B.; Furuya, T.; Choi, D. C.; Hooker, J. M.; Ritter, T. A Fluoride-Derived Electrophilic Late-Stage Fluorination Reagent for PET Imaging" *Science* **2011**, *334*, 639–642.

   *denotes equal contribution

2. Furuya, T*; Kamlet, A. S.*; Ritter, T. Catalysis for fluorination and trifluoromethylation. *Nature* **2011***, 473,* 470–477.

   *denotes equal contribution

3. Chen, Y.; Kamlet, A.S.; Steinman, J.B.; Liu, D.R. A Biomolecule-Compatible Visible Light-Induced Azide Reduction from a DNA-Encoded Reaction Discovery System. *Nature Chem.* **2011**, *3*, 146-153.

4. Gorin, D. J.; Kamlet, A. S.; Liu, D. R. Reactivity-Dependent PCR: Direct, Solution-Phase *In Vitro* Selection for Bond Formation. *J. Am. Chem. Soc.* **2009**, *131*, 9189-9191.

1. INTRODUCTION

1.1 Positron Emission Tomography

Positron emission tomography (PET) is a powerful, non-invasive imaging technology that can be used to identify and characterize human disease. PET can provide critical information about normal or aberrant human physiology. Experiments using PET can be designed to provide two distinct types of information: i) the disposition (i.e., pharmacokinetics and biodistribution) of a radiolabeled compound; and ii) the measurement of a physiological parameter using a radiotracer (e.g., receptor concentration/occupancy, enzyme activity, or metabolism).[1] These two "classes" of imaging experiments are synergistic and provide a means for direct characterization of drug interactions and their downstream biological consequences.[2]

PET imaging employs molecules labeled with positron-emitting isotopes, such as carbon-11 (^{11}C), nitrogen-13 (^{13}N), oxygen-15 (^{15}O), and fluorine-18 (^{18}F) (Table 1.1). During an experiment, in which a radiolabeled molecule is injected into a subject, decay will occur, and the emitted positron will encounter its anti-matter partner, an electron. They annihilate and produce two high energy gamma rays that travel in anti-parallel directions. The timing and location of detection of the gamma rays by a PET scanner allows for the computed tomography of the place of annihilation, and therefore the location of the molecule *in vivo*. Summation of the annihilation events leads to a PET image of the radiolabeled molecule.

Currently, PET is most recognized as a clinical tool for the diagnosis of cancer[3] due to

---

1. Serdons, K.; Terwinghe, C.; Van Vermaelen, P.; Laere, K.; Kung, H.; Mortelmans, L.; Bormans, G.; Verbruggen, A. *J. Med. Chem.* **2009**, *52*, 1428.

2. (a) Antoni, G.; Langstrom, B. *Handb. Exp. Pharmacol.* **2008**, 177; (b) Fowler, J. S.; Wolf, A. P. *Acc. Chem. Res.* **1997**, *30*, 181.

3. (a) Wood, K. A.; Hoskin, P. J.; Saunders, M. I. *Clin. Oncol.* **2007**, *19*, 237; (b) Weber, W. A. *J. Clin. Oncol.* **2006**, *24*, 3282; (c) Oriuchi, N.; Higuchi, T.; Ishikita, T.; Miyakubo, M.; Hanaoka, H.; Iida, Y.; Endo, K. *Cancer Sci.* **2006**, *97*, 1291;

the radiotracer 2-[^{18}F]fluoro-2-deoxy-D-glucose ([^{18}F]FDG),[4] Over two million PET scans are performed each year with [^{18}F]FDG. [^{18}F]FDG has revolutionized clinical practices in oncology,[5] and its role in medical research and patient care is rapidly evolving.[6] Over the past decade, PET imaging has had an impact in studying neurological diseases,[7] and gene therapy.[8] Importantly, PET is also beginning to expedite the development of new pharmaceuticals.[8a, 9]

Table 1.1. Commonly employed PET isotopes with half-lives, nuclear reaction, target, and target products.

(d) Jadvar, H.; Alavi, A.; Gambhir, S. S. *J. Nucl. Med.* **2009**, *50*, 1820.

4. (a) Gambhir, S. S. *Nat. Rev. Cancer* **2002**, *2*, 683; (b) Rigo, P.; Paulus, P.; Kaschten, B. J.; Hustinx, R.; Bury, T.; Jerusalem, G.; Benoit, T.; Foidart Willems, J. *Eur. J. Nucl. Med.* **1996**, *23*, 1641.

5. (a) Gambhir, S. S.; Czernin, J.; Schwimmer, J.; Silverman, D. H. S.; Coleman, R. E.; Phelps, M. E. *J. Nucl. Med.* **2001**, *42*, 1S; (b) Rohren, E. M.; Turkington, T. G.; Coleman, R. E. *Radiology* **2004**, *231*, 305.

6. (a) Kelloff, G.; Hoffman, J. M.; Johnson, B.; Scher, H. I.; Siegel, B. A.; Cheng, E. Y.; Cheson, B. D.; O'Shaughnessy, J.; Guyton, K. Z.; Mankoff, D. A.; Shankar, L.; Larson, S. M.; Sigman, C. C.; Schilsky, R. L.; Sullivan, D. C. *Clin. Cancer Res.* **2005**, *11*, 2785; (b) Patterson, J. C., 2nd; Mosley, M. L. *Mol. Imaging Biol.* **2005**, *7*, 197.

7. (a) Herholz, K.; Heiss, W. D. *Mol. Imaging Biol.* **2004**, *6*, 239; (b) Jacobs, A. H.; Li, H.; Winkeler, A.; Hilker, R.; Knoess, C.; Ruger, A.; Galldiks, N.; Schaller, B.; Sobesky, J.; Kracht, L.; Monfared, P.; Klein, M.; Vollmar, S.; Bauer, B.; Wagner, R.; Graf, R.; Wienhard, K.; Herholz, K.; Heiss, W. D. *Eur. J. Nuc. Med. Mol. Imaging* **2003**, *30*, 1051.

8. (a) Winkeler, A.; Sena-Esteves, M.; Paulis, L. E. M.; Li, H.; Waerzeggers, Y.; Ruckriem, B.; Himmelreich, U.; Klein, M.; Monfared, P.; Rueger, M. A.; Heneka, M.; Vollmar, S.; Hoehn, M.; Fraefel, C.; Graf, R.; Wienhard, K.; Heiss, W. D.; Jacobs, A. H. *PLoS ONE* **2007**, *2*, 1; (b) Raty, J. K.; Liimatainen, T.; Kaikkonen, M. U.; Grahn, O.; Airenne, K. J.; Yla-Herttuala, S. *Mol. Ther.* **2007**, *15*, 1579; (c) Kang, J. H.; Chung, J. K. *J. Nucl. Med.* **2008**, *49*, 164S; (d) Massoud, T. F.; Singh, A.; Gambhir, S. S. *Am. J. Neuroradiol.* **2008**, *29*, 229; (e) Massoud, T. F.; Singh, A.; Gambhir, S. S. *Am. J. Neuroradiol.* **2008**, *29*, 409.

9. (a) Hargreaves, R. J. *Clin. Pharmacol. Ther.* **2008**, *83*, 349; (b) Wang, J. L.; Maurer, L. *Curr. Top. Med. Chem.* **2005**, *5*, 1053; (c) Wagner, C. C.; Muller, M.; Lappin, G.; Langer, O. *Curr. Opin. Drug Discov. Devel.* **2008**, *11*, 104.

radioisotope	half-life (min)	nuclear reaction	target	product
^{11}C	20	$^{14}N(p,\alpha)^{11}C$	$N_2(+O_2)$	$[^{11}C]CO_2$
			$N_2(+H_2)$	$[^{11}C]CH_4$
^{13}N	10	$^{16}O(p,\alpha)^{13}N$	H_2O	$[^{13}N]NO_x$
			H_2O+EtOH	$[^{13}N]NH_3$
^{15}O	2	$^{15}N(d,n)^{15}O$	$N_2(+O_2)$	$[^{15}O]O_2$
^{18}F	110	$^{20}Ne(d,\alpha)^{18}F$	$Ne(+F_2)$	$[^{18}F]F_2$
		$^{18}O(p,n)^{18}F$	$[^{18}O]H_2O$	$^{18}F^-$

While several positron-emitting nuclei are available for PET imaging as noted above, the non-natural isotope fluorine-18 (^{18}F) is the nucleus of choice for many applications in PET imaging due to its half-life of 110 minutes, which provides an opportunity for radiotracer distribution in the subject,[10] as well as its widespread availability. The ^{18}F-nucleus is typically attached by a carbon–fluorine (C–F) bond in ^{18}F-PET tracers.[11] Carbon–fluorine bond formation is extremely challenging.[12] While simple molecules such as [^{18}F]FDG can be efficiently prepared (see Figure 1.5), more complex, biomedically interesting molecules often cannot. Furthermore [^{18}F]FDG contains a C_{sp3}–F bond. Generally, C_{sp3}–F bonds are easier to synthesize than C_{sp2}–F bonds through nucleophilic displacement reactions or enol/enolate chemistry. Methods to form C_{sp2}–F bonds will be discussed in the following section.

1.2 Late-Stage Fluorination of Arenes

Methods to form of C_{sp2}–F bonds in complex substrates has been a long-standing challenge in synthetic organic chemistry. Traditionally, aryl fluorides have been synthesized

---

10. Miller, P. W.; Long, N. J.; Vilar, R.; Gee, A. D. *Angew. Chem., Int. Ed.* **2008**, *47*, 8998.

11. Schirrmacher, R.; Wangler, C.; Schirrmacher, E. *Mini-Rev. Org. Chem.* **2007**, *4*, 317.

12. (a) Furuya, T.; Kuttruff, C. A.; Ritter, T. *Curr. Opin. Drug Discov. Devel.* **2008**, *11*, 803 (12) Grushin, V. V. *Acc. Chem. Res.* **2010**, *43*, 160; (b) Furuya, T.; Klein, E. M. N.; Ritter, T. *Synthesis* **2010**, 1804.

through the Balz-Schiemann reaction[13] and the Wallach reaction[14] (Figure 1.1). The Balz Schiemann reaction is the thermolysis of aryl diazonium tetrafluoroborates and the Wallach reaction is the acidic decomposition of triazenes. Due to the harsh condition employed for these transformations (heat and/or strong acid), sensitive functionality should not be present during the reaction. As such, the substrate scope of these classic reactions is limited.

Nucleophilic aromatic substitution is widely used for the construction of aryl fluorides.[15] With an appropriate electron-withdrawing group on the arene (e.g., nitro, cyano, carboxyl, carboxyl derivative, keto), fluoride can replace an appropriate leaving group (e.g., nitro, cyano, halo, trialkyl ammonium). Electron-neutral and electron-rich aromatic rings are rarely or cannot be employed in nucleophilic aromatic substitution reactions.

There are properties of fluorine that make synthesis with the element difficult and have hindered the development of more robust reactions than the traditional one described above.[16] Elemental fluorine is highly reactive and difficult to work with. The invention of alternative electrophilic fluorination reagents, such as xenon difluoride, pyridinium fluorides, and Selectfluor® (F-TEDA), has been instrumental in electrophilic fluorine chemistry research. Fluoride, on the other hand, has the smallest ionic radius, is a strong base when dry, and is weakly nucleophilic when wet due to the high hydration energy.[17]

---

13. Balz, G.; Schiemann, G. *Ber. Dtsch. Chem. Ges.* **1927**, *60*, 1186.

14. Wallach, O. *Liebigs Ann. Chem.* **1886**, *235*, 233.

15. (a) Gottlieb, H. B. *J. Am. Chem. Soc.* **1936**, *58*, 532; (b) Adams, D. J.; Clark, J. H. *Chem. Soc. Rev.* **1999**, *28*, 225.

16. O'Hagan, D. *Chem. Soc. Rev.* **2008**, *37*, 308.

17. Emsley, J. *Chem. Soc. Rev.* **1980**, *9*, 91.

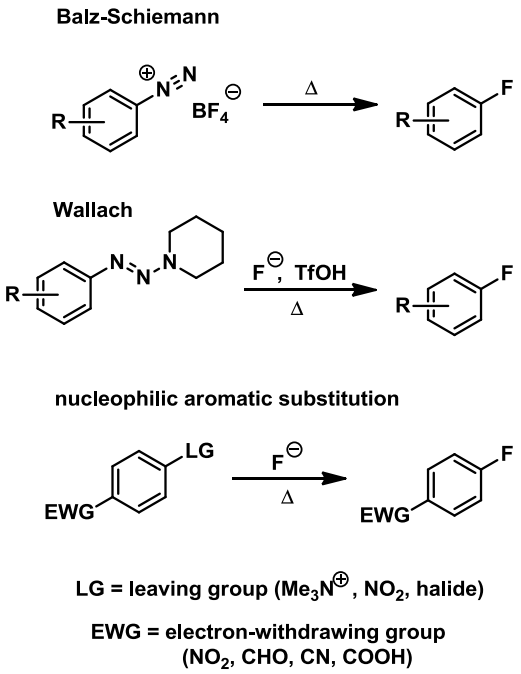

Figure 1.1. Traditional methods to synthesize aryl fluorides.

Yet, despite the difficulty of working with electrophilic fluorine and nucleophilic fluoride, incorporation of the element into small molecules and polymers is desirable.[18] Fluorine uniquely affects the properties of organic molecules through strong polar interactions due to the atom's high electronegativity.[16] For pharmaceuticals, fluorine can make a molecule more bioavailable, lipophilic, and metabolically stable, and can increase the strength of a compound's interactions with a target protein.[18b] Fluorine chemistry research has therefore been an active pursuit. Recent advances in transition-metal-mediated fluorination reactions of arenes will be highlighted here.

In 2002, the late transition metal copper, in the form of the electrophilic fluorination

---

18. (a) Kirk, K. L. *Org. Process Res. Dev.* **2008**, *12*, 305; (b) Muller, K.; Faeh, C.; Diederich, F. *Science* **2007**, *317*, 1881; (c) Purser, S.; Moore, P. R.; Swallow, S.; Gouverneur, V. *Chem. Soc. Rev.* **2008**, *37*, 320; (d) Hung, M. H.; Farnham, W. B.; Feiring, A. E., Rozen, S. In *Fluoropolymers*; Hougham, G.; Cassidy, P. E.; Johns, K.; Davidson, T. Eds, Plenum Publishing Co: New York, 1999.

reagent CuF_2, was used in the oxidation of benzene to fluorobenzene at 450 °C.[19] The copper reagent can be regenerated after fluorination, and this reaction approach has the potential to lead to a practical copper-catalyzed synthesis of simple fluorinated arenes. Currently, only structurally simple arenes, such as fluorobenzene, fluorotoluenes and difluorobenzenes, can be synthesized with the CuF_2-mediated process, and the reaction is characterized by low regioselectivity when substituents are present on the arene.

Regioselective functionalization of C_{aryl}–H (Ar–H) bonds by transition metals under less harsh conditions has been achieved through the use of directing groups.[20] Covalently attached to the aryl ring, directing groups coordinate to a transition metal and lower the activation energy for C–H bond cleavage preferentially, by positioning the transition metal in proximity to specific C–H bonds. The direct transformation of a C–H bond to a C–F bond is an attractive feature of directed electrophilic fluorination in terms of efficiency. Application of the directing group strategy to arene fluorination was first reported in 2006 by the Sanford Group[21] (Equation 1.1). Phenyl pyridine derivatives were fluorinated at the ortho positions in the presence of $Pd(OAc)_2$ and an electrophilic fluorination reagent. A similar palladium-catalyzed directed electrophilic fluorination of Ar–H bonds of N-benzyltriflamide derivatives was reported by the Yu Group in 2009[22] (Equation 1.2). The triflamide directing group (–NHTf) can be easily converted into a variety of other functional groups. Current limitations of the directing group approach include the restriction that fluorine can only be incorporated at the position ortho to the directing group, the

---

19. Subramanian, M. A.; Manzer, L. E. *Science* **2002**, *297*, 1665.

20. Cope, A. C.; Siekman, R. W. *J. Am. Chem. Soc.* **1965**, *87*, 3272.

21. Hull, K. L.; Anani, W. Q.; Sanford, M. S. *J. Am. Chem. Soc.* **2006**, *128*, 7134.

22. Wang, X.; Mei, T. S.; Yu, J. Q. *J. Am. Chem. Soc.* **2009**, *131*, 7520.

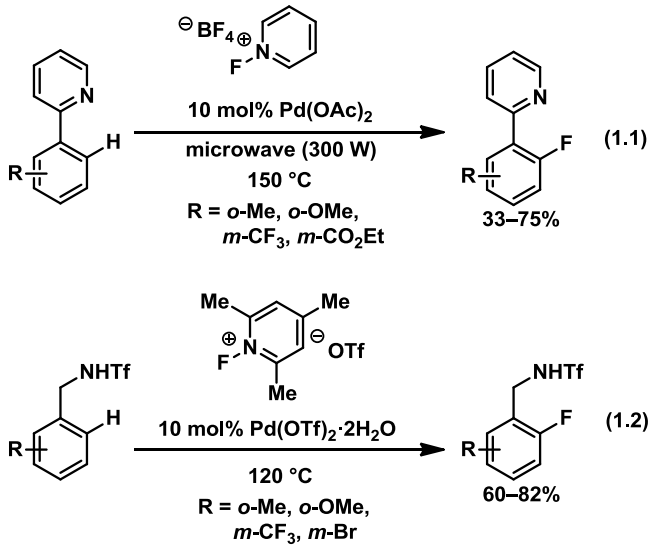

requirement for blocking groups to prevent ortho,ortho'-difluorination, and the need for a directing group itself. If the directing group is part of the desired molecule, the approach is efficient, but directing groups and functional groups that are derived from directing groups are often not desired in the final molecule, and easily removable directing groups are rare.

The mechanisms of the directed electrophilic fluorination reactions shown in Equations 1.1 and 1.2 are still unknown. After cyclopalladation, the key C–F bond-forming event could occur either from a Pd(II) center without change in the oxidation state of the metal (as in the electrophilic fluorination of an aryl Grignard reagent[23]), or from a higher oxidation state palladium complex (such as a dinuclear Pd(III)[24] or a Pd(IV)[25] complex) via C–F reductive elimination. Reductive elimination from transition metal complexes to form C–F bonds was long

---

23. (a) Yamada, S.; Gavryushin, A.; Knochel, P. *Angew. Chem., Int. Ed.* **2010**, *49*, 2215; (b) Anbarasan, P.; Neumann, H.; Beller, M. *Angew. Chem., Int. Ed.* **2010**, *49*, 2219.

24. (a) Powers, D. C.; Ritter, T. *Nat. Chem.* **2009**, *1*, 302; (b) Powers, D. C.; Geibel, M. A. L.; Klein, J.; Ritter, T. *J. Am. Chem. Soc.* **2009**, *131*, 17050; (c) Powers, D. C.; Xiao, D. Y.; Geibel, M. A. L.; Ritter, T. *J. Am. Chem. Soc.* **2010**, *132*, 14530; (d) Powers, D. C.; Benitez, D.; Tkatchouk, E.; Goddard, W. A.; Ritter, T. *J. Am. Chem. Soc.* **2010**, *132*, 14092.

25. (a) Kaspi, A. W.; Yahav-Levi, A.; Goldberg, I.; Vigalok, A. *Inorg. Chem.* **2008**, *47*, 5; (b) Ball, N. D.; Sanford, M. S. *J. Am. Chem. Soc.* **2009**, *131*, 3796.

unknown. Only in 2008 was an isolated aryltransition metal fluoride complex reported to undergo C–F reductive elimination.[26]

Carbon–fluorine reductive elimination was studied by the Ritter Group in the context of isolated Pd(II)–Ar complexes synthesized by transmetalation from aryl boronic acids. In 2008, it was discovered that a variety of functionalized arylboronic acids are suitable substrates for transmetalation onto a palladium(II) complex; subsequent treatment with the electrophilic fluorination reagent F-TEDA-BF_4 afforded the corresponding aryl fluorides (Figure 1.2).[27] It was postulated that C–F bond formation occurred via fluorination of the transition metal, followed by C–F reductive elimination. Studies on isolated arylpalladium(IV) fluoride complexes established the viability of Ar–F reductive elimination from a transition metal complex.[26]

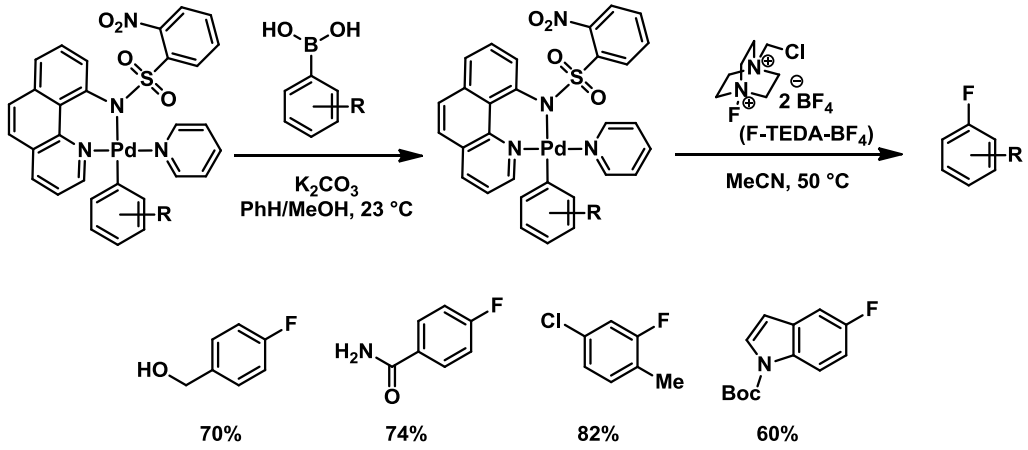

Figure 1.2. Palladium-mediated fluorination of aryl boronic acids with F-TEDA. (Yields given are for fluorination.)

Transition-metal-catalyzed cross coupling between an electrophile and a nucleophile is potentially a general approach for C–F bond formation. Studies of the use of palladium-, rhodium- and copper-based cross-coupling reactions for C–F bond formation have been

---

26. (a) Furuya, T.; Ritter, T. *J. Am. Chem. Soc.* **2008**, *130*, 10060; (b) Furuya, T.; Benitez, D.; Tkatchouk, E.; Strom, A. E.; Tang, P. P.; Goddard, W. A.; Ritter, T. *J. Am. Chem. Soc.* **2010**, *132*, 3793.

27. Furuya, T.; Kaiser, H. M.; Ritter, T. *Angew. Chem., Int. Ed.* **2008**, *47*, 5993.

documented since the late 1990s,[28] but only recently has successful fluorination by catalysis been achieved, due in large part to the development of metal complexes that can undergo C–F reductive elimination.

Theoretical studies of the fundamental difficulties associated with C–F reductive elimination from arylpalladium(II) fluoride complexes were reported in 2007.[29] Reductive elimination should occur most readily from a mononuclear, three-coordinate, 'T'-shaped palladium complex, with the aryl ligand and the fluoride ligand oriented cis to each other. However, 'T'-shaped arylpalladium(II) fluoride complexes are often less stable than their corresponding dimeric form, in which two 'T'-shaped palladium complexes come together, with both fluorine ligands bound to both palladium atoms. Reductive elimination from such a bis-μ-fluoride dimer is significantly more difficult than from the T-shaped monomer; in fact, to date, it has not been observed. Large ligands on palladium destabilize the dimer relative to the monomer and therefore increase the concentration of the mononuclear three-coordinate arylpalladium(II) fluoride complex for subsequent C–F reductive elimination. In line with this reasoning, the use of the bulky monodentate phosphine ligand *t*-Bu-XPhos resulted in C–F bond formation from an arylpalladium(II) fluoride complex, albeit in only 10% yield. This was a significant and promising result, but conclusive evidence for concerted C–F reductive elimination was not obtained and other mechanisms of C–F bond formation are possible.[30]

The first palladium(0)-catalyzed Ar–F bond-forming cross-coupling reaction was reported in 2009 using aryl triflates (ArOTf) and CsF as a nucleophilic fluorine source (Figure

---

28. (a) Fraser, S. L.; Antipin, M. Y.; Khroustalyov, V. N.; Grushin, V. V. *J. Am. Chem. Soc.* **1997**, *119*, 4769; (b) Pilon, M. C.; Grushin, V. V. *Organometallics* **1998**, *17*, 1774; (c) Grushin, V. V. *Chem.-Eur. J.* **2002**, *8*, 1006.

29. Yandulov, D. V.; Tran, N. T. *J. Am. Chem. Soc.* **2007**, *129*, 1342.

30. Grushin, V. V.; Marshall, W. J. *Organometallics* **2007**, *26*, 4997.

1.3).[31] As predicted by theory, the use of a bulky monodentate phosphine ligand, *t*-BuBrettPhos,[32] to access three-coordinate arylpalladium(II) fluoride complexes was the key to success. An arylpalladium(II) fluoride complex supported by *t*-BuBrettPhos was shown to be effective for C–F reductive elimination. Arenes with a wide range of electronic properties and a variety of heterocycles could be fluorinated with this method. Sterically congested arenes and arenes bearing electrophilic and nucleophilic functional groups could be fluorinated as well. For a few substrates, undesired constitutional isomers were formed as by-products when para-electron-donating or meta-electron withdrawing groups were present. Although the mechanism for the formation of the constitutional isomers has not yet been elucidated, the isomers could arise from a competing benzyne pathway, owing to high reaction temperatures and dried, basic fluoride. It has also been shown that the phosphine ligand can undergo *in situ* modification to generate a triaryl phosphine that is responsible for C–F bond formation for some substrates.[33] The reaction

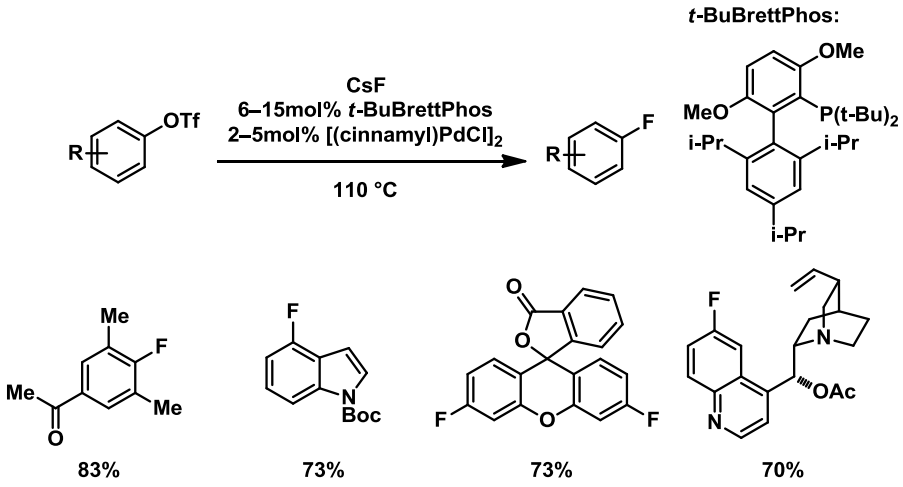

Figure 1.3. Palladium-catalyzed cross-coupling reaction to form aryl fluorides using aryl triflates and cesium fluoride.

---

31. Watson, D. A.; Su, M. J.; Teverovskiy, G.; Zhang, Y.; Garcia-Fortanet, J.; Kinzel, T.; Buchwald, S. L. *Science* **2009**, *325*, 1661.

32. Fors, B. P.; Watson, D. A.; Biscoe, M. R.; Buchwald, S. L. *J. Am. Chem. Soc.* **2008**, *130*, 13552.

33. Maimone, T. J.; Milner, P. J.; Kinzel, T.; Zhang, Y.; Takase, M. K.; Buchwald, S. L. *J. Am. Chem. Soc.* **2011**, *133*, 18106.

must be performed under anhydrous conditions, and substrates with protic functional groups were not demonstrated to undergo fluorination, possibly owing to the tendency of fluoride to form strong hydrogen bonds. Hydrogen-bond formation between protic functional groups or water with arylpalladium(II) fluorides could stabilize the ground state of the arylpalladium(II) fluoride complex, which increases the activation barrier to C–F reductive elimination.[29] Water could also result in hydrolysis of the Pd–F bond at a rate faster than the rate of C–F reductive elimination.

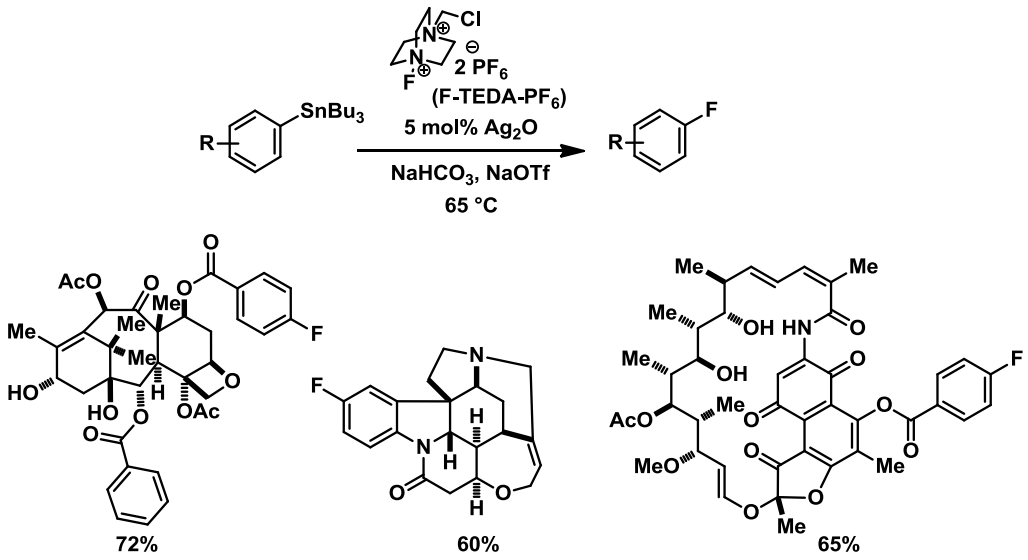

Figure 1.4. Silver-catalyzed fluorination of aryl stannanes with the electrophilic fluorination reagent F-TEDA.

Reductive elimination of C–F bonds from transition metal fluorides need not be limited to palladium. The late transition metal silver has been shown to mediate the electrophilic fluorination of arylboronic acids[34] and aryl stannanes.[35] Following the initial discovery of general silver-mediated fluorination of arenes, a silver-catalyzed electrophilic A–F bond-forming reaction for aryl stannanes using Ag_2O and the electrophilic fluorination reagent F-TEDA-PF_6 was

34. Furuya, T.; Ritter, T. *Org. Lett*. **2009**, *11*, 2860.

35. Furuya, T.; Strom, A. E.; Ritter, T. *J. Am. Chem. Soc*. **2009**, *131*, 1662.

developed (Figure 1.4).[36] Several functional groups are tolerated under the reaction conditions. The reaction is applicable to late-stage fluorination of complex small molecules, including taxol, strychnine, and rifamycin derivatives. Few nucleophilic functional groups—including certain amines and sulfides that are generally compatible with nucleophilic fluorination reactions—are incompatible with the electrophilic fluorination reaction. Current challenges associated with the silver-catalyzed electrophilic fluorination include the use of toxic aryl stannane starting materials and the additional synthetic steps required for their preparation from Ar–OH or Ar–H bonds, typically via aryl triflates or aryl halides.[37]

1.3 Synthesis with ^{18}F

Using the position-emitting ^{18}F isotope exacerbates the challenge of C_{sp2}–F bond formation. The relatively short half-life of ^{18}F dictates severe restrictions on the chemical synthesis of PET tracers.[10, 38] Introduction of ^{18}F must occur at a late stage of the synthesis, ideally as the last step to avoid unproductive decay of the ^{18}F-nucleus before injection into the body. Due to the limited functional group compatibility of fluorination reactions employed today and the short half-life of 110 minutes, the synthesis of PET tracers is currently limited to a fairly small number of simple molecules.[11, 39] Examples of the late-stage fluorination of ^{18}F-PET tracers ([^{18}F]FDG,[40] [^{18}F]fallypride,[41] [^{18}F]F-DOPA[42]) are shown in Figure 1.5. In these examples,

---

36. Tang, P. P.; Furuya, T.; Ritter, T. *J. Am. Chem. Soc*. **2010**, *132*, 12150.

37. Azizian, H.; Eaborn, C.; Pidcock, A. *J. Organomet. Chem.* **1981**, *215*, 49.

38. (a) Cai, L.; Lu, S.; Pike, V. W. *Eur. J. Org. Chem.* **2008**, *2008*, 2853; (b) Fowler, J. S.; Wolf, A. P. *Acc. Chem. Res.* **1997**, *30*, 181.

39. (a) Lasne, M. C.; Perrio, C.; Rouden, J.; Barre, L.; Roeda, D.; Dolle, F.; Crouzel, C. In *Contrast Agents II*; Springer: Berlin, 2002; Vol. 222, p 201; (b) Schubiger, P. A.; Lehmann, L.; Friebe, M. *PET Chemistry: The Driving Force in Molecular Imaging*; Springer: New York, 2007.

40. Hamacher, K.; Coenen, H. H.; Stocklin, G. *J. Nucl. Med.* **1986**, *27*, 235.

reaction times are short and there may or may not be a deprotection of sensitive functional groups after C–F bond formation.

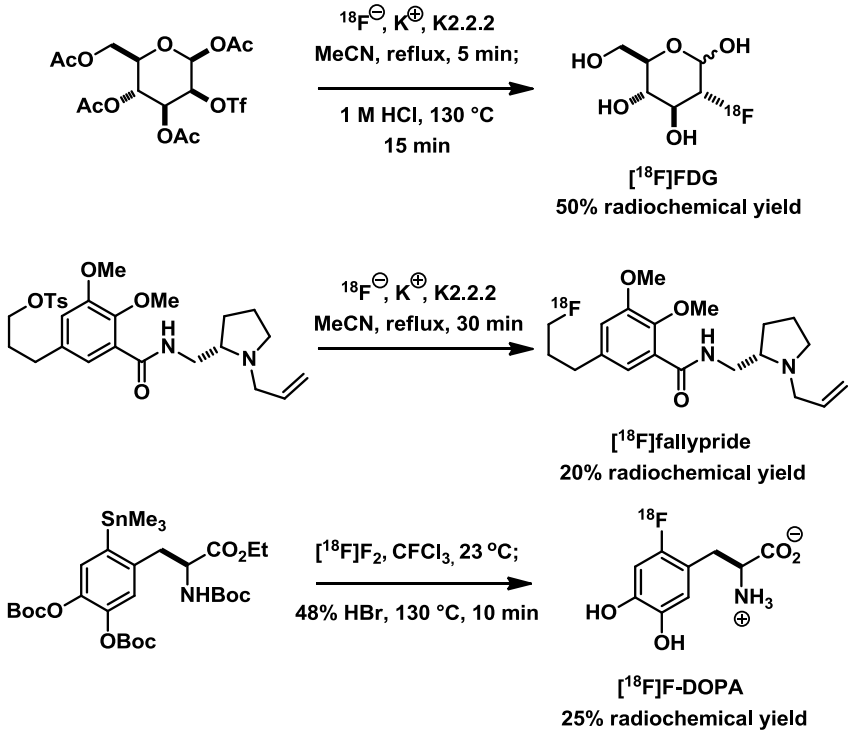

Figure 1.5. Example late-stage fluorination to synthesize ^{18}F-PET tracers.

However, substrate scope and reaction time are not the only constraints of ^{18}F-PET chemistry. It is desirable to obtain PET images using high specific activity isotopes. Specific activity is a measurement of isotopic enrichment (i.e. the ratio of position-emitting nuclei to natural, non-positron emitting nuclei), and is typically measured in terms of amount of

41. Mukherjee, J.; Yang, Z. Y.; Das, M. K.; Brown, T. *Nucl. Med. Biol.* **1995**, *22*, 283.

42. Namavari, M.; Bishop, A.; Satyamurthy, N.; Bida, G.; Barrio, J. R. *Appl. Radiat. Isot.* **1992**, *43*, 989.

radioactivity per moles of sample.[10] For ^{18}F chemistry, the ^{18}F can be made either as [^{18}F]fluoride or [^{18}F]F_2 ("F^-" or "F^+"). [^{18}F]Fluoride ([^{18}F]F^-) is much more widely available, easier to use, and is made at a specific activity typically 2 orders of magnitude greater than [^{18}F]F_2.[43] High specific activity [^{18}F]F^- provides higher quality images compared to [^{18}F]F_2 and is the preferred source of ^{18}F.[38a, 44] Nevertheless, using high specific activity isotopes means that the total amount of material is small, on the order nanomoles. This dictates a need for unusually high chemical reaction rates and efficiencies, which are met by only a handful of methods.

Recent advances in the synthesis of ^{18}F-labeled molecules include work by Pike and Gouverneur. Pike has shown that fluorination of diaryl iodinium salts is an efficient method to form aryl fluorides (Equation 1.3).[45] The method has been applied a variety of useful molecules.[46] The drawbacks of the method include the general difficulty to prepare diaryl iodonium salts, which can be unstable and lack functional group tolerance, and the lack of selectivity in C–F bond formation. Gouverneur has demonstrated that more useful and selective electrophilic fluorination reagents (compared to fluorine gas) can be synthesized with ^{18}F. This has allowed her to employ recently discovered electrophilic fluorination reactions in for the synthesis of ^{18}F-labeled aryl fluorides (for example, see Equation 1.4).[47] However, the ^{18}F-labeled electrophilic fluorination reagents are ultimately derived from [^{18}F]F_2, which cannot be made in specific activities as high as [^{18}F]fluoride.[43]

---

43. Bergman, J.; Solin, O. *Nucl. Med. Biol.* **1997**, *24*, 677.

44. (a) Ametamey, S. M.; Honer, M.; Schubiger, P. A. *Chem. Rev.* **2008**, *108*, 1501.

45. (a) Pike, V. W.; Aigbirhio, F. I. *J. Chem. Soc., Chem. Commun.* **1995**, 2215; (b) Ross, T.; Ermert, J.; Coenen, H. H. *J. Labelled Compd. Radiopharm.* **2005**, *48*, S153.

46. (a) Zhang, M. R.; Kumata, K.; Suzuki, K. *Tetrahedron Lett.* **2007**, *48*, 8632; (b) Lee, B. C.; Kim, J. S.; Kim, B. S.; Son, J. Y.; Hong, S. K.; Park, H. S.; Moon, B. S.; Jung, J. H.; Jeong, J. M.; Kim, S. E. *Bioorg. Med. Chem.* **2011**, *19*, 2980.

47. (a) Teare, H.; Robins, E. G.; Kirjavainen, A.; Forsback, S.; Sandford, G.; Solin, O.; Luthra, S. K.; Gouverneur, V. *Angew. Chem., Int. Ed.* **2010**, *49*, 6821; (b) Teare, H.; Robins, E. G.; Arstad, E.; Sajinder, K. L.; Gouverneur, V. *Chem. Commun.* **2007**, 2330.

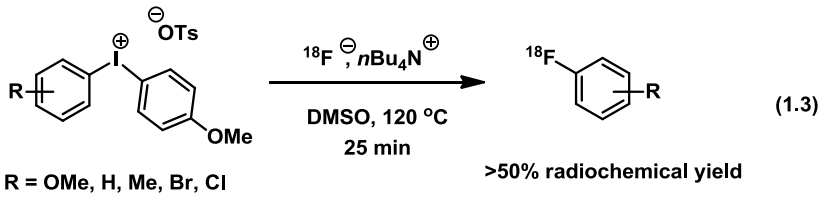

(1.3)

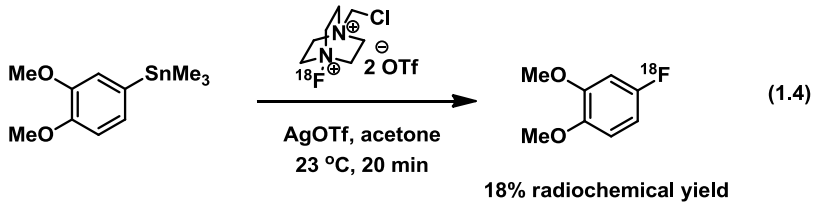

(1.4)

Given the above considerations, a general method to synthesize ^{18}F-labeled aryl fluorides employing [^{18}F]F^{-} as the source of ^{18}F would be a breakthrough in the field of PET imaging.

2. RESULTS AND DISCUSSION

Note: For context, the initial developments of this research project, which preceded my contributions, are presented in this chapter (Section 2.1). Dr. Takeru Furuya and Dan Choi observed the electrophilic nature of a Pd(IV)–F complex and used the complex for Pd-mediated C–F bond formation. Dr. David Powers improved the efficiency of C–F bond formation and synthesized Pd(IV)–F complexes from fluoride via ligand metathesis. Dr. Eunsung Lee synthesized and developed the route to the Pd(IV)–F complex from fluoride that we use in this research as well as performed the DFT calculations that are alluded to. Dr. Eunsung Lee and I collaborated on the initial transition to radiochemistry (Section 2.3).

2.1 Design and Synthesis of an Electrophilic Fluorination Reagent Derived from Fluoride

During the course of an investigation into C–F reductive elimination and high-valent palladium reactivity, the Ritter Group synthesized a Pd(IV)–F complex containing a tetrapyrazolylborate ligand (Figure 2.1).[48] The complex was synthesized from a Pd(II)–Ar complex using a pyridinium fluoride electrophilic fluorination reagent. C–F reductive elimination from the complex was not observed. However, when treated with triphenylphosphine, P–F bond formation was observed, suggesting that a

48. Choi, D. *Harvard University* **2008**.

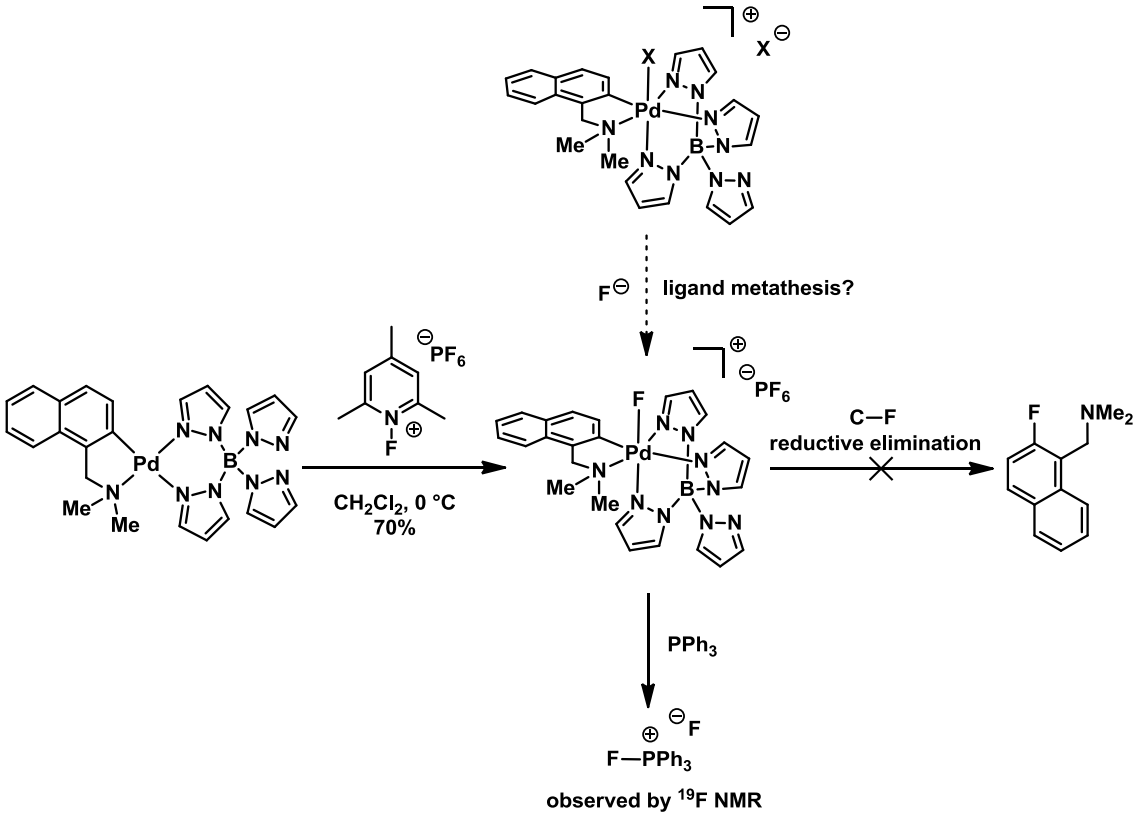

Figure 2.1. Initial observation that a Pd(IV)–F could behave as an electrophilic fluorination reagent.

Pd(IV)–F could serve as an electrophilic fluorination reagent. If a Pd(IV)–F could be synthesized from fluoride and a Pd(IV) complex through ligand metathesis of an X- or L-type ligand, then electrophilic fluorination reactions could be a means to make high specific activity ^{18}F-PET tracers. Specifically, ^{18}F radiochemistry combined with the general, functional-group-tolerant electrophilic fluorination reactions described in Section 1.2 could drastically expand access to ^{18}F-PET tracers.

Previously, the Ritter Group reported the fluorination of palladium aryl complexes with the electrophilic fluorination reagent F-TEDA (Figure 1.2).[49] F-TEDA can oxidize Pd(II)–Ar complexes, which subsequently afford aryl fluorides by C–F reductive elimination from

49. Furuya, T.; Kaiser, H. M.; Ritter, T. *Angew. Chem., Int. Ed.* **2008**, *47*, 5993.

arylpalladium(IV) fluoride complexes.[50] Replacement of F-TEDA by a fluorination reagent that mimics the function of F-TEDA, but is made from fluoride has the potential for use in the synthesis of high specific activity ^{18}F radiotracers. We designed and synthesized an organometallic complex made from fluoride (**2.1** → **2.2**, Equation 2.1) that behaves as an electrophilic fluorination reagent, and can use the reagent for the synthesis of small molecules via late-stage fluorination.

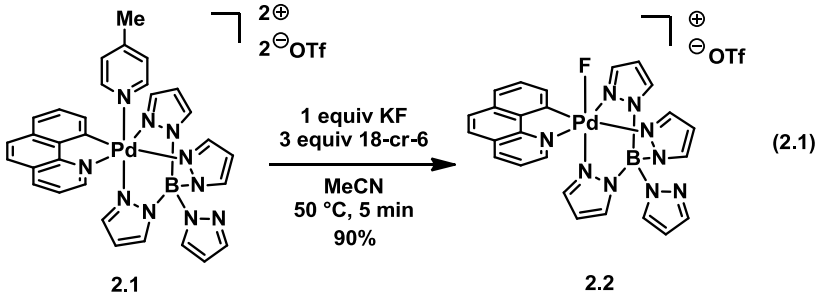

Palladium complex **2.2** was envisioned to accomplish oxidative fluorine transfer by serving as an electrophile in S_N2 reactions with nucleophilic attack occurring at the fluorine substituent. The complexes **2.1** and **2.2** were designed based on the following five considerations: i) The palladium center in **2.1** carries three formal positive charges (counter charges to two triflate anions and one negatively charged borate ligand) and should therefore capture negatively charged fluoride from solution. High fluorophilicity of the palladium complex **2.1** is required for radiochemistry applications due to the low effective concentration of fluoride in solution (roughly 10^{-4} M). ii) The palladium centers in **2.1** and **2.2** are in the oxidation state +IV (Pd(IV)), a high oxidation state for palladium. Late transition metals such as palladium, when in a high oxidation state, can function as an oxidant and transfer a ligand to a nucleophile,

50. (a) Furuya, T.; Ritter, T. *J. Am. Chem. Soc.* **2008**, *130*, 10060; (b) Furuya, T.; Benitez, D.; Tkatchouk, E.; Strom, A. E.; Tang, P. P.; Goddard, W. A.; Ritter, T. *J. Am. Chem. Soc.* **2010**, *132*, 3793.

while being reduced in the process to a lower oxidation state.[51] The palladium in **2.2** can function as an electron acceptor, which rationalizes the reactivity of **2.2** as an oxidant. iii) The supporting benzo[*h*]quinolyl and tetrapyrazole borate (Tp) ligands are multidentate ligands that were selected to impart stability on both **2.1** and **2.2** toward undesired reductive processes such as C–F reductive elimination. Reductive elimination from **2.2** would likely require dissociation of one ligand to form a pentacoordinate palladium complex,[50] and multidentate ligands such as Tp are less likely to dissociate and hence reduce the rate of potential reductive elimination. iv) An octahedral Pd(IV) complex was chosen to avoid undesired nucleophilic attack at the transition metal. The Pd–F bond is polarized toward fluorine, with partial negative charge on fluorine and positive charge on palladium. Solely based on coulombic interactions, nucleophilic attack is expected at palladium rather than fluorine. However, the orbitals available for nucleophilic attack on octahedral $(t_{2g})^6(e_g)^0$ Pd(IV) complexes, the d_{x2-y2} and d_{z2} orbitals, are high in energy, and nucleophilic attack on high energy orbitals is disfavored.[52] v) The multidentate supporting ligands in **2.2** feature aromatic substituents to prevent nucleophilic attack on the carbon and nitrogen atoms coordinated to palladium. Complex **2.2** was devised to act as an electrophilic fluorination reagent through nucleophilic attack at the antibonding palladium–fluorine-based orbital (σ*Pd–F) at fluorine in an S_N2 reaction. In such a putative S_N2 reaction, palladium would function as a leaving group, with concomitant reduction to the oxidation state +II (Pd(II)). Nucleophilic attack would occur at the lowest unoccupied molecular orbital (LUMO) of 2. The calculated LUMO of **2.2** (Figure 2.2), shows that only the lobe on fluorine points into unoccupied space; no other LUMO lobe is available for nucleophilic attack because the aromatic ligands block the trajectories.

---

51. Stahl, S. S.; Labinger, J. A.; Bercaw, J. E. *Angew. Chem., Int. Ed.* **1998**, *37*, 2181.

52. Cotton, F. *Chemical Applications of Group Theory*; 3 ed.; Wiley: New York, 1990.

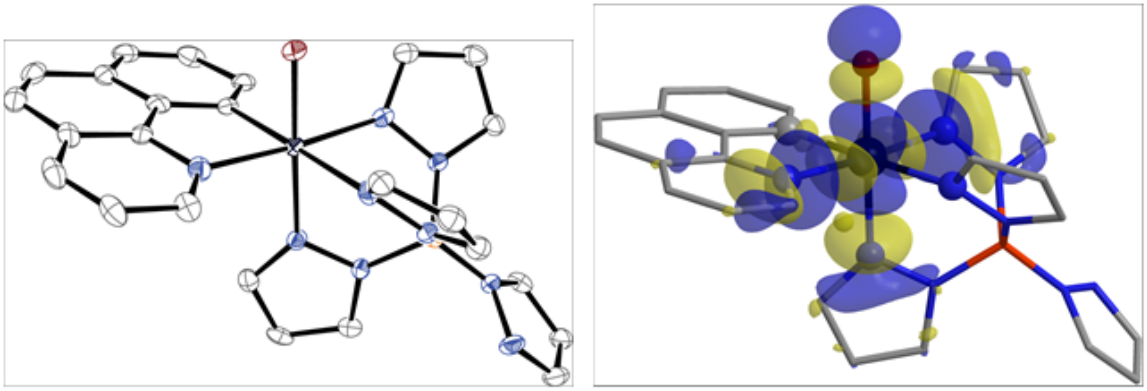

Figure 2.2. X-ray structure and calculated LUMO of **2.2**.

Treatment of the palladium complex **2.1** with nucleophilic fluoride (KF) afforded the palladium fluoride complex **2.2** within five minutes in 90% yield (Equation 2.1). The ability of **2.2** to function as an electrophilic fluorination reagent was confirmed by fluorination of Pd(II) aryl complexes. Two model substrates with limited functionality were chosen. Pd(II)–Ar complexes **2.3** and **2.4** were treated with one equivalent of **2.2** at 85 °C in acetone in a sealed vial for 10 minutes (Figure 2.3) Aryl fluorides **2.5** and **2.6** were obtained in high yield. We propose that Pd(IV)–F complex **2.2** oxidizes the Pd(II)–Ar complexes by fluorine transfer to form high-valent arylpalladium(IV) fluoride complexes, from which C–F reductive elimination can occur to form aryl fluoride products **2.5** and **2.6**.

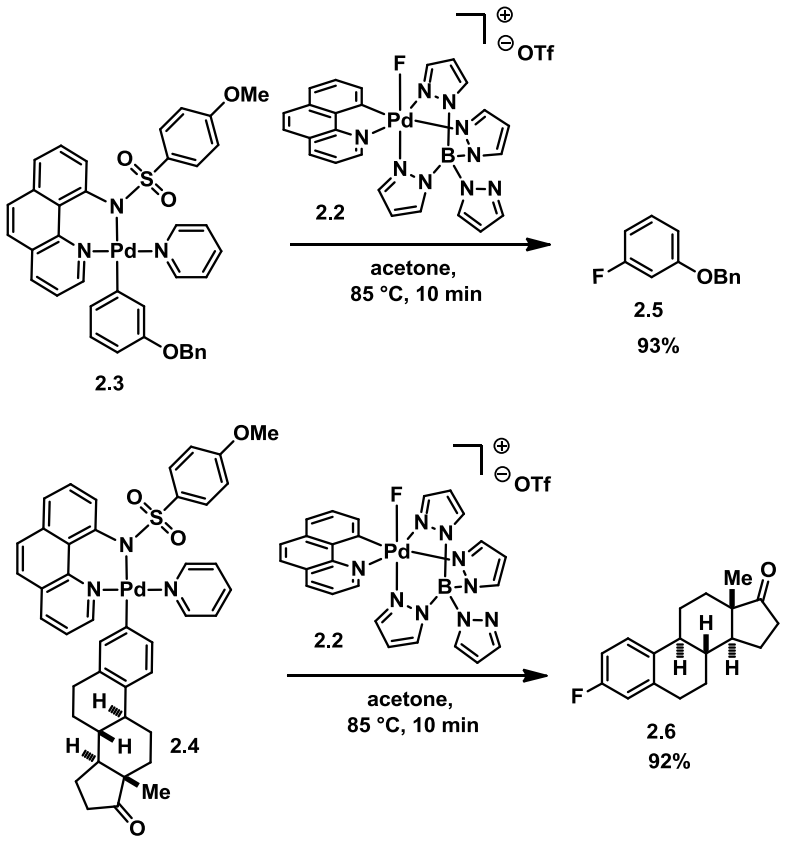

Figure 2.3. Complex **2.2** can behave as an electrophilic reagent in a Pd-mediated fluorination reaction.

Oxidative fluorine transfer from **2.2** to **2.3**, for example, could proceed by S_N2 reaction as designed, with nucleophilic attack of the d_{z^2}-based orbital on palladium of **2.3** on the σ* Pd–F-based orbital of the LUMO of **2.2**, or via electron transfers[53] from **2.3** to **2.2** with interposed or subsequent fluorine transfer. Current data cannot distinguish between these mechanisms. In addition, other pathways that intercept putative arylpalladium(IV) fluoride intermediates could potentially be used for C–F bond formation. Palladium complex **2.2** is both an oxidant and a fluoride donor. The oxidation equivalents are inherent in the transition metal oxidation state, and the fluorine substituent is negatively polarized, because fluorine is the most electronegative element. But oxidation of **2.3** with an external oxidant followed by reaction with an independent

53. (a) Taube, H.; Myers, H. *J. Am. Chem. Soc.* **1954**, *76*, 2103; (b) Haim, A. *Prog. Inorg. Chem.* **1983**, *30*, 273.

fluoride source could also provide arylpalladium(IV) fluoride intermediates. In such a stepwise approach, potential side reactions of putative intermediates, such as undesired reductive elimination reactions, must be prevented. Conceptually, several combinations of an oxidant and a fluoride source are conceivable for successful oxidative fluorination.

Scheme 2.1. Synthesis of electrophilic fluorination reagent **2.2** from fluoride.

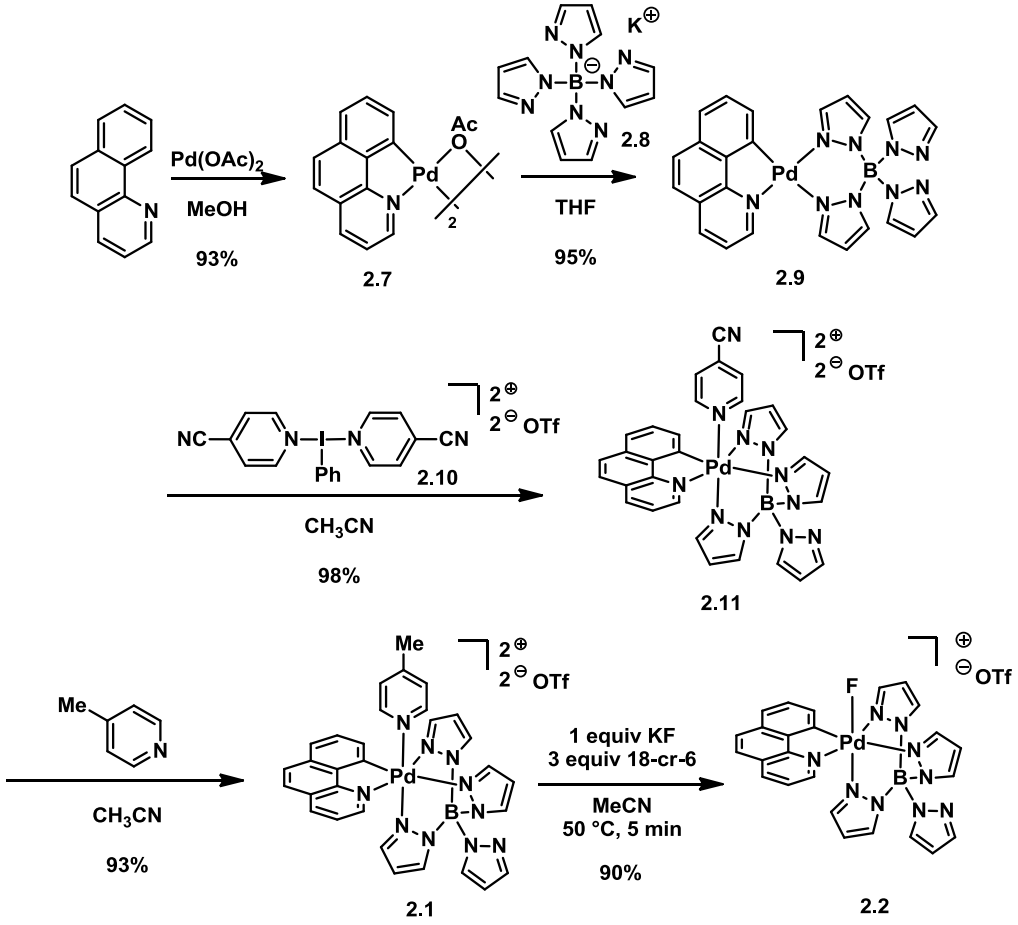

Pd(IV)–F was synthesized according to Scheme 2.1. Cyclometalation using $Pd(OAc)_2$ with benzo[*h*]quinoline afforded the palladium dimer **2.7**. Ligand exchange with potassium tetrapyrazolylborate (**2.8**) gave the Pd(II) complex **2.9** that was oxidized to Pd(IV) using hypervalent iodine reagent **2.10**. While the oxidation was efficient with **2.10**, the 4-cyanopyridine was subsequently exchanged with picoline to provide a more stable complex **2.1**.

Pd(IV) complex **2.1** efficiently captures fluoride as described above to give electrophilic fluorination reagent **2.2**.

Pd(II)–aryl complexes are synthesized in a modular fashion (Scheme 2.2).[49] First, using the same palladium dimer **2.7** from Scheme 2.1, chloride for acetate ligand exchange afforded **2.12**, which underwent a nitrene insertion using the oxidant **2.13** of the PhINTs variety. Pd(II)–Cl complex **2.14** was then converted into Pd(II)–OAc complex **2.15**. This complex is the direct precursor to the Pd(II)–aryl complexes. Transmetalation of an aryl boronic acids or pinacol esters on to the Pd center gives, for example, Pd(II)–aryl **2.3**.

Scheme 2.2. Synthesis of example Pd(II)–Ar complex **2.3**.

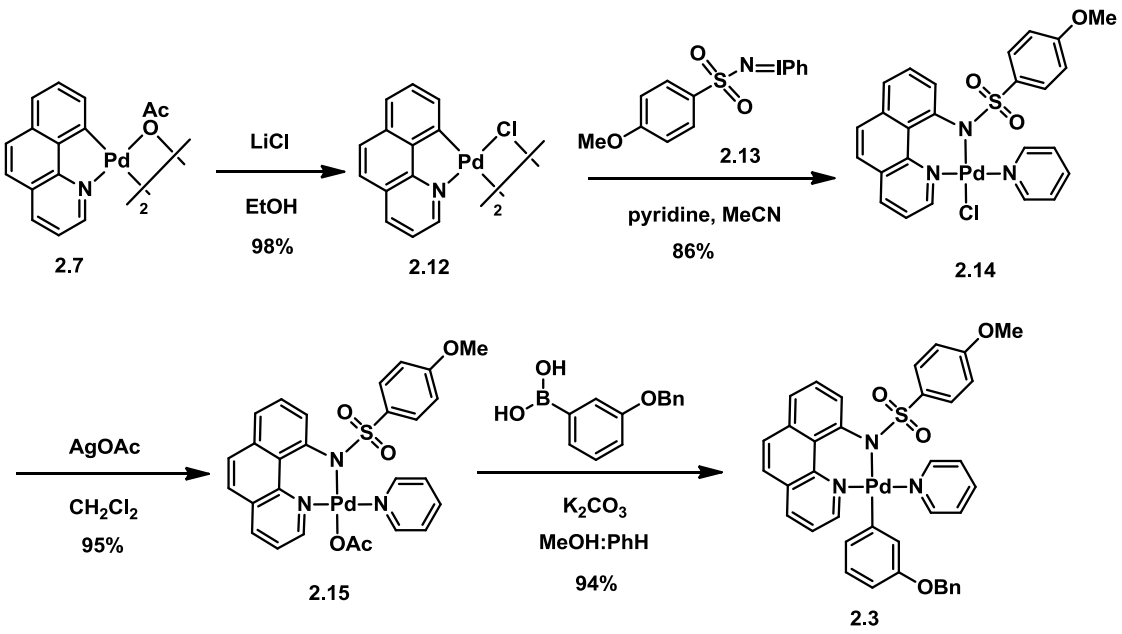

2.2 Application of New Electrophilic Fluorination Reagent to Late-Stage Fluorination of Complex Molecules

The fluorination reagent **2.2** was subsequently evaluated for late-stage fluorination. Fluorination of the Pd(II) aryl complexes **2.16**–**2.18** afforded aryl fluorides **2.19**–**2.21** in 67–72% yield (Figure 2.4). The parent aryl fluorides (without protecting groups) of the molecules shown

in Figure 2.4 were selected in part based on their structure and exhibition of a variety of functional groups, akin to potential small-molecule PET tracers.[54] The molecules are electron-rich arenes, which would be challenging to prepare by conventional fluorination reactions with [^{18}F]fluoride. The protic functional groups of the molecules in Figure 2.4 are masked with protecting groups that are quickly removable with exposure to acidic conditions; protection is necessary for efficient fluorination. Currently, arenes that have a non-hydrogen substituent ortho to the site of fluorine substitution cannot be used for late-stage fluorination with reagent **2.2**. Tertiary amines are also not tolerated by the method.

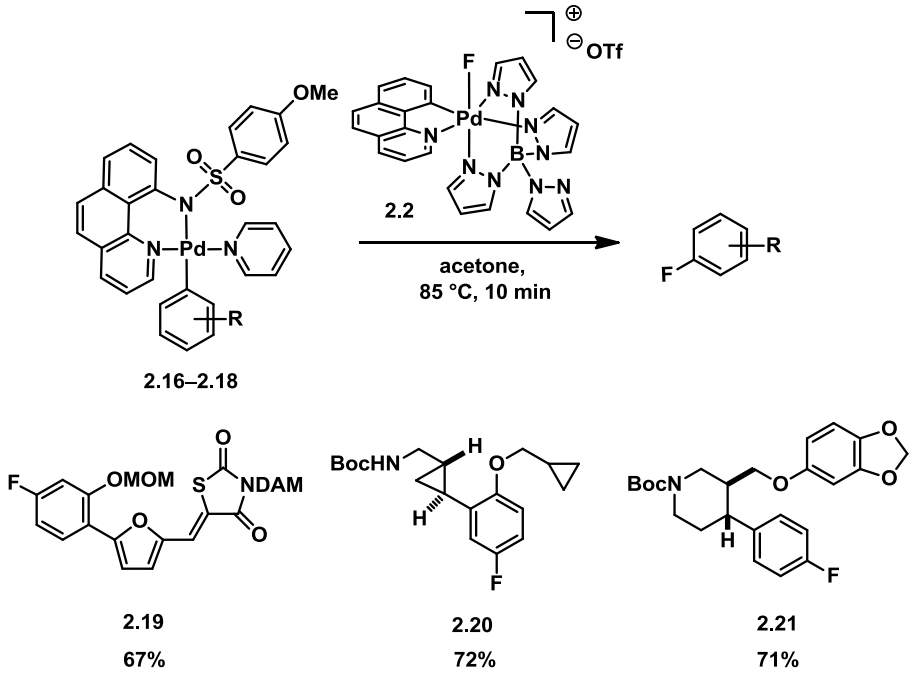

Figure 2.4. Late-stage fluorination of complex small molecules with **2.2**.

Complex Pd(II)–aryl species such as **2.16**–**2.18** are prepared from the boronic esters. For

54. (a) Kozikowski, A. P.; Cho, S. J.; Jensen, N. H.; Allen, J. A.; Svennebring, A. M.; Roth, B. L. *ChemMedChem* **2010**, *5*, 1221; (b) Pomel, V.; Klicic, J.; Covini, D.; Church, D. D.; Shaw, J. P.; Roulin, K.; Burgat-Charvillon, F.; Valognes, D.; Camps, M.; Chabert, C.; Gillieron, C.; Francon, B.; Perrin, D.; Leroy, D.; Gretener, D.; Nichols, A.; Vitte, P. A.; Carboni, S.; Rommel, C.; Schwarz, M. K.; Ruckle, T. *J. Med. Chem.* **2006**, *49*, 3857; (c) Petersen, E. N.; Bechgaard, E.; Sortwell, R. J.; Wetterberg, L. *Eur. J. Pharmacol.* **1978**, *52*, 115.

2.16, a Sandmeyer reaction starting with 2-amino-5-chlorophenol gave aryl iodide **2.22** (Scheme 2.3). MOM protection of the phenol afforded **2.23**, ready for two successive Pd-catalyzed cross-coupling reactions. First, the more reactive C–I bond was used in a Suzuki cross-coupling reaction with (5-formylfuran-2-yl)boronic acid to yield **2.24**. Subsequently, the C–Cl bond was used in a Pd-catalyzed borylation using modified conditions reported by Buchwald[55] to install the requisite pinacol boronic ester of **2.25**. Knoevenagel reaction with an N-protected thiazolidinedione **2.26** led to the entire carbon skeleton. The thiazolidinedione was protected with a dianisylmethyl (DAM) group. It was discovered that an acidic N–H bond was not tolerated during the reaction and needed to be protected. A protecting group that would remain intact during the transmetalation reaction and fluorination reaction and then be easily removed at the same time as the MOM group was desired. The DAM protecting group[56] satisfied these considerations. Transmetalation of **2.27** on to complex **2.15** gave **2.16** ready for fluorination.

---

55. Billingsley, K. L.; Barder, T. E.; Buchwald, S. L. *Angew. Chem., Int. Ed.* **2007**, *46*, 5359.

56. Carlier, P. R.; Zhao, H.; MacQuarrie-Hunter, S. L.; DeGuzman, J. C.; Hsu, D. C. *J. Am. Chem. Soc.* **2006**, *128*, 15215.

Scheme 2.3. Synthesis of Pd(II)–Ar complex **2.16**.

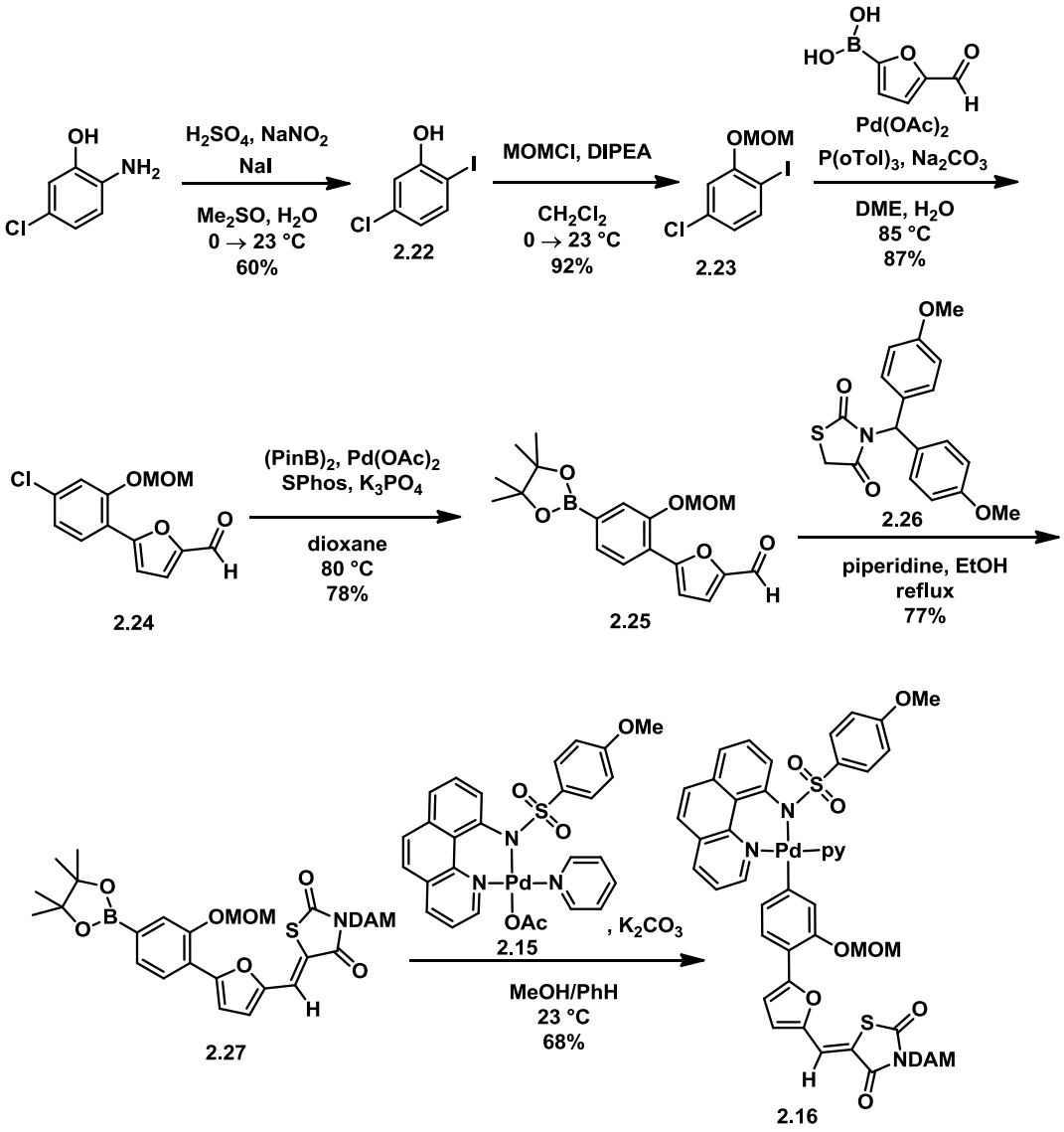

For **2.17**, commercially available 5-bromo-2-hydroxybenzaldehyde was alkylated with (bromomethyl)cyclopropane to afford **2.28** (Scheme 2.4). A Horner-Wadsworth-Emmons olefination reaction gave **2.29**, which was reduced with DIBAL-H to afford allylic alcohol **2.30**. A Charette asymmetric cyclopropanation using a chiral non racemic dioxaborolane reagent was

employed to afford the cyclopropane **2.31** in high yield and high enantiomeric excess (*ee*).[57] Mesylation and displacement with azide gave **2.32**. A one-pot reduction-protection afforded the Boc-protected compound **2.33**. Aryl bromide **2.33** could be recrystallized to afford material that was greater than 99% *ee*. Pd-catalyzed borylation gave **2.34** that was then used in the standard transmetalation reaction to afford Pd(II)–aryl complex **2.17**.

Complex **2.18** was synthesized according to Scheme 2.5. Alkylation of 4-methoxyaniline with 1-(4-bromophenyl)-3-chloropropan-1-one gave **2.35**. Acylation, cyclization, and decarboxylation gave dihydropyridone **2.36**. Asymmetric conjugate reduction using a method developed by Buchwald [58] led to enantioenriched lactam **2.37**. Claisen reaction was diastereoselective giving **2.38** as the only detectable isomer. Reduction of the ester and amide led to alcohol **2.39**. A protecting group swap was needed to ease final deprotection after radiofluorination. As such, the PMP group was removed using CAN and replaced with a Boc group in **2.40**. Sesamol was then used as the nucleophile in a Mitsunobu reaction to form aryl alkyl ether **2.41**. Borylation to afford **2.42** proceeded smoothly, which was followed by transmetalation on to **2.15** under standard conditions to give **2.18**.

---

57. Charette, A. B.; Juteau, H.; Lebel, H.; Molinaro, C. *J. Am. Chem. Soc.* **1998**, *120*, 11943.

58. Hughes, G.; Kimura, M.; Buchwald, S. L. *J. Am. Chem. Soc.* **2003**, *125*, 11253.

Scheme 2.4. Synthesis of Pd(II)–Ar complex **2.17**.

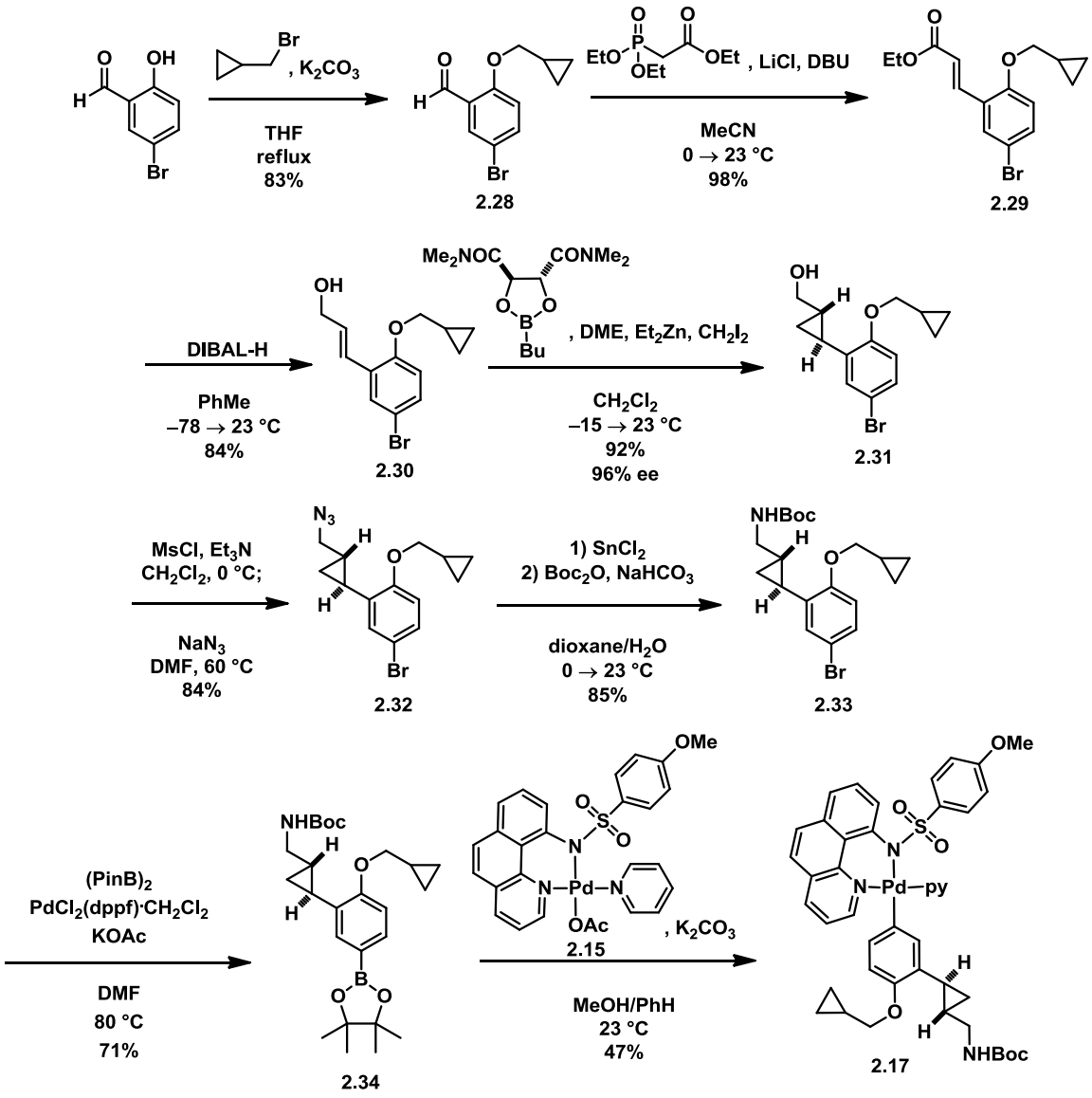

Scheme 2.5. Synthesis of Pd(II)–Ar complex **2.18**.

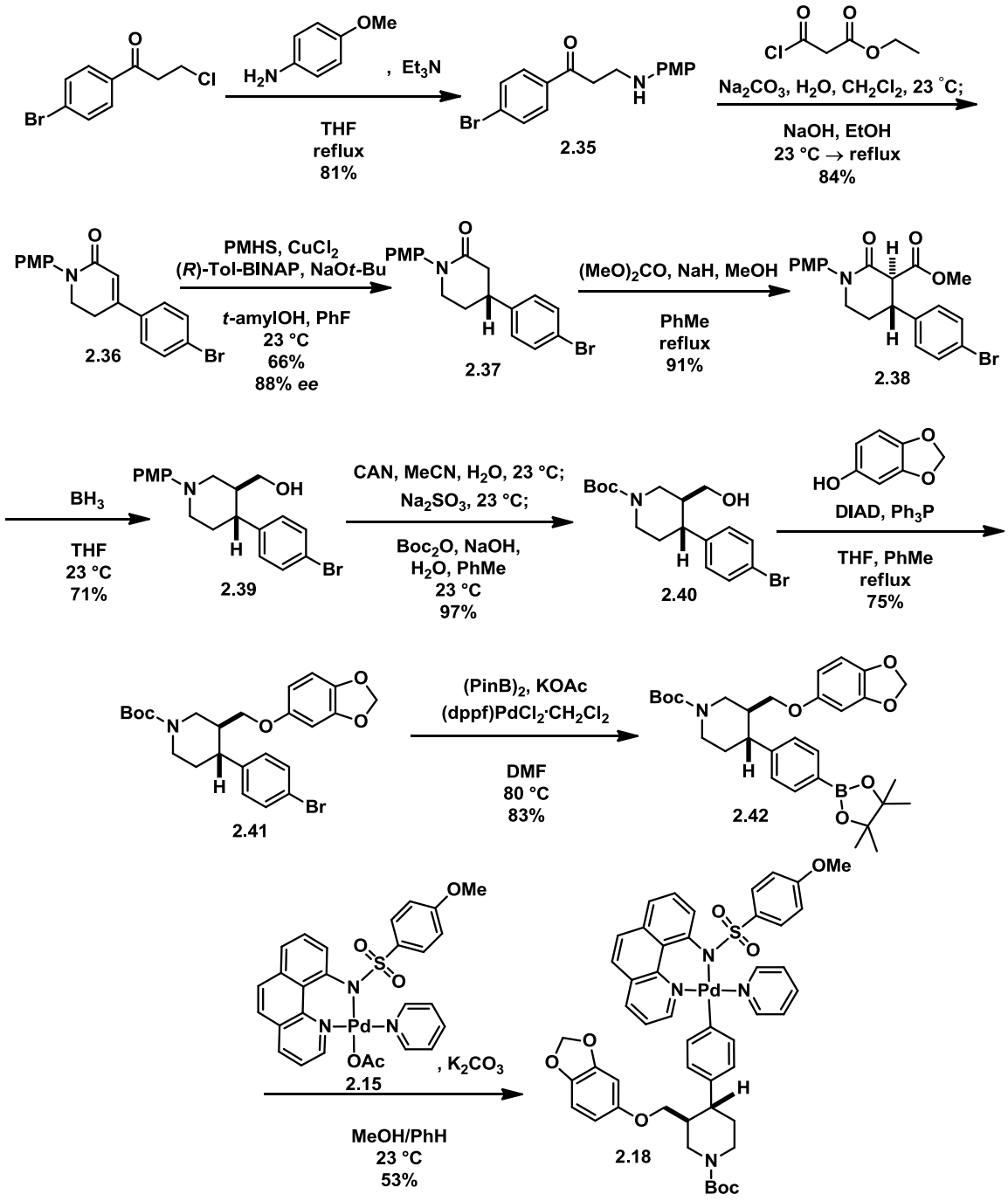

2.3 Transition from ^{19}F Chemistry to ^{18}F Radiochemistry

The transition from ^{19}F chemistry to ^{18}F chemistry is challenging because the concentration of the limiting reagent, fluoride, changes from mM to μM, and syntheses must be performed in the presence of ionizing radiation and under a time constraint due to the 110-minute half-life of ^{18}F.[59] Therefore, reaction chemistry applicable to ^{18}F chemistry must be robust and as simple as possible for broad applications in medical imaging. Organometallic synthesis in a hospital setting would be impractical. However, the palladium complexes discussed here can be prepared conveniently on scale, stored, and subsequently transported to imaging sites when needed. The Pd(II)–Ar complexes such as **2.4** and **2.16**–**2.18** can be purified by chromatography or recrystallization and can be stored and transported in air at ambient temperature. Palladium complex **2.1** is stable at room temperature and can be manipulated briefly in air. Palladium complex **2.2** is stable toward heat (no observed decomposition for 24 hours at 100 ºC), and water (no observed decomposition in 10% aqueous acetonitrile solution after 3 hours at 23 ºC). Thermal stability and tolerance toward water are beneficial for practical PET applications, because reaction mixtures are often heated to increase reaction rates and [^{18}F]fluoride is made from ^{18}O-enriched water.

We devised procedures to adapt our "cold" reaction to "hot" conditions such that the synthesis of ^{18}F-radiolabeled molecules is operationally simple. Pd(IV) complex **2.1** reacts with conventionally prepared solutions of potassium [^{18}F]fluoride in acetone with 18-crown-6 and forms the ^{18}F-reagent **[^{18}F]2.2** within 10 minutes (Figure 2.5). Subsequent filtration over a polymer-supported resin and addition of the Pd(II)–Ar complexes such as **2.4** and **2.16**–**2.18** afforded, upon heating for 10 minutes, the ^{18}F-labeled aryl fluorides **[^{18}F]2.6** and **[^{18}F]2.19**–**2.21**,

---

59. (a) Fowler, J. S.; Wolf, A. P. *Acc. Chem. Res.* **1997**, *30*, 181; (b) Cai, L. S.; Lu, S. Y.; Pike, V. W. *Eur. J. Org. Chem.* **2008**, 2853.

respectively. Azeotropic drying of aqueous [^{18}F]fluoride, the two-step reaction sequence (fluoride capture (**2.1** → **[^{18}F]2.2**) followed by fluorine transfer (e.g., **2.4** → **[^{18}F]2.6**)), results in an overall synthesis time of less than 40 minutes. The efficiency of radiochemical synthesis is given in radiochemical yield, which is based on decay-corrected radioactivity rather than on mass of isolated material.[60] Radiochemical yields (RCYs) as high as possible are desired, but even low RCYs can provide meaningful amounts of radiolabeled compounds for PET imaging, given enough starting [^{18}F]fluoride.[61] The ^{18}F-fluorination method described here has afforded RCYs higher than 30%.

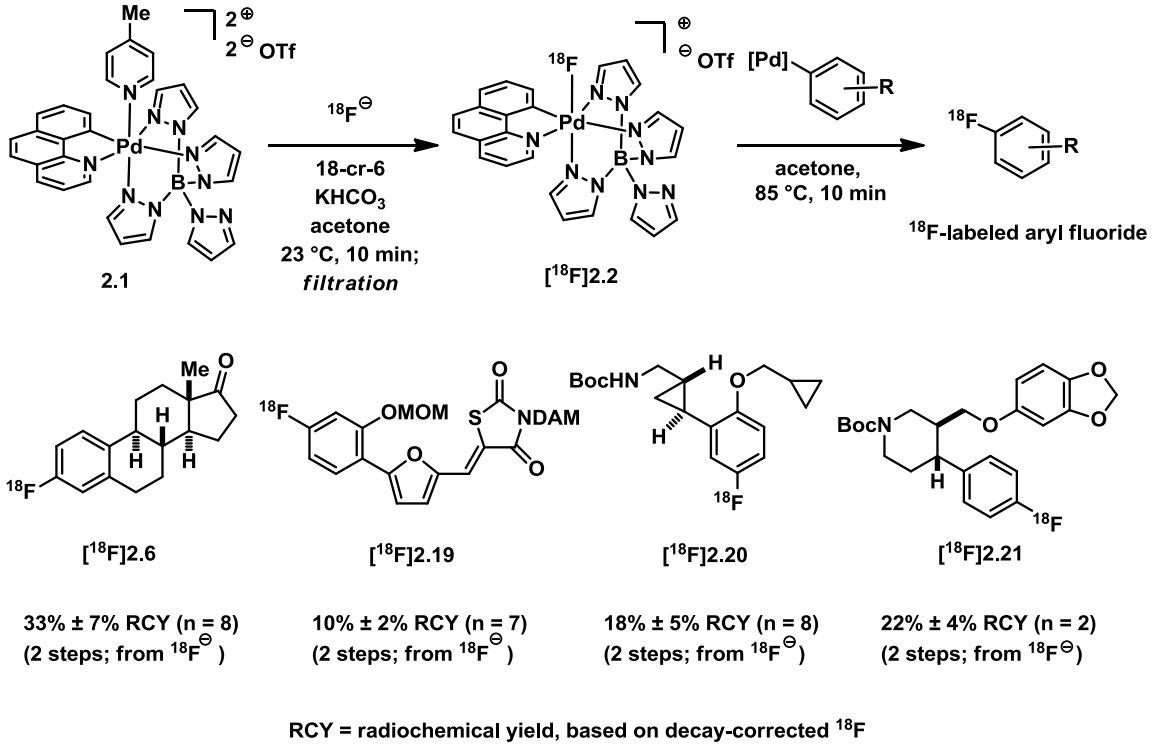

Figure 2.5. Two-step late-stage radiofluorination of complex small molecules.

Adapting the "hot" procedures described here to allow for the production of an amount of

60. Miller, P. W.; Long, N. J.; Vilar, R.; Gee, A. D. *Angew. Chem., Int. Ed.* **2008**, *47*, 8998.

61. Chin, F. T.; Namavari, M.; Levi, J.; Subbarayan, M.; Ray, P.; Chen, X. Y.; Gambhir, S. S. *Mol. Imaging Biol.* **2008**, *10*, 82.

radioactivity suitable for imaging primates (5–10 mCi of final product per experiment) required the use of automation for safety reasons. Eckert and Ziegler automated synthesis modules were programmed to perform the two-step radiochemistry reactions. First [^{18}F]fluoride in water is dried in a vial using acetonitrile and then acetone. Then a solution of Pd(IV) complex **2.1** in acetone is added and stirred for 7.5 minutes. The solution is then passed through a column of the polymer-supported resin via positive nitrogen pressure into a new vial containing the Pd(II)–Ar complex. The procedures are modular and any of the Pd(II)–Ar complexes can be used. After washing the first vial and the resin with 2-butanone, the combined organic solutions are heated at 90 °C for 10 minutes. The solvent is removed in favor of a mixture of hexanes and ethyl acetate. The reaction mixture is passed through a silica column and concentrated. If, after the synthesis of both **[^{18}F]2.20** and **[^{18}F]2.21**, for example, a deprotection step is required, it can be accomplished by a short exposure to trifluoroacetic acid. Concentration and dissolving in a minimal amount of aqueous acetonitrile followed by purification by HPLC, leads to chemically and radiochemically pure radiolabeled aryl fluorides **[^{18}F]2.43** and **[^{18}F]2.44** (see Figure 2.6) . Reformulation into a sterile saline solution for injection into a subject is then performed. The entire method from end of bombardment (production of ^{18}F) through reformulation can take less than 100 minutes.

It should be noted that stoichiometric amounts of precious transition metals such as palladium are typically avoided in syntheses of health care products due to toxicity and cost considerations. However, such considerations are different for the synthesis of PET tracers due to the small amount that is required.[62] High-specific activity PET tracers are administered at a dose at least two orders of magnitude smaller than is common for pharmaceuticals because

---

62. Toyohara, J.; Sakata, M.; Wu, J.; Ishikawa, M.; Oda, K.; Ishii, K.; Iyo, M.; Hashimoto, K.; Ishiwata, K. *Ann. Nucl. Med.* **2009**, *23*, 301.

pharmacological effects are not sought,[63] and purification is often straightforward due to the small amount of tracer to be purified. For example, inductively coupled plasma mass spectrometry (ICP-MS) analysis of a saline solution of **[^{18}F]2.43**, purified by conventional HPLC technique afforded material with less than 5 parts per billion (ppb) palladium residue, commensurate with international recommendations on the palladium impurity profile for samples injected into humans, which demand less than 1000 ppb palladium.[64] Similarly, the synthesis cost for the palladium complexes is small compared to the cost of ^{18}F-isotope infrastructure and the cost associated with clinical imaging.[65]

2.4 PET Imaging in Rats and Baboons Using ^{18}F-Aryl Fluorides Derived from Pd(IV)–F

We chose to focus our initial PET imaging experiments on neuroactive molecules. We chose two molecules that are known to interact with the serotonergic system, **2.43** and **2.44** (Figure 2.6). Aryl fluoride **2.43** is a selective serotonin 2C receptor subtype (5-HT$_{2C}$) agonist.[54a] To date, 5-HT$_{2C}$ radioligands for autoradiography and 5-HT$_{2C}$ radiotracers for imaging have not been described, and our basic understanding of these receptors is deficient. This is in spite of growing associations between the 5-HT$_{2C}$ receptor subtype and brain-related disorders including depression[66] and schizophrenia,[67] as well as drug abuse,[68] Parkinson's disease,[69] anxiety,[70] and

---

63. U.S. Department of Health and Human Services, Food and Drug Administration, www.fda.gov/downloads/Drugs/GuidanceComplianceRegulatoryInformation/Guidances/ucm078933.pdf

64. European Medicines Agency, www.ema.europa.eu/docs/en_GB/document_library/Scientific_guideline/2009/09/WC500003587.pdf

65. Buck, A. K.; Herrmann, K.; Stargardt, T.; Dechow, T.; Krause, B. J.; Schreyogg, J. *J. Nucl. Med.* **2010**, *51*, 401.

66. (a) Millan, M. J.; Gobert, A.; Lejeune, F.; Dekeyne, A.; Newman-Tancredi, A.; Pasteau, V.; Rivet, J. M.; Cussac, D. *J. Pharmacol. Exp. Ther.* **2003**, *306*, 954; (b) Millan, M. J.; Girardon, S.; Dekeyne, A. *Psychopharmacology* **1999**, *142*, 432; (c) Dekeyne, A.; Millan, M. J. *Behav. Pharmacol.* **2003**, *14*, 391.

67. (a) Marquis, K. L.; Sabb, A. L.; Logue, S. F.; Brennan, J. A.; Piesla, M. J.; Comery, T. A.; Grauer, S. M.; Ashby, C. R.; Nguyen, H. Q.; Dawson, L. A.; Barrett, J. E.; Stack, G.; Meltzer, H. Y.; Harrison, B. L.; Rosenzweig-Lipson, S. *J.*

obesity.[71] Unfortunately, direct links between the diseases listed above and 5-HT_{2C} receptor abnormalities have been difficult to discern due to the lack of a method to determine 5-HT_{2C} receptor concentration *in vivo*. Thus, the development of a selective 5-HT_{2C} PET radiotracer could have a transformative impact on neuroscience research in this area.

Paroxetine (**2.44**) is a selective serotonin reuptake inhibitor (SSRI), which functions by inhibiting the reuptake of presynaptic serotonin.[72] The synthesis of [^{18}F]paroxetine has not been previously accomplished. Its synthesis could allow for the observation of paroxetine interacting with the serotonin transporter *in vivo* using PET imaging.[71] The ability to study the binding properties of paroxetine could provide insight into the interactions between the serotonin transporter and small molecules, potentially useful for the development of more potent and selective antidepressants.[73] Importantly, synthesis of **[^{18}F]2.43** and **[^{18}F]2.44** would demonstrate that ^{18}F-labeled versions of CNS active drugs may be accessed more straightforwardly using our method, ultimately influencing for the development of pharmaceuticals development with our

---

Pharmacol. Exp. Ther. **2007**, *320*, 486; (b) Siuciak, J. A.; Chapin, D. S.; McCarthy, S. A.; Guanowsky, V.; Brown, J.; Chiang, P.; Marala, R.; Patterson, T.; Seymour, P. A.; Swick, A.; Iredale, P. A. *Neuropharmacology* **2007**, *52*, 279.

68. (a) Pandey, S. C.; Pandey, G. N. *Behav. Brain Res.* **1996**, *73*, 235; (b) Pandey, S. C.; Lumeng, L.; Li, T. K. *Alcohol. Clin. Exp. Res.* **1996**, *20*, 1038.

69. (a) Fox, S. H.; Brotchie, J. M. *Eur. J. Pharmacol.* **2000**, *398*, 59; (b) Fox, S. H.; Brotchie, J. M. *Mov. Disord.* **2000**, *15*, 1064.

70. Heisler, L. K.; Zhou, L.; Bajwa, P.; Hsu, J.; Tecott, L. H. *Genes Brain Behav.* **2007**, *6*, 491.

71. Tecott, L. H.; Sun, L. M.; Akana, S. F.; Strack, A. M.; Lowenstein, D. H.; Dallman, M. F.; Julius, D. *Nature* **1995**, *374*, 542.

72. (a) *J. Affect. Disorderes* **1990**, *18*, 289; (b) Owens, M. J.; Morgan, W. N.; Plott, S. J.; Nemeroff, C. B. *J. Pharmacol. Exp. Ther.* **1997**, *283*, 1305.

73. Glennon, R. A. In *The Serotonin Receptors*; Roth, B. L., Ed.; Humana Press: 2006, p 91.

method.

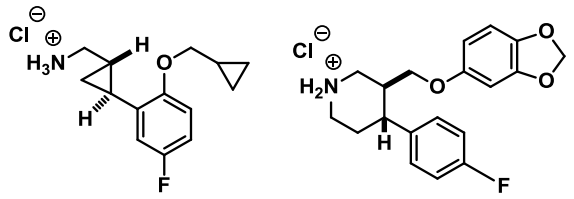

2.43 **2.44**
paroxetine

5-HT$_{2C}$ agonist **SSRI**

Figure 2.6. Two small molecules known to interact with the serotonergic system and chosen for PET imaging.

The syntheses of the required Pd(II)–aryl complexes were described in Section 2.2 and the large radioactivity scale reaction procedures via automation were described in Section 2.3. Starting with over 1 Ci of radioactive [^{18}F]fluoride in water, 14 mCi of **[^{18}F]2.43** was produced after reformulation and **[^{18}F]2.44** was produced twice, furnishing 16 and 13 mCi after reformulation. The procedures afford an amount of radiolabeled small molecule sufficient for imaging non-human primates (~5 mCi) and even humans (~10 mCi). The specific activities of the samples were measured and, at the time of injection, the specific activity was at least 1 Ci/μmol. Standard GMP guidelines were followed to test the pH, sterility, pyrogenicity of the solutions, and the purity of the radiolabeled molecules. All tests passed inspection.

Typically, two anesthetized rats were scanned at a time. One was administered a dose of the unlabeled molecule via a tail vein injection and then both were administered approximately 300–500 μCi of radiolabeled aryl fluoride. PET scanning proceeded for 90 minutes followed by a CT scan. Images were reconstructed and biodistribution and pharmacokinetic data of the two radiolabeled molecules was obtained.

For the 5-HT$_{2C}$ agonist, two adult Sprague Dawley rats were anesthetized. One rat was administered via the tail vein 1.0 mg of **2.43** followed by 322 μCi of **[^{18}F]2.43**. The other rat was administered via the tail vein 385 μCi of **[^{18}F]2.43**. The experiment lasted 90 minutes followed

by a CT scan.

After scanning, the rats were sacrificed and biodistribution determined by measuring the radioactivity of various organs. A normalized summary is shown in Figure 2.7. In rats, **[^{18}F]2.43** was not successfully blocked in the brain by pretreatment with **2.43**, suggesting ample nonspecific binding.

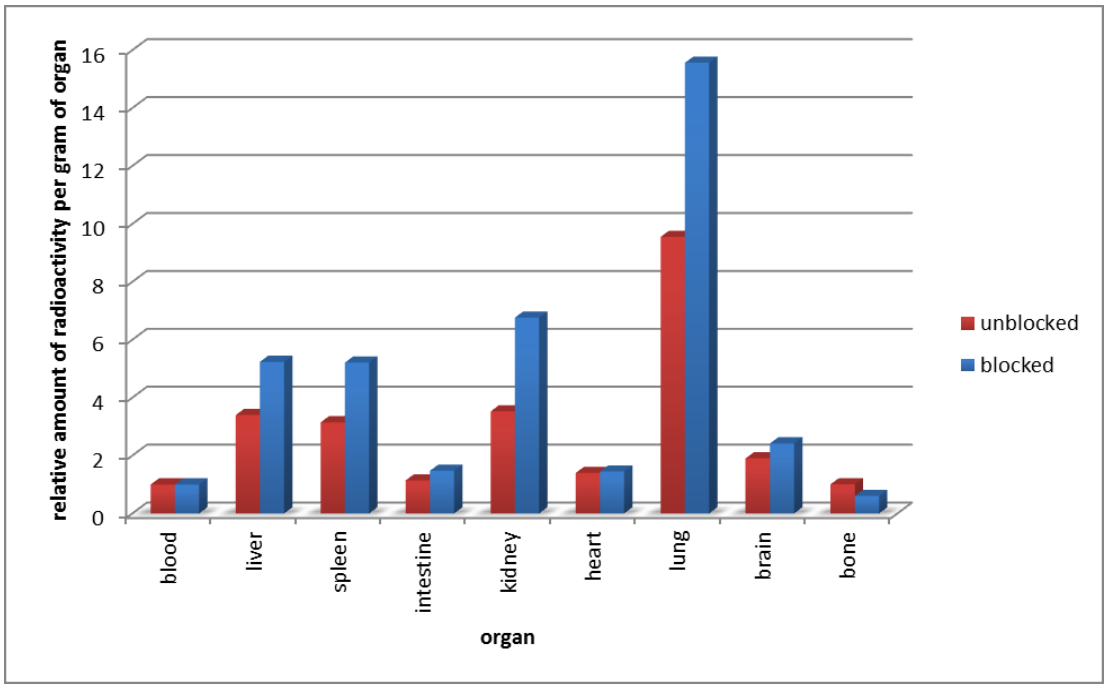

Figure 2.7. Biodistribution of **[^{18}F]2.43** in rats.

With non-human primates, an adult male baboon weighing 7.9 kg was administered 4.47 mCi of **[^{18}F]2.43** and scanned for 120 minutes followed by an MRI scan (see Figures 2.8 and 2.9).

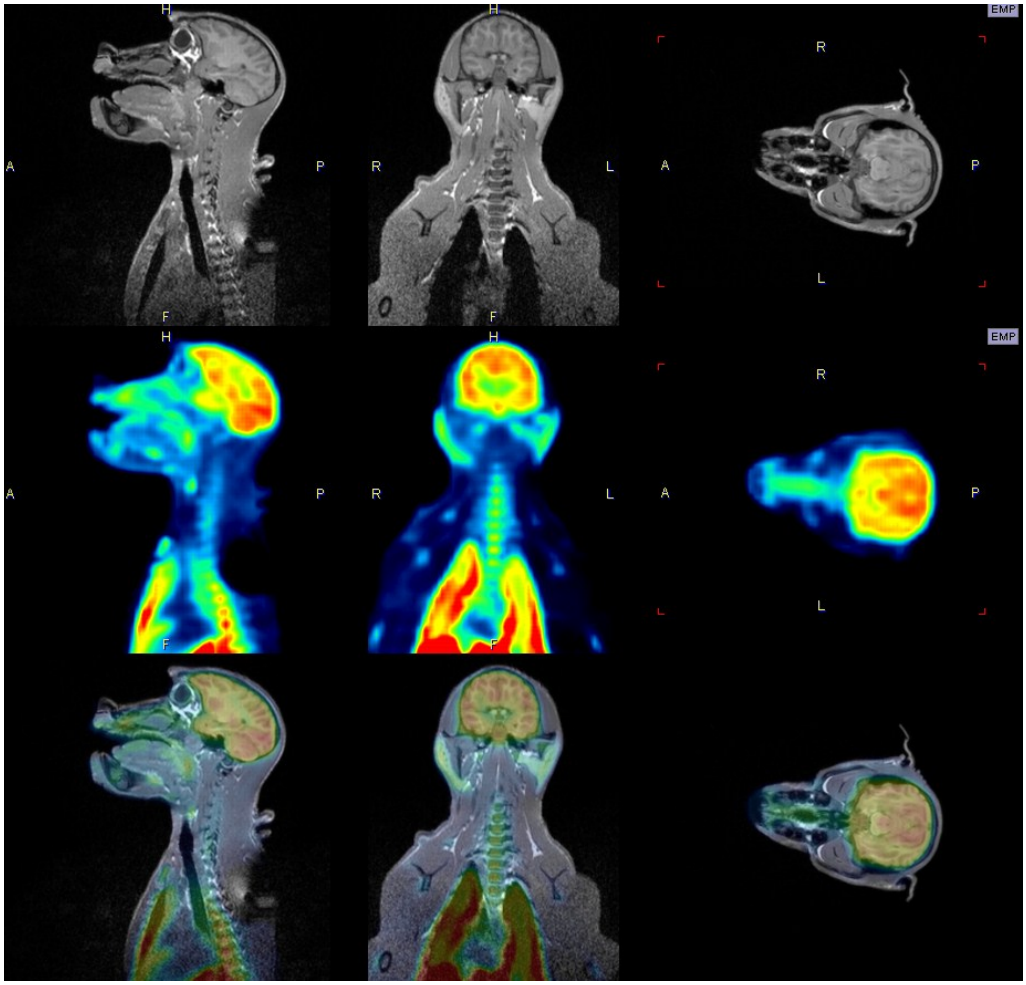

Figure 2.8. PET/MR scan of **[^{18}F]2.43** averaged over 120 minutes of upper body of baboon.

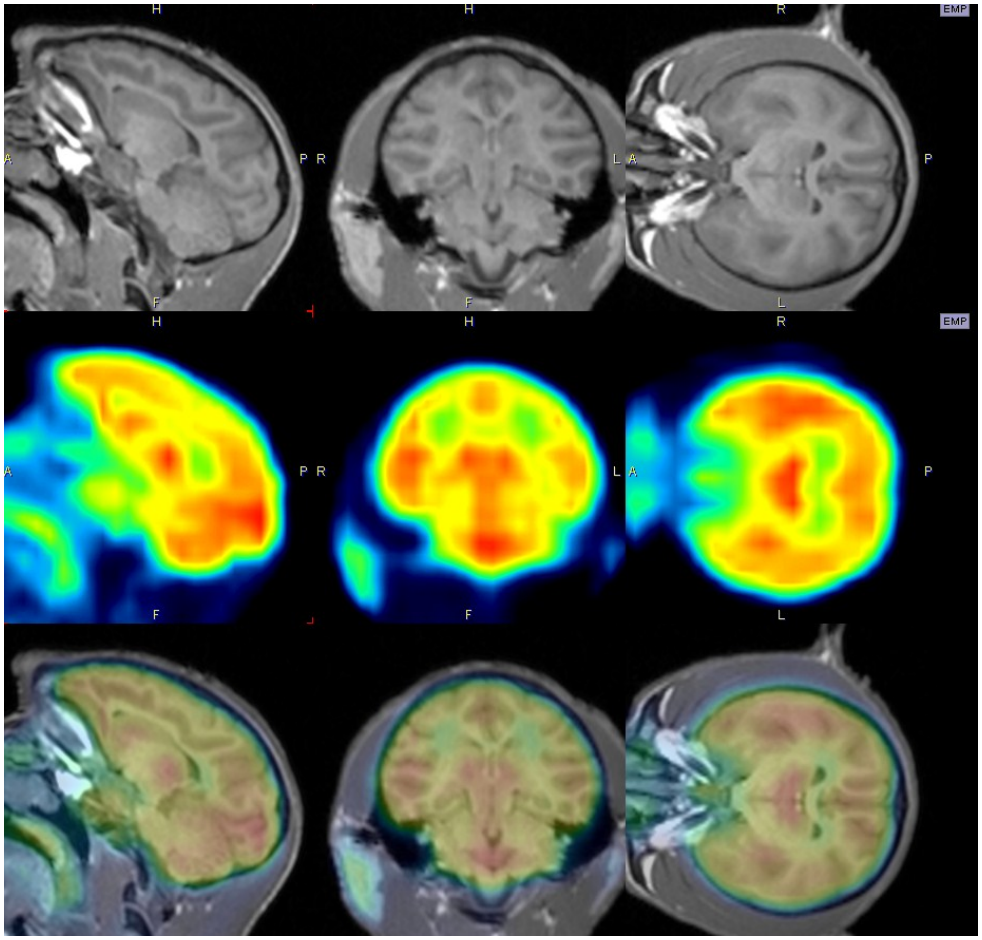

Figure 2.9. PET/MR scan of **[^{18}F]2.43** averaged over 120 minutes of brain of baboon.

Time activity curves of radioactivity throughout the portions animal and different regions of the brain are shown in Figure 2.10. As expected, there is a large initial spike in the heart and lungs due to intravenous injection of **[^{18}F]2.43** into the baboon. Agonist **[^{18}F]2.43** efficiently crosses the blood-brain barrier (as also seen for rats), but fails to differentiate itself in regions of the brain known to have varying amounts of 5-HT_{2C} receptor concentrations.[74]

74. Filip, M.; Bader, M. D. *Pharmacol. Rep.* **2009**, *61*, 761.

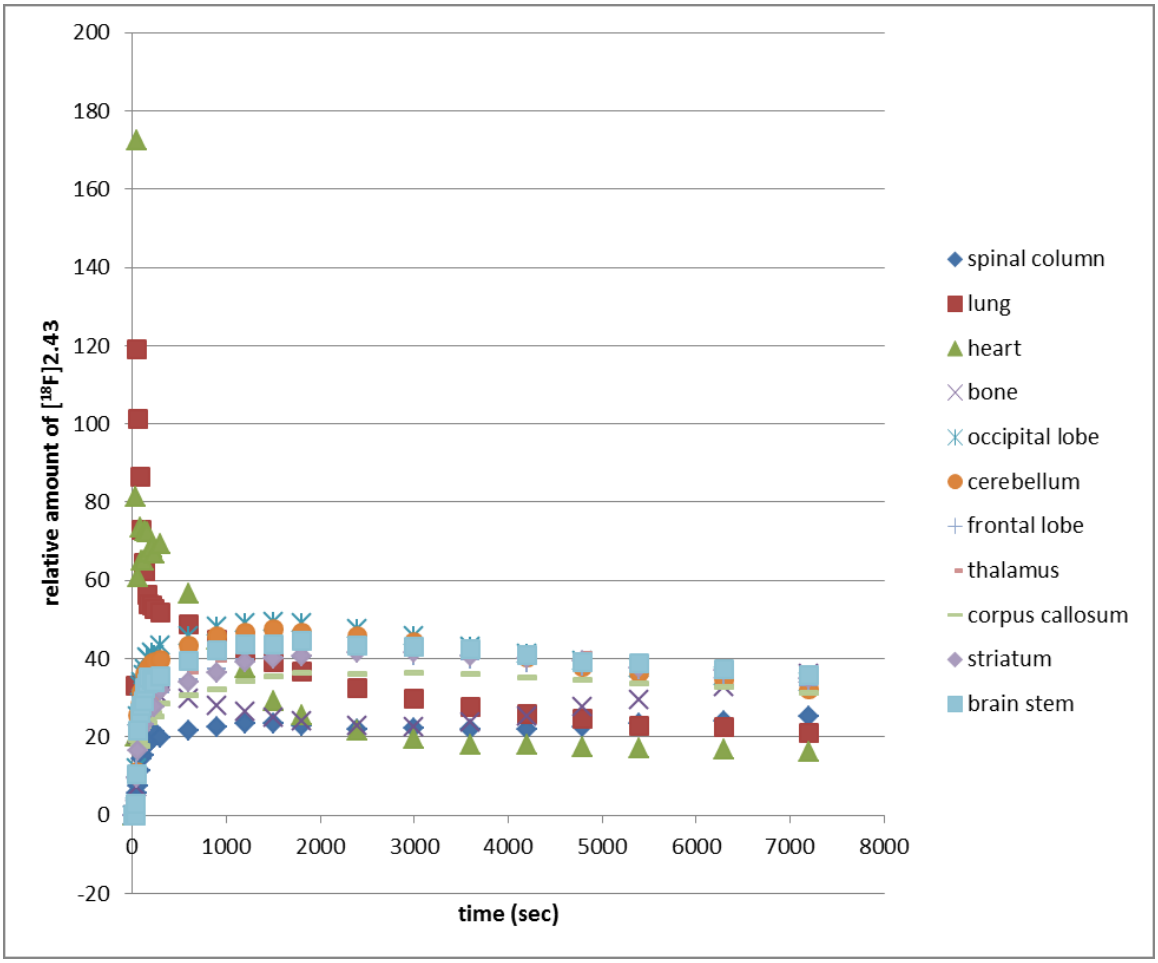

Figure 2.10. Time activity curves (decay corrected) for **[^{18}F]2.43** in baboon.

PET imaging with radiolabeled paroxetine was also performed. Two adult Sprague Dawley rats were anesthetized. One rat was administered 1.0 mg of **2.44** followed by 522 µCi of **[^{18}F]2.44** via the tail vein. The other rat was administered 457 µCi of **[^{18}F]2.44**. Both rats were scanned simultaneously for 90 minutes followed by a CT scan.

The rats were then sacrificed and their organs harvested to determine biodistribution of**[^{18}F]2.44**. Results are summarized in Figure 2.11. Similarly to **2.43**, preadministration of **2.44** failed to block significantly in the brain. Non-specific binding is problematic with **[^{18}F]2.44.**

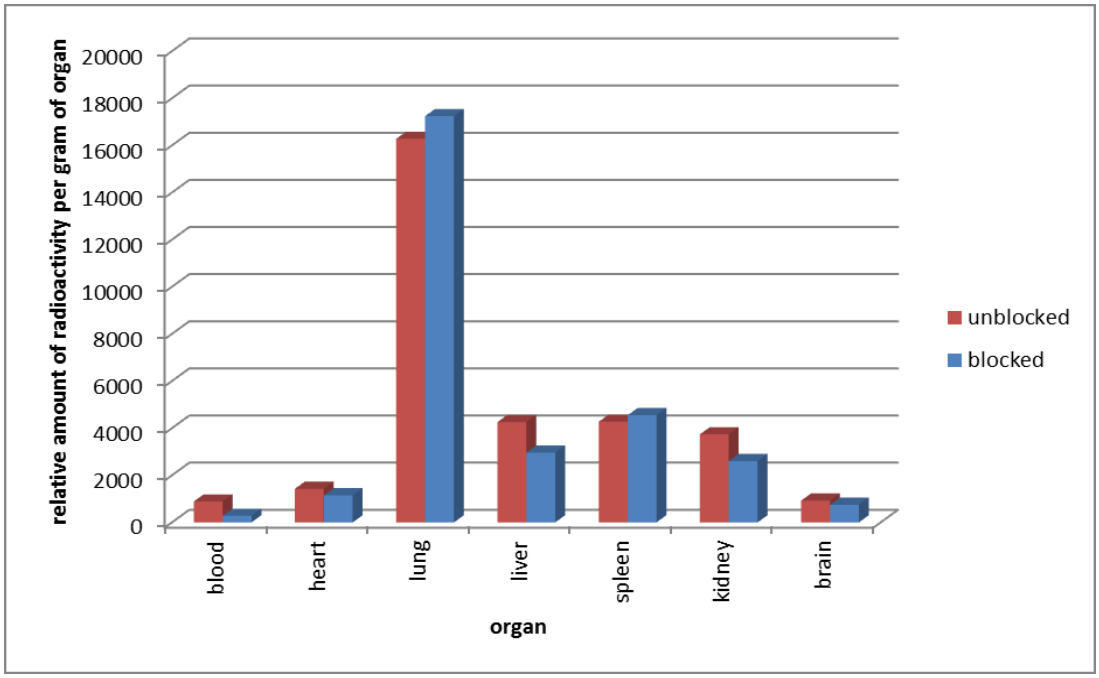

Figure 2.11. Biodistribution of **[^{18}F]2.44** in rats.

Radiolabeled paroxetine was also administered to baboons. An adult baboon weighing 6.9 kg was intravenously administered 4.4 mCi of **[^{18}F]2.44** and scanned for 90 minutes followed by an MRI scan. Additionally, an adult baboon weighing 6.6 kg was intravenously administered 33 mg of citalopram followed by 3.40 mCi of **[^{18}F]2.44** and scanned for 180 minutes followed by an MRI scan. Data was reconstructed and images data compared between the baseline (unblocked) and challenge (pretreated/blocked) experiments. Figures 2.12 and 2.13 show PET, MRI, overlay close ups of the two baboon brain averaged over the respective experiments.

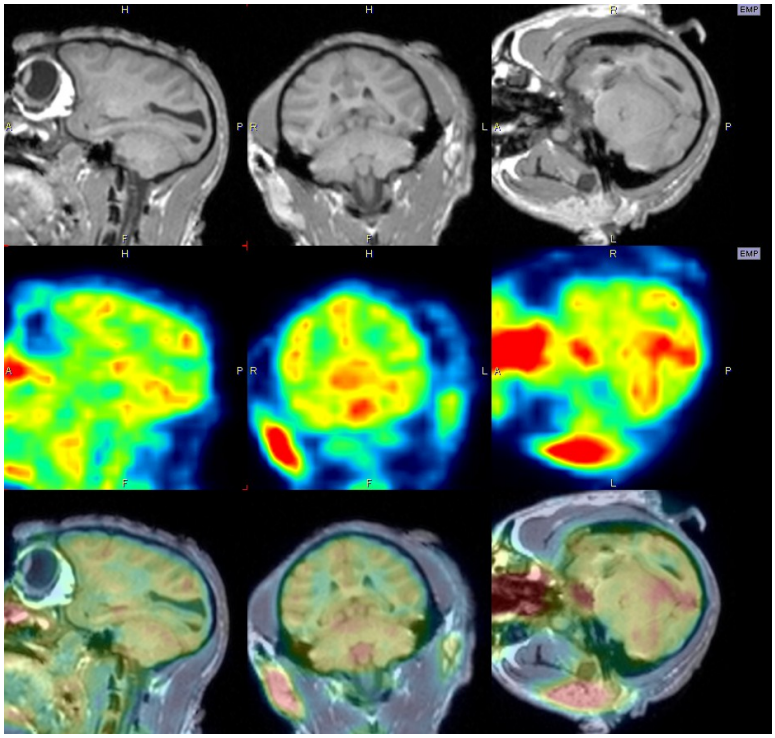

Figure 2.12. PET/MR scan of **[^{18}F]2.44** averaged over 90 minutes of brain of baboon.

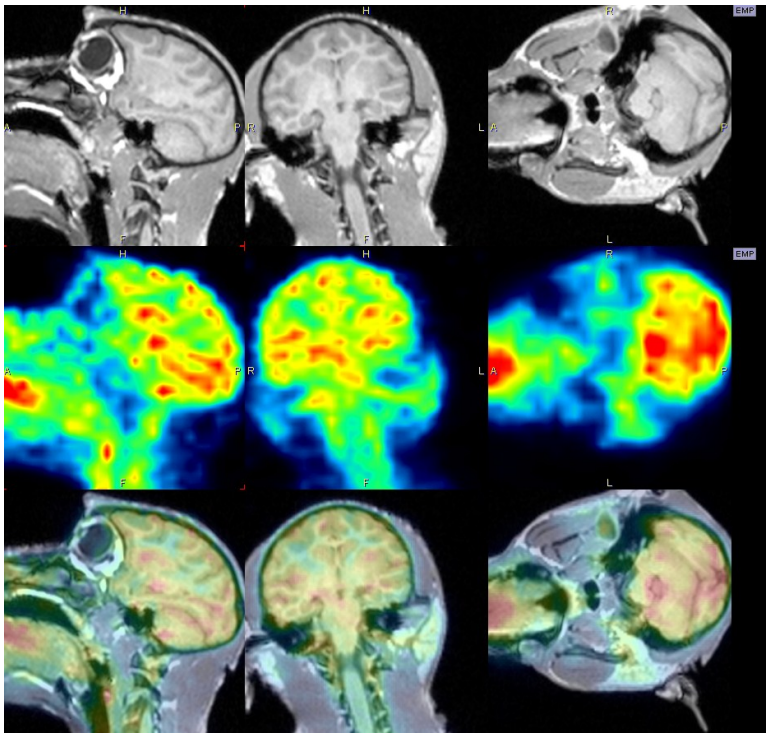

Figure 2.13. PET/MR scan of **[^{18}F]2.44** averaged over 90 minutes of brain of baboon pretreated with citalopram.

Similarities between the two experiments despite the challenge are also borne out in time activity curves of different regions of the brain (Figures 2.14 and 2.15). While regions of the brain (with large amounts of white matter) like the corpus callosum that would be expected to have low uptake of **2.44**, do show low uptake, other regions of the baboon brain are not differentiated. For example, effective SERT imaging would show a large ratio for thalamus/hypothalamus to cerebellum due to the known densities of SERT in these regions.[75]

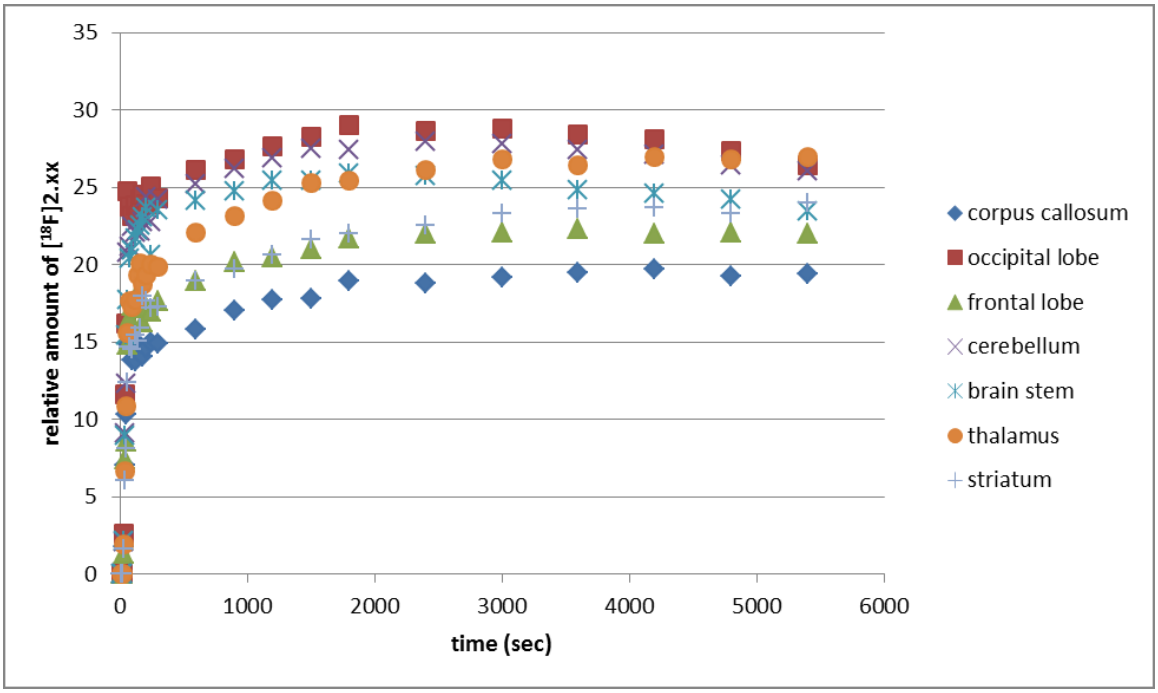

Figure 2.14. Time activity curves (decay corrected) for **[^{18}F]2.44** in baboon brain.

75. (a) Wilson, A. A.; Ginovart, N.; Hussey, D.; Meyer, J.; Houle, S. *Nucl. Med. Biol.* **2002**, *29*, 509; (b) Wilson, A. A.; Ginovart, N.; Schmidt, H.; Meyer, J. H. Threlkeld, P. G.; Houle, S. *J. Med. Chem.* **2000**, *43*, 3103.

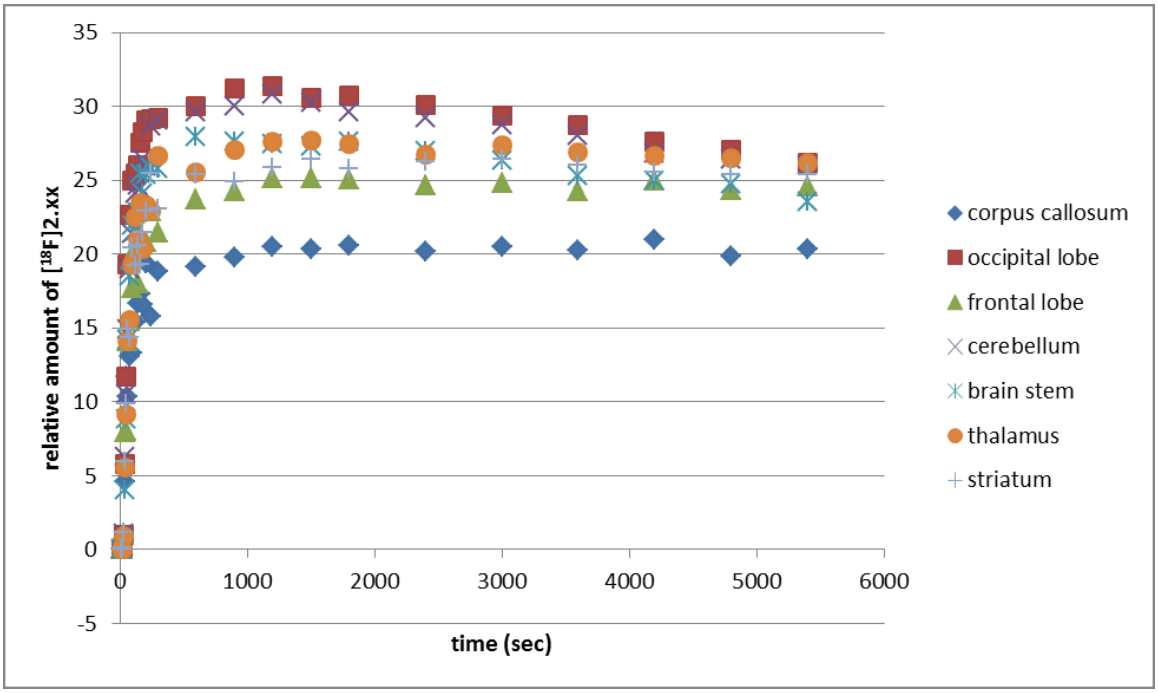

Figure 2.15. Time activity curves (decay corrected) for **[^{18}F]2.44** in baboon brain pretreated with citalopram.

In summary, both radiolabeled molecules **[^{18}F]2.43** and **[^{18}F]2.44** efficiently crossed the blood-brain barrier in rats and baboons. From imaging and pharmacokinetic analysis, due to non-specific binding and lack of blocking, these radiolabeled molecules will not find widespread use as PET tracers. The key challenge moving forward will be to use our radiofluorination reaction to synthesize molecules that have the potential to have widespread use as PET tracers.

3. CONCLUSION AND OUTLOOK

This thesis described the translational research from fundamental organometallic observations and experiments to applications in non-human primate molecular PET imaging. A new electrophilic fluorination reagent was discovered that could be used in the late-stage fluorination of complex molecules. Importantly, the electrophilic fluorination reagent can be derived from fluoride for the synthesis of high specific activity PET tracers. We can now access ^{18}F-labeled functionalized molecules, which would be particularly difficult to prepare with conventional fluorination reactions. We have advanced the method to the point where we can now prepare sufficient amounts of radiolabeled molecules for PET imaging on a primate scale.

The future goals of this research vary from chemistry advances to medical applications. From a fundamental chemistry standpoint, the ability of a Pd(IV) complex to capture fluoride and then behave as an electrophilic fluorination reagent is not well understood. Can other complexes, palladium-based or otherwise, act in a similar manner? A series of tuned electrophilic fluorination reagents, each with slightly varying reactivity would be beneficial in order to address the diverse substrate scope that is inherent in ^{18}F-PET chemistry. Specifically, a fluorination reaction that proceeds in the presence of tertiary amines, and a reaction that can fluorinate arenes with ortho substitution to the eventual place of fluorine would drastically widen substrate scope and utility.

Since our power to predict radiolabeled molecules that will become useful PET tracers is limited, a means to rapidly access and assess small molecules for use as imaging agents is needed. Given current abilities, turning **2.43** and **2.44** into useful PET tracers would require a significant amount of time and effort. We would need to maintain binding interactions with the target while modifying the structure to minimize nonspecific binding. Each derivative would need to be synthesized, evaluated *in vitro*, radiolabeled, and imaged, which is impractical. More modular chemistry and screening methods may be used to overcome this obstacle.

Finally, the chemistry and radiochemistry is at a point where it can be disseminated throughout the PET imaging community in order to reach its full potential. The procedures to produce ^{18}F-labeled molecules are reliable and sufficient for use in non-human primate imaging. Human imaging is well within reach and where this translation research will have its greatest societal impact.

4. EXPERIMENTAL FOR CHAPTERS 1–3[76]

76. I thank Dr. Eunsung Lee for performing experiments in the following chapter including the development and synthesis of **2.2** (see note at the beginning of Chapter 2).

4.1 Materials and Methods

All air- and moisture-insensitive reactions were carried out under an ambient atmosphere, magnetically stirred, and monitored by thin layer chromatography (TLC) using EMD TLC plates pre-coated with 250 μm thickness silica gel 60 F254 plates and visualized by fluorescence quenching under UV light. Flash chromatography was performed on Dynamic Adsorbents Silica Gel 40–63 μm particle size using a forced flow of eluent at 0.3–0.5 bar pressure. All air- and moisture-sensitive manipulations were performed using oven-dried glassware, including standard Schlenk and glovebox techniques under an atmosphere of nitrogen. Methylene chloride was purged with nitrogen, dried by passage through activated alumina, and stored over 3Å molecular sieves.[77] Benzene, benzene-d_6, diethyl ether, toluene, pentane, dioxane, and THF were distilled from deep purple sodium benzophenone ketyl. Methylene chloride-d_2 was dried over CaH_2 and vacuum-distilled. Acetonitrile and acetonitrile-d_3 were dried over P_2O_5 and vacuum-distilled. Pyridine was dried over CaH_2 and distilled. DMSO was distilled from sodium triphenylmethanide and stored over 3Å sieves.[78] Acetone was distilled over B_2O_3. MeOH was degassed at –30 ºC under dynamic vacuum (10^{-4} Torr) for one hour and stored over 3Å sieves. Anhydrous DMF and dioxane bottles equipped with a SureSeal™ were purchased from Sigma Aldrich®. 18-Crown-6 was sublimed. KF was ground finely and dried at 200 ºC under dynamic vacuum (10^{-4} Torr) before use. Chloroform-d_1, D_2O, $Pd(OAc)_2$, AgOAc, and all other chemicals were used as received. All deutrated solvents were purchased from Cambridge Isotope Laboratories. $Pd(OAc)_2$, AgOAc, KBH_4, and 18-crown-6 were purchased from Strem Chemicals. Benzo[*h*]quinoline was purchased from TCI. (Diacetoxyiodo)benzene, potassium fluoride, 4-cyanopyridine, α-tetralone, pyrrolidine, *p*-toluenesulfonic acid, *p*-methoxybenzenesulfonamide, and F-TEDA-BF_4 (Selectfluor®) were purchased from Sigma-Aldrich®. Pyrazole, TMSOTf, and trifluoroacetic acid were purchased from Oakwood Products. Soda lime glass bottles were purchased from Qorpak®. NMR spectra were recorded on either a Varian Unity/Inova 600 spectrometer operating at 600 MHz for ^1H

---

77. Pangborn, A. B.; Giardello, M. A.; Grubbs, R. H.; Rosen, R. K.; Timmers, F. J. *Organometallics* **1996**, *15*, 1518.

78. Matthews, W. S.; Bares, J. E.; Bartmess, J. E.; Bordwell, F. G.; Cornforth, F. J.; Drucker, G. E.; Margolin, Z.; McCallum, R. J.; McCollum, G. J.; Vanier, N. R. *J. Am. Chem. Soc.* **1975**, *97*, 7006.

acquisitions, a Varian Unity/Inova 500 spectrometer operating at 500 MHz and 125 MHz for ^{1}H and ^{13}C acquisitions, respectively, a Varian Mercury 400 spectrometer operating at 375 MHz and 101 MHz for ^{19}F and ^{13}C acquisitions, respectively, or a Varian Mercury 300 spectrometer operating at 100 MHz for ^{11}B acquisitions. Chemical shifts were referenced to the residual proton solvent peaks (^{1}H: $CDCl_3$, δ 7.26; C_6D_6, δ 7.16; CD_2Cl_2, δ 5.32; D_2O, δ 4.79; $(CD_3)_2SO$, δ 2.50; CD_3CN, δ 1.94), solvent ^{13}C signals ($CDCl_3$, δ 77.16; C_6D_6, δ 128.06; CD_2Cl_2, δ 53.84; CD_3CN, δ 1.32, $(CD_3)_2SO$, δ 39.52),[79] dissolved or external neat PhF (^{19}F, δ –113.15 relative to $CFCl_3$) or dissolved 3-nitrofluorobenzene (–112.0 ppm). Signals are listed in ppm, and multiplicity identified as s = singlet, br = broad, d = doublet, t = triplet, q = quartet, quin = quintet, sep = septet, m = multiplet; coupling constants in Hz; integration. Concentration under reduced pressure was performed by rotary evaporation at 25–30 ºC at appropriate pressure. Purified compounds were further dried under high vacuum (0.01–0.05 Torr). Yields refer to purified and spectroscopically pure compounds. Elemental analysis was performed by Robertson Microlit Laboratories.

---

79. Fulmer, G. R.; Miller, A. J. M.; Sherden, N. H.; Gottlieb, H. E.; Nudelman, A.; Stoltz, B. M.; Bercaw, J. E.; Goldberg, K. I. *Organometallics* **2010**, *29*, 2176.

4.2 Experimental Procedures and Compound Characterization

Synthesis of Pd(IV) complex 2.1

Benzo[*h*]quinolinyl palladium acetate dimer (2.7)

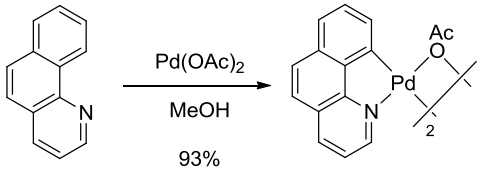

2.7

Based on a reported procedure:[80] To benzo[*h*]quinoline (1.79 g, 10.0 mmol, 1.00 equiv) in MeOH (100 mL) in a round-bottom flask open to air at 23 ºC was added $Pd(OAc)_2$ (2.25 g, 10.0 mmol, 1.00 equiv). After stirring for 17 hours at 23 ºC, the solid was collected by filtration and washed with MeOH (50 mL) and diethyl ether (50 mL) to afford 3.19 g of the title compound as a yellow solid (93% yield).

NMR Spectroscopy: ^{1}H NMR (500 MHz, $CDCl_3$, 23 ºC, δ): 7.80 (dd, J = 5.5, 1.5 Hz, 1H), 7.43 (dd, J = 8.0, 1.5 Hz, 1H), 7.24–7.18 (m, 3H), 7.08 (dd, J = 7.0, 1.5 Hz, 1H), 6.97 (d, J = 9.0 Hz, 1H), 6.46 (dd, J = 7.5, 5.0 Hz, 1H), 2.38 (s, 3H). ^{13}C NMR (125 MHz, $CDCl_3$, 23 ºC, δ): 182.3, 152.9, 148.6, 148.5, 139.7, 135.0, 132.2, 128.7, 127.6, 127.4, 124.7, 122.6, 121.8, 119.5, 24.9. These spectroscopic data correspond to previously reported data.

Potassium tetra(1*H*-pyrazol-1-yl)borate (2.8)

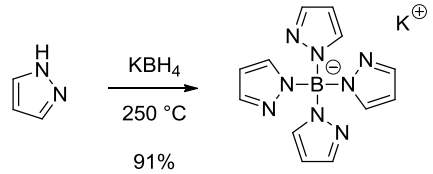

2.8

80. Dick, A. R.; Hull, K. L.; Sanford, M. S. *J. Am. Chem. Soc.* **2004**, *126*, 2300.

Based on a reported procedure:[81] As solids, KBH_4 (7.00 g, 0.130 mol, 1.00 equiv) and pyrazole (44.2 g, 0.649 mol, 5.00 equiv) were combined in a round-bottom flask equipped with a reflux condenser under a N_2 atmosphere. This mixture was heated at 250 ºC for 16 hours. The melt was then cooled to 23 °C. The residue was dissolved in methanol (200 mL). The solution was added to diethyl ether (600 mL). A precipitate formed that was isolated by filtration. The precipitate was washed with additional diethyl ether (2 × 100 mL), affording 37.6 g of the title compound as a colorless solid (91% yield).

Melting Point: 248–249 ºC. NMR Spectroscopy: ^{1}H NMR (600 MHz, D_2O, 23 ºC, δ): 7.49 (s, 4H), 7.19 (d, J = 2.0 Hz, 4H), 6.14 (s, 4H). ^{13}C NMR (125 MHz, D_2O, 23 ºC, δ): 138.9, 132.8, 102.4. ^{11}B NMR (100 MHz, D_2O, 23 ºC, δ): –1.3. Mass Spectrometry: LRMS-FIA (m/z): calcd for $C_{12}H_{12}BN_8$ $[M - K]^-$, 279.1; found, 279.1. These spectroscopic data correspond to previously reported data (*81*).

Benzo[*h*]quinolinyl (tetrapyrazolylborate)palladium (2.9)

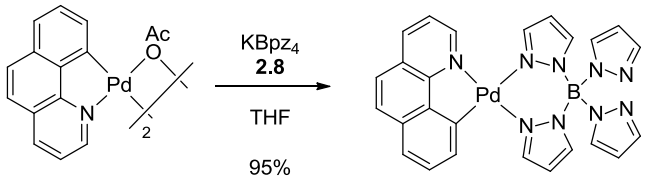

2.7 **2.9**

Based on a reported procedure:[82] To benzo[*h*]quinolinyl palladium acetate dimer (**2.7**) (2.11 g, 3.07 mmol, 1.00 equiv) in a round-bottom flask open to air in THF (120 mL) was added potassium tetra(1*H*-pyrazol-1-yl)borate ($KBpz_4$) (**2.8**) (1.95 g, 6.13 mmol, 2.00 equiv) in one portion at 23 ºC. The solution was stirred at 23 °C for 12 hours and then concentrated *in vacuo*. The residue was dissolved in CH_2Cl_2 (200 mL), filtered through Celite eluting with additional CH_2Cl_2 (50 mL), and the solution was concentrated *in vacuo*. The residual solid was triturated with diethyl ether (100 mL), collected by filtration, and subsequently dried to afford 3.28 g of the title compound as a light yellow solid (95%).

NMR Spectroscopy: ^{1}H NMR (400 MHz, $CDCl_3$, 23 ºC, δ): 8.50 (d, J = 4.8 Hz, 1H), 8.19 (d, J = 8.6 Hz,

---

81. Niedenzu, K.; Niedenzu, P. M. *Inorg. Chem.* **1984**, *23*, 3713.

82. Onishi, M.; Yushichiro, O.; Sugimura, K.; Hiraki, K. *Chem. Lett.* **1976**, 955.

1H), 7.95 (br s, 1H), 7.89 (br s, 1H), 7.75 (br s, 1H), 7.69 (d, *J* = 8.6 Hz, 1H), 7.66 (br s, 1H), 7.60 (br s, 1H), 7.57 (d, *J* = 7.6 Hz, 1H), 7.48 (d, *J* = 8.6 Hz, 1H), 7.43 (dd, *J* = 7.6, 7.6 Hz, 1H), 7.36 (dd, *J* = 7.0, 5.7 Hz, 1H), 7.30 (d, *J* = 7.6 Hz, 1H), 6.92 (br s, 1H), 6.43 (br s, 2H), 6.29 (br s, 1H), 6.01 (br s, 1H). ^{1}H NMR (400 MHz, $CDCl_3$, –25 ºC, δ): 8.46 (d, *J* = 5.1 Hz, 1H), 8.10 (d, *J* = 8.1 Hz, 1H), 7.94 (s, 1H), 7.89 (s, 1H), 7.75 (s, 1H), 7.67 (d, *J* = 2.6 Hz, 1H), 7.60 (d, *J* = 9.0, 1H), 7.55–7.52 (m, 3H), 7.43 (dd, *J* = 7.5, 7.5 Hz, 1H), 7.38 (d, *J* = 6.5 Hz, 1H), 7.37 (s, 1H), 7.33–7.29 (m, 2H), 6.83 (d, *J* = 2.1, 1H), 6.44 (d, *J* = 1.7, 2H), 6.30 (dd, *J* = 1.9, 1.9 Hz, 1H), 6.05 (s, 1H). ^{13}C NMR (125 MHz, $CDCl_3$, 23 ºC, δ): 155.5, 152.4, 148.2, 144.0 (br), 142.4 (br), 141.9 (br), 141.7, 141.1 (br), 137.5, 137.4 (br), 137.0 (br), 135.7 (br), 134.1 (br), 133.4, 132.1, 129.5, 128.6, 126.9, 123.1, 121.1, 106.3 (br), 106.2 (br), 105.3 (br). ^{13}C NMR (101 MHz, $CDCl_3$, –25 ºC, δ): 155.0, 152.3, 148.0, 144.0, 142.4, 142.1, 141.3, 141.3, 137.5, 137.1, 136.7, 135.7, 134.0, 133.1, 131.9, 129.1, 128.5, 126.6, 123.1, 123.1, 121.1, 106.5, 106.3, 105.5, 105.2. Anal: calcd for $C_{25}H_{20}BN_9Pd$: C, 53.27; H, 3.58; N, 22.36; found: C, 53.09; H, 3.64; N, 22.17.

1,1'-(phenyl-λ^3-iodanediyl)bis(4-cyanopyridinium) bis(trifluoromethanesulfonate) (2.10)

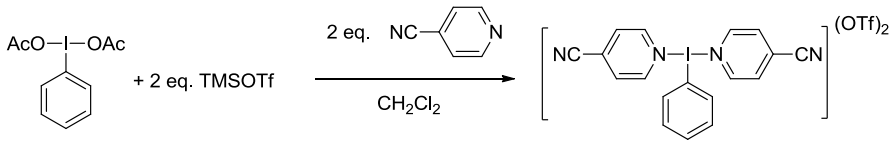

2.10

Based on a reported procedure:[83] All manipulations were carried out in a dry box under a N_2 atmosphere. To (diacetoxyiodo)benzene (2.00 g, 6.21 mmol, 1.00 equiv) dissolved in CH_2Cl_2 (100 mL) in a round-bottom flask was added TMSOTf (2.83 g, 12.7 mmol, 2.00 equiv) dropwise over 1 minute at 23 °C. 4-Cyanopyridine (1.29 g, 12.7 mmol, 2.00 equiv) in CH_2Cl_2 (10 mL) was added to the solution dropwise over 5 minutes to give a colorless precipitate and the mixture was stirred for 30 min vigorously at 23 °C. The solid was filtered off and washed with CH_2Cl_2 (3 × 10 mL) and subsequently dried under vacuum to afford 3.80 g of the title compound as a colorless solid (86%).

---

83. Weiss, R.; Seubert, J. *Angew. Chem., Int. Ed. Engl.* **1994**, *33*, 891.

NMR Spectroscopy: ^{1}H NMR (500 MHz, CD_3CN, 23 ºC, δ): 9.21 (d, J = 5.3 Hz, 4H), 8.74 (d, J = 7.5 Hz, 2H), 8.11 (d, J = 6.4 Hz, 4H), 7.87 (t, J = 7.5 Hz, 1H), 7.71 (dd, J = 8.0, 8.0 Hz, 2H). ^{13}C NMR (125 MHz, CD_3CN, 23 ºC, δ): 150.1, 137.4, 136.8, 134.7, 132.4, 128.8, 124.0, 121.9 (q, J = 319 Hz, triflate), 115.4. ^{19}F NMR (375 MHz, CD_3CN, 23 ºC, δ): –77.5. Anal: calcd for $C_{20}H_{13}F_6IN_4O_6S_2$: C, 33.82; H, 1.84; N, 7.89; found: C, 33.63; H, 1.67; N, 7.68.

Benzo[*h*]quinolinyl (tetrapyrazolylborate) Pd(IV) 4-cyanopyridine trifluoromethanesulfonate (2.11)

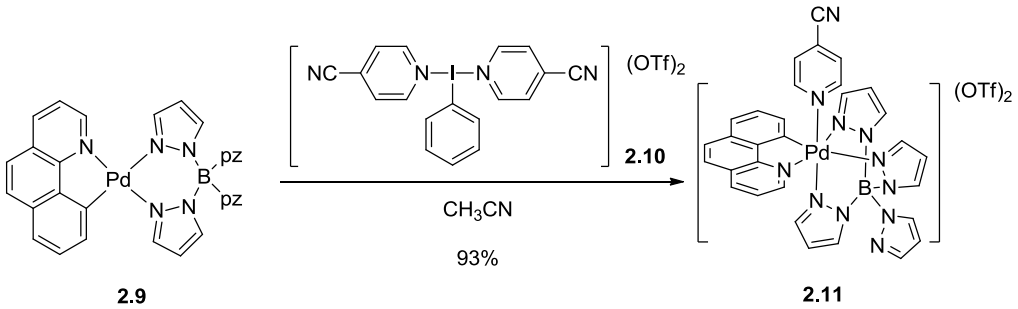

2.9 **2.11**

All manipulations were carried out in a dry box under a N_2 atmosphere. To benzo[*h*]quinolinyl (tetrapyrazolylborate)palladium (**2.9**) (3.00 g, 5.32 mmol, 1.00 equiv) in a round-bottom flask in CH_3CN (50 mL) at 23 ºC was added 1,1'-(phenyl-λ^3-iodanediyl)bis(4-cyanopyridinium) bis(trifluoromethanesulfonate) (**2.10**) (3.89 g, 5.48 mmol, 1.03 equiv). After stirring for 30 minutes, the reaction mixture was concentrated *in vacuo*. The resulting residue was triturated with THF (3 × 30 mL) and collected by filtration as a light brown solid. The solid was re-dissolved in CH_3CN (10 mL), and the solution was concentrated *in vacuo* to afford 4.80 g of the title compound as a brown solid (93%).

NMR Spectroscopy: ^{1}H NMR (500 MHz, CD_3CN, 23 ºC, δ): 9.10 (d, J = 8.6 Hz, 1H), 8.97 (s, 1H), 8.97 (d, J = 9.6 Hz, 1H), 8.49 (d, J = 8.5 Hz, 1H), 8.41 (d, J = 9.6 Hz, 1H), 8.39 (d, J = 7.5 Hz, 1H), 8.35 (s, 1H), 8.26 (d, J = 2.1 Hz, 1H), 8.09 (s, 1H), 8.06 (d, J = 2.1 Hz, 1H), 8.05 (s, 1H), 7.97 (dd, J = 7.0, 7.0 Hz, 1H), 7.85 (dd, J = 8.0, 8.0 Hz, 1H), 7.77–7.70 (m, 5H), 7.43 (d, J = 2.3 Hz, 1H), 6.86 (s, 1H), 6.82 (dd, J = 2.7, 2.7 Hz, 1H), 6.80 (s, 1H), 6.21 (d, J = 2.1 Hz, 1H), 6.10 (dd, J = 2.1, 2.1 Hz, 1H). ^{13}C NMR (125 MHz, CD_3CN, 23 ºC): 169.5, 153.5, 152.3, 148.2, 144.5, 144.4, 144.1, 144.0, 142.7, 140.8, 140.4, 140.0, 139.8, 137.7, 134.0, 133.7, 133.5, 132.0, 131.7, 130.4, 130.3, 128.7, 127.7, 127.0, 121.9 (q, J = 319 Hz, triflate),

115.1, 112.2, 110.5, 110.5, 110.4, 109.6. ^{19}F NMR (375 MHz, CD_3CN, 23 ºC, δ): –77.5. Anal: calcd for $C_{33}H_{24}BF_6N_{11}O_6PdS_2$: C, 41.03; H, 2.50; N, 15.95; found: C, 40.78; H, 2.47; N, 15.67.

Benzo[*h*]quinolinyl (tetrapyrazolylborate) Pd(IV) 4-picoline trifluoromethanesulfonate (2.1)

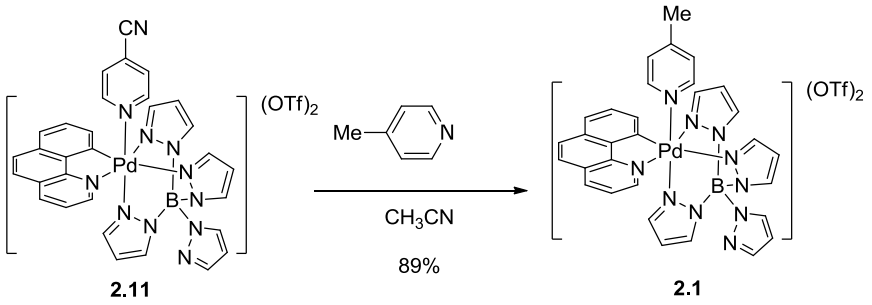

All manipulations were carried out in a dry box under a N_2 atmosphere. To benzo[*h*]quinolinyl (tetrapyrazolylborate) Pd(IV) 4-cyanopyridine trifluoromethanesulfonate (**2.11**) (5.00 g, 5.16 mmol, 1.00 equiv) in a round-bottom flask in CH_3CN (15 mL) at 23 ºC was added 4-picoline (769 mg, 8.26 mmol, 1.60 equiv). After stirring for 2 minutes the reaction mixture was added dropwise over 5 minutes to 200 mL of diethyl ether (200 mL) while stirring vigorously at 23 ºC. The resulting precipitate was collected by filtration as a light brown solid. The solid was re-dissolved in CH_3CN (10 mL), and the solution was concentrated *in vacuo* to afford 4.40 g of the title compound as a brown solid (89%).

NMR Spectroscopy: ^{1}H NMR (500 MHz, CD_3CN, 23 ºC, δ): 9.09 (d, J = 8.5 Hz, 1H), 8.97 (d, J = 8.5 Hz, 1H), 8.97 (s, 1H), 8.47 (d, J = 9.6 Hz, 1H), 8.40 (d, J = 8.5 Hz, 1H), 8.38 (d, J = 8.6 Hz, 1H), 8.27 (d, J = 9.6 Hz, 2H), 8.08 (s, 1H), 8.05 (d, J = 2.1 Hz, 1H), 7.98–7.95 (m, 2H), 7.84 (dd, J = 8.1, 8.1 Hz, 1H), 7.73 (d, J = 8.5 Hz, 1H), 7.40 (d, J = 3.2 Hz, 1H), 7.32 (d, J = 7.5 Hz, 2H), 7.20 (d, J = 6.4 Hz, 2H), 6.85 (dd, J = 2.1, 2.1 Hz, 1H), 6.81 (s, 2H), 6.20 (d, J = 2.1 Hz, 1H), 6.09 (dd, J = 2.1, 2.1 Hz, 1H), 2.38 (s, 3H). ^{13}C NMR (125 MHz, CD_3CN, 23 ºC, δ): 169.2, 158.7, 152.0, 151.1, 148.5, 144.4, 144.3, 144.1, 143.9, 142.6, 140.6, 140.2, 139.9, 139.6, 137.7, 134.3, 133.5, 133.4, 131.7, 130.4, 130.2, 130.0, 128.6, 126.9, 121.9 (q, J = 319 Hz, triflate), 112.0, 110.3, 110.3, 109.6, 21.2. ^{19}F NMR (375 MHz, CD_3CN, 23 ºC, δ): –77.5. Anal: calcd for $C_{33}H_{27}BF_6N_{10}O_6PdS_2$: C, 41.50; H, 2.85; N, 14.67; found: C, 41.45; H, 2.72; N, 14.41. X-ray quality crystals were obtained from 1.0 mL CH_3CN solution that contained 20 mg of the title compound

layered slowly with 0.5 mL diethyl ether at 23 ºC.

Synthesis of Pd(IV) fluoride complex 2.2

Benzo[*h*]quinolinyl (tetrapyrazolylborate) Pd(IV) fluoride trifluoromethanesulfonate (2.2)

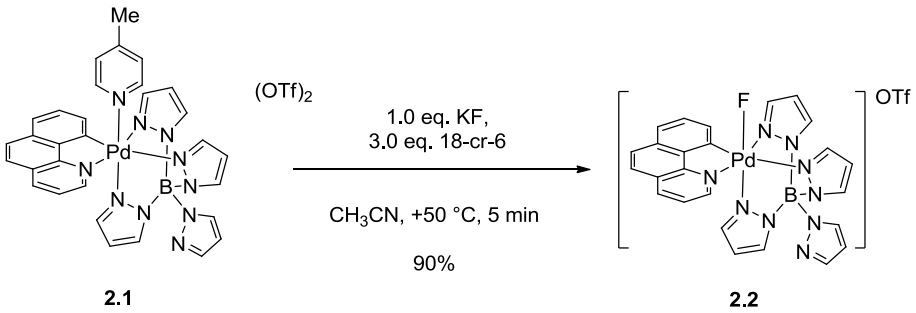

In a glove box, to benzo[*h*]quinolinyl (tetrapyrazolylborate) Pd(IV) 4-picoline trifluoromethanesulfonate (**2.1**) (284 mg, 0.297 mmol, 1.00 equiv) dissolved in CH_3CN (15 mL) in a soda lime glass bottle was added KF (17.3 mg, 0.297 mmol, 1.00 equiv) and 18-crown-6 (235 mg, 0.891 mmol, 3.00 equiv) in one portion at 23 ºC. The bottle was sealed, taken out of the glove box, sonicated at 23 °C for 5 minutes, immersed in an oil bath heated at 50 °C for 5 minutes while vigorously stirring the suspension. CH_3CN (10 mL) was added to the solution, and the solution was filtered through Celite, eluting with additional CH_3CN (10 mL). The filtrate was concentrated *in vacuo*. The residue was triturated with THF (3 × 15 mL) and subsequently dried *in vacuo* to afford 195 mg of the title compound as an orange solid (90%).

NMR Spectroscopy: ^{1}H NMR (500 MHz, CD_3CN, 23 ºC, δ): 9.01 (d, J = 5.3 Hz, 1H), 8.96 (d, J = 8.5 Hz, 1H), 8.79 (d, J = 3.2 Hz, 1H), 8.32 (s, 2H), 8.29 (d, J = 9.6 Hz, 1H), 8.27 (d, J = 2.1 Hz, 1H), 8.23 (d, J = 8.6 Hz, 1H), 8.21 (d, J = 8.6 Hz, 1H), 8.16 (s, 1H), 7.97 (d, J = 5.4 Hz, 1H), 7.96 (d, J = 6.4 Hz, 1H), 7.83 (dd, J = 8.1, 8.1 Hz, 1H), 7.62 (d, J = 8.5 Hz, 1H), 6.79–6.72 (m, 4H), 6.54 (d, J = 2.1 Hz, 1H), 6.11 (s, 1H). ^{13}C NMR (125 MHz, DMSO-d_6, 23 ºC, δ): 165.0, 149.4, 149.2, 149.4, 149.2, 143.4, 143.0, 142.7, 142.7, 142.2, 138.5, 137.6, 137.6, 137.0, 136.7, 134.8, 132.1, 130.3, 129.6, 127.6, 127.6, 126.4, 120.7 (q, J = 323 Hz, triflate), 109.9, 109.6, 108.5, 108.5. ^{19}F NMR (375 MHz, CD_3CN, 23 ºC, δ): –77.5 (s), –319.5 (s). Anal: calcd for $C_{26}H_{20}BF_4N_9O_3PdS$: C, 42.67; H, 2.75; N, 17.23; found: C, 42.95; H, 2.95; N, 17.04. X-ray quality crystals were obtained from 4 mL CH_3CN solution that contained 20.0 mg of the title compound

slowly layered with 3.0 mL diethyl ether at 23 ºC.

Thermal stability of **2.2**: **2.2** was placed in a vial and heated for 24 hours at 100 ºC under dynamic vacuum (10^{-4} Torr). The solid was analyzed by ^{1}H and ^{19}F NMR spectroscopy, and showed no decomposition.

Tolerance of **2.2** toward water: 2.4 mg of **2.2** (3.3 μmol) and THF (2.0 μL) (internal standard) were dissolved in CD_3CN (0.55 mL) in an NMR tube. D_2O (61 μL) was added to the solution. The solution was kept at +23 ºC for 3 hours and monitored by ^{1}H and ^{19}F NMR spectroscopy, which showed no decomposition (Figure 4.1).

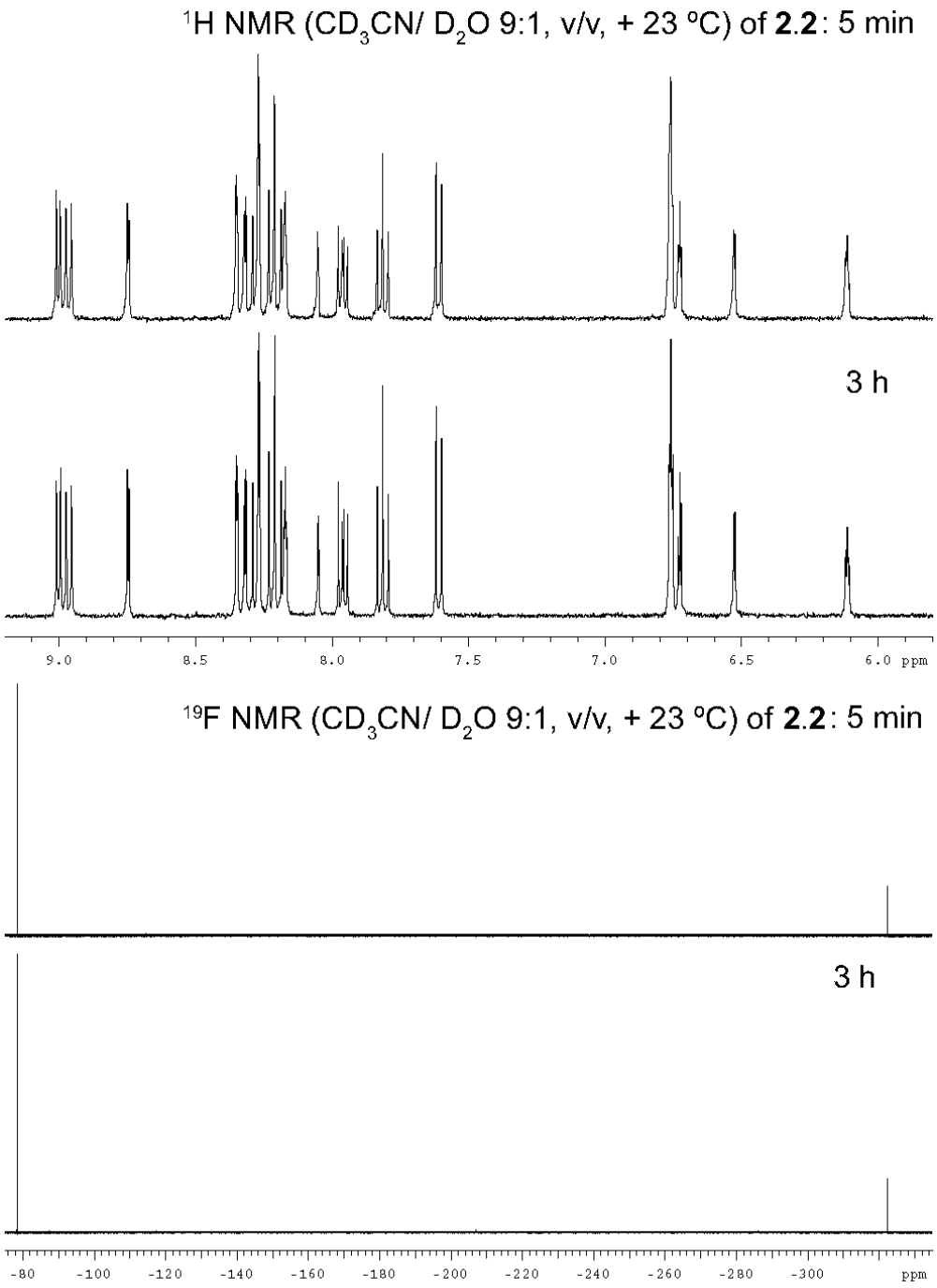

Figure 4.1. NMR Spectra of **2.2** in 10% aqueous acetonitrile solution.

Synthesis of aryl palladium complexes (2.3–2.4 and 2.16–2.18)

Benzo[*h*]quinolinyl palladium chloro dimer (2.12)

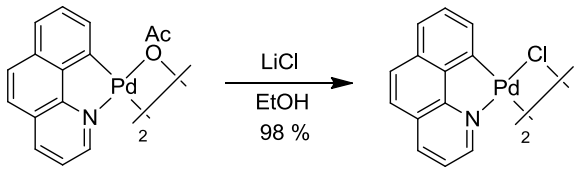

2.7 **2.12**

Based on a reported procedure:[84] To benzo[*h*]quinolinyl palladium acetate dimer (**2.7**) (4.27 g, 12.4 mmol, 1.00 equiv) in a round-bottom flask open to air in EtOH (100 mL) at 0 ºC was added lithium chloride (10.5 g, 24.8 mmol, 20.0 equiv). The reaction mixture was warmed to 23 ºC and stirred for 1.0 hours. The reaction mixture was filtered and the filter cake was washed with water (3 × 100 mL), MeOH (2 × 100 mL), and diethyl ether (100 mL) to afford 3.89 g of the title compound as a pale yellow solid (98% yield).

NMR Spectroscopy: ^{1}H NMR (500 MHz, DMSO-d_6, 23 ºC, δ): 9.44 (d, J = 4.5 Hz, 1H), 8.72 (br, 0.25H), 8.67 (d, J = 7.5 Hz, 1H), 8.61 (br, 0.25H), 8.22 (d, J = 7.0 Hz, 1H), 7.91 (d, J = 9.0 Hz, 1H), 7.86–7.74 (m, 3H), 7.73 (br, 0.25H), 7.60 (br, 0.25H), 7.53 (dd, J = 7.5, 7.0 Hz 1H), 7.38 (br, 0.25H); ^{13}C NMR (125 MHz, DMSO-d_6, 23 ºC, δ): 153.9, 152.2, 150.7, 150.6, 148.0, 141.7, 139.9, 134.4, 130.8, 129.6, 129.4, 127.5, 125.1, 124.4, 123.0, 122.9. Note: The complicated ^{1}H and ^{13}C NMR spectra are probably due to a mixture of the title compound and solvent adduct in DMSO-d_6. The title compound was not soluble in non-coordinating solvents.

[{(4-Methoxyphenyl)sulfonyl}imino]phenyliodinane (2.13)

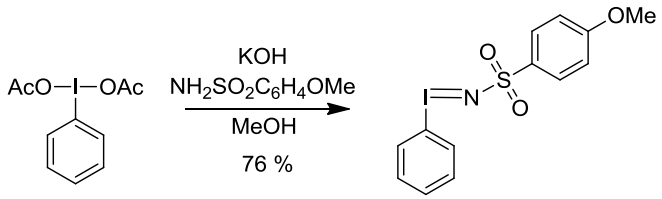

2.13

84. Hartwell, G. E.; Lawrence, R. V.; Smas, M. J. *J. Chem. Soc. D Chem. Comm.* **1970**, 912.

Based on a reported procedure:[85]: To *p*-methoxybenzenesulfonamide (5.00 g, 26.7 mmol, 1.00 equiv) in a round-bottom flask open to air in methanol (100 mL) at 23 ºC was added potassium hydroxide (3.75 g, 66.8 mmol, 2.50 equiv). The reaction mixture was stirred at 23 ºC for 10 minutes and subsequently cooled to 0 ºC. To the reaction mixture at 0 ºC was added iodobenzene diacetate (8.60 g, 26.7 mmol, 1.00 equiv). The reaction mixture was stirred at 0 ºC for 10 minutes and further stirred at 23 ºC for 2.0 hours. The reaction mixture was poured into cold water (700 mL) and kept at 0 ºC for 4 hours. The suspension was filtered and the filter cake was washed with water (2 × 200 mL) and methanol (2 × 200 mL) to afford 7.90 g of the title compound as a colorless solid (76% yield).

NMR Spectroscopy: ^{1}H NMR (500 MHz, DMSO-d_6, 23 ºC, δ): 7.70 (d, J = 7.5 Hz, 2H), 7.49–7.44 (m, 3H), 7.32–7.28 (m, 2H), 6.78 (d, J = 8.5 Hz, 2H), 3.74 (s, 3H). ^{13}C NMR (125 MHz, DMSO-d_6, 23 ºC, δ): 160.6, 136.9, 133.2, 130.5, 130.2, 128.0, 117.0, 113.4, 55.4. These spectroscopic data correspond to previously reported data.[86]

Chloro palladium complex 2.14

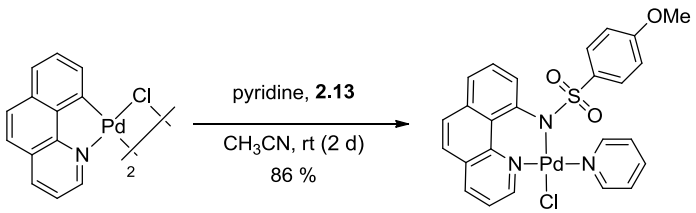

2.12 **2.14**

Based on a reported procedure:[87] In a glove box under a N_2 atmosphere, to chloropalladium dimer **2.12** (6.00 g, 18.7 mmol, 1.00 equiv) in a round-bottom flask in CH_3CN (100 mL) at 23 ºC was added pyridine (6.06 mL, 75.0 mmol, 4.00 equiv) and [{(4-methoxyphenyl)sulfonyl}imino]phenyliodinane (**2.13**) (10.9 g, 28.1 mmol, 1.50 equiv). The reaction mixture was stirred at 23 ºC for 48 hours and subsequently taken out

85. Muller, P.; Baud, C.; Jacquier, Y. *Can. J. Chem.* **1998**, *76*, 738.

86. Taylor, S.; Gullick, J.; McMorn, P.; Bethell, D.; Page, P. C. B.; Hancock, F. E.; King, F.; Hutchings, G. J. *J.Chem. Soc. Perk. Trans. 2* **2001**, 1714.

87. Dick, A. R.; Remy, M. S.; Kampf, J. W.; Sanford, M. S. *Organometallics* **2007**, *26*, 1365.

of the glove box. The reaction mixture was filtered and the filter cake was washed with diethyl ether (3 × 30 mL) to afford 9.70 g of the title compound as a yellow solid (86% yield).

NMR Spectroscopy: ^{1}H NMR (500 MHz, $CDCl_3$, 23 ºC, δ): 9.21 (dd, *J* = 5.2, 1.5 Hz, 1H), 9.01–8.99 (m, 2H), 8.08 (dd, *J* = 7.9, 1.8 Hz, 1H), 7.88–7.73 (m, 5H), 7.47–7.43 (m, 3H), 7.35 (dd, *J* = 7.9, 5.5 Hz, 1H), 7.11–7.08 (m, 2H), 6.19–6.15 (m, 2H), 3.56 (s, 3H); 13C NMR (125 MHz, $CDCl_3$, 23 ºC, δ): 160.9, 154.2, 152.6, 141.9, 139.0, 138.6, 138.4, 136.0, 134.3, 130.4, 129.8, 128.4, 128.1, 127.7, 126.8, 125.6, 125.0, 124.2, 122.1, 112.4, 55.4.

Acetato palladium complex 2.15

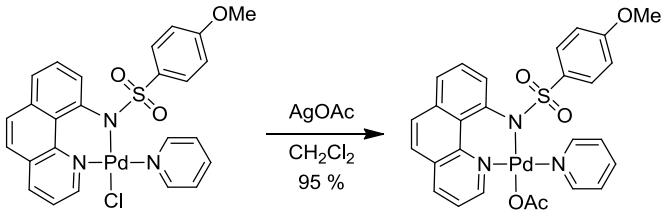

2.14 **2.15**

To chloro palladium complex **2.14** (5.00 g, 8.34 mmol, 1.00 equiv) in a round-bottom flask fitted with a reflux condenser open to air in CH_2Cl_2 (300 mL) at 23 ºC was added AgOAc (4.87 g, 29.2 mmol, 3.50 equiv). The suspension was stirred at 40 ºC for 3 hours. After cooling to 23 ºC, the suspension was filtered through a plug of Celite, eluting with additional CH_2Cl_2 (50 mL). The filtrate was concentrated *in vacuo* and the residue was triturated with diethyl ether (100 mL). The solid was collected by filtration and washed with diethyl ether (2 × 50 mL) to afford 5.07 g of the title compound as a yellow solid (95% yield).

NMR Spectroscopy: ^{1}H NMR (500 MHz, $CDCl_3$, 23 ºC, δ): 8.93 (d, *J* = 5.5 Hz, 2H), 8.70 (d, *J* = 5.5 Hz, 1H), 8.01 (d, *J* = 7.9 Hz, 1H), 7.83 (d, *J* = 6.7 Hz, 1H), 7.80 (t, *J* = 7.6 Hz, 1H), 7.74–7.68 (m, 3H), 7.41–7.36 (m, 3H), 7.27 (dd, *J* = 7.6, 5.2 Hz, 1H), 7.15 (d, *J* = 8.5 Hz, 2H), 6.13 (d, *J* = 8.5 Hz, 2H), 3.48 (s, 3H), 1.78 (s, 3H); ^{13}C NMR (125 MHz, $CDCl_3$, 23 ºC, δ): 177.4, 160.7, 151.6, 151.2, 141.7, 139.0, 138.4, 138.2, 135.8, 134.4, 130.1, 129.9, 128.9, 128.1, 127.3, 126.7, 125.5, 124.8, 124.0, 121.8, 112.3, 55.2, 23.8. Anal: calcd for $C_{27}H_{23}N_3O_5PdS$: C, 53.34; H, 3.81; N, 6.91; found: C, 53.31; H, 3.69; N, 6.89.

Aryl palladium complex 2.3

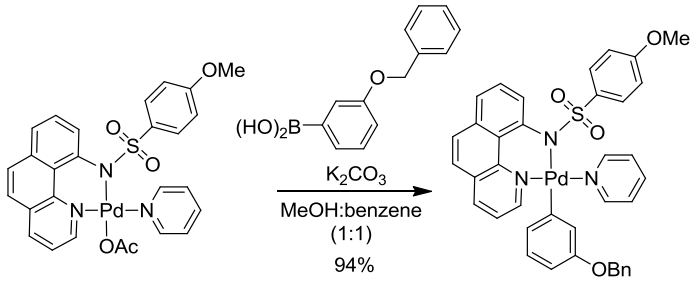

2.15 **2.3**

To acetato palladium complex **2.15** (0.550 g, 0.996 mmol, 1.00 equiv) in a round-bottom flask open to air in MeOH (10 mL) and benzene (10 mL) at 23 ºC was added (3-benzyloxyphenyl)boronic acid (0.268 g, 1.18 mmol, 1.30 equiv) and K_2CO_3 (0.188 g, 1.36 mmol, 1.50 equiv). The reaction mixture was stirred at 23 ºC for 10 hours and then concentrated *in vacuo*. To the solid residue was added CH_2Cl_2 (80 mL) and the solution was filtered through Celite, eluting with additional CH_2Cl_2 (30 mL). The solution was washed with water (3 × 20 mL), dried with Na_2SO_4, and concentrated *in vacuo*. The residue was recrystallized by dissolving the solid in CH_2Cl_2 (10 mL) and layering with pentane (100 mL). After 3 hours, the solid was collected by filtration to afford 624 mg of the title compound as a yellow solid (94% yield).

NMR Spectroscopy: ^{1}H NMR (500 MHz, $CDCl_3$, 23 ºC, δ): 8.96 (d, *J* = 4.9 Hz, 2H), 8.30 (dd, *J* = 5.5, 1.2 Hz, 1H), 7.90 (d, *J* = 7.9 Hz, 1H), 7.69–7.57 (m, 5H), 7.32 (d, *J* = 8.5 Hz, 1H), 7.27–7.20 (m, 7H), 7.09 (d, *J* = 8.5 Hz, 2H), 6.95 (dd, *J* = 7.3, 5.5 Hz, 1H), 6.69 (t, *J* = 7.6 Hz, 1H), 6.54 (d, *J* = 1.8 Hz, 1H), 6.50 (d, *J* = 7.3 Hz, 1H), 6.44 (dd, *J* = 7.9, 1.8 Hz, 1H), 6.14 (d, *J* = 8.5 Hz, 2H), 4.85 (d, *J* = 12.2 Hz, 1H), 4.79 (d, *J* = 12.2 Hz, 1H), 3.49 (s, 3H); ^{13}C NMR (125 MHz, $CDCl_3$, 23 ºC, δ): 160.1, 158.1, 156.4, 153.8, 153.2, 144.7, 143.4, 137.6, 137.5, 136.2, 136.1, 130.0, 129.8, 128.5, 127.7, 127.7, 127.6, 127.4, 127.3, 127.1, 127.1, 124.8, 124.1, 123.5, 121.1, 120.7, 112.2, 109.9, 69.5, 55.2. Anal: calcd for $C_{38}H_{31}N_3O_4PdS$: C, 62.34; H, 4.27; N, 5.74; found: C, 62.42; H, 4.19; N, 5.72. X-ray quality crystals were obtained from the saturated MeOH solution of the title compound at 23 ºC.

Aryl palladium complex 2.4

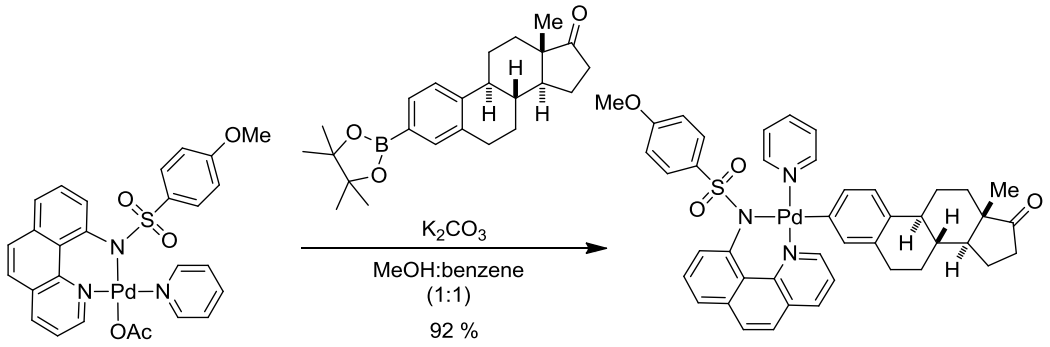

2.15 **2.4**

3-Pinacolatoboroestra-1,3,5-(10)-triene-17-one was prepared by modification of a published method:[88] To a mixture of 3-(trifluoromethanesulfonyl)estrone (11.0 g, 27.3 mmol, 1.00 equiv) and $Pd(dppf)Cl_2{\cdot}CH_2Cl_2$ (1.12g, 1.37 mmol, 0.0500 equiv) in a round-bottom flask in dioxane (100 ml) under a N_2 atmosphere were added Et_3N (22.9 ml, 16.6 g, 164 mmol, 6.00 equiv) and 4,4,5,5-tetramethyl-1,3,2-dioxaborolane (11.5 ml, 10.1 g, 79.0 mmol, 2.89 equiv).[89] The reaction mixture was heated at 100 °C for 20 hours while stirring. The reaction mixture was cooled to 23 ºC and concentrated *in vacuo*. The residue was dissolved in EtOAc/hexanes (1:3 (v/v), 100 mL) and the solution was filtered through a pad of silica gel to remove palladium residue, eluting with additional EtOAc/hexanes (1:3 (v/v), 50 mL). The filtrate was concentrated *in vacuo* and the residue was washed with cold (–15 ºC) pentane (3 × 10 mL) to afford 8.30 g of 3-pinacolatoboroestra-1,3,5-(10)-triene-17-one as a colorless solid (80% yield).

NMR Spectroscopy: ^{1}H NMR (500 MHz, $CDCl_3$, 23 ºC, δ): 7.60 (d, J = 7.8 Hz, 1H), 7.57 (s, 1H), 7.32 (d, J = 7.8 Hz, 1H), 2.95–2.88 (m, 2H), 2.53–2.44 (m, 2H), 2.35–2.29 (m, 1H), 2.18–1.95 (m, 4H), 1.67–1.40 (m, 6H), 1.34 (s, 12 H), 0.91 (s, 3H). ^{13}C NMR (125 MHz, $CDCl_3$, 23 ºC, δ): 220.8, 143.2, 135.9, 135.6, 132.2, 124.8, 83.7, 50.6, 48.0, 44.8, 38.1, 35.9, 31.7, 29.2, 26.5, 25.7, 24.9, 24.9, 21.7, 13.9.

To acetato palladium complex **2.15** (1.00 g, 1.64 mmol, 1.00 equiv) in a round-bottom flask in MeOH (30 mL) and benzene (30 mL) under a N_2 atmostphere at 23 ºC were added 3-pinacolatoboroestra-1,3,5-(10)-triene-17-one (0.625 g, 1.64 mmol, 1.00 equiv) and K_2CO_3 (0.340 g, 2.47 mmol, 1.50 equiv). The reaction

88. Ahmed, V.; Liu, Y.; Silvestro, C.; Taylor, S. D. *Bioorgan.Med. Chem.* **2006**, *14*, 8564.

89. Furuya, T.; Strom, A. E.; Ritter, T. *J. Am. Chem. Soc.* **2009**, *131*, 1662.

mixture was stirred at 23 ºC for 20 hours, and then concentrated *in vacuo*. To the solid residue was added CH_2Cl_2 (100 mL) and the solution was filtered through Celite, eluting with additional CH_2Cl_2 (50 mL). The solution was washed with water (3 × 20 mL), dried with Na_2SO_4, and concentrated *in vacuo*. The residue was recrystallized by dissolving the solid in CH_2Cl_2 (20 mL) and layering with pentane (100 mL). After 6 hours, the solid was collected by filtration to afford 1.22 g of the title compound as a yellow solid (92% yield).

NMR Spectroscopy: ^{1}H NMR (500 MHz, $CDCl_3$, 23 ºC, δ): 9.04 (d, *J* = 5.3 Hz, 2H), 8.37 (dd, *J* = 4.3, 4.3 Hz, 1H), 7.98 (dd, *J* = 7.5, 2.1 Hz, 1H), 7.75–7.60 (m, 5H), 7.39 (d, *J* = 8.6 Hz, 1H), 7.31 (dd, *J* = 7.0, 7.0 Hz, 2H), 7.11 (d, *J* = 8.6 Hz, 2H), 7.08–7.06 (m, 1H), 6.68 (dd, *J* = 7.5, 4.3 Hz, 1H), 6.55–6.49 (m, 2H), 6.18 (d, *J* = 8.6 Hz, 2H), 3.54 (s, 3H), 2.72–2.51 (m, 2H), 2.46 (dd, *J* = 19.1, 10.8 Hz, 1H), 2.26–2.24 (m, 1H), 2.15–2.06 (m, 2H), 2.02–1.97 (m, 1H), 1.88–1.85 (m, 2H), 1.60–1.22 (m, 6H), 0.86 (s, 3H); ^{13}C NMR (125 MHz, $CDCl_3$, 23 ºC, δ): 221.3, 160.2, 154.2, 154.2, 153.4, 151.9, 144.9, 143.6, 137.5, 137.4, 136.3, 136.2, 135.3, 135.2, 134.6, 134.5, 132.3, 132.2, 130.1, 129.9, 127.8, 127.7, 127.6, 127.3, 127.2, 124.8, 124.8, 124.1, 123.5, 123.4, 123.4, 121.2, 121.1, 112.2, 55.3, 50.7, 50.7, 48.2, 44.3, 44.3, 38.3, 36.0, 31.8, 29.4, 26.9, 26.8, 25.7, 25.6, 21.7, 14.1, 14.0. Anal: calcd for $C_{43}H_{41}N_3O_4PdS$: C, 64.37; H, 5.15; N, 5.24; found: C, 64.06; H, 5.21; N, 5.21.

5-Chloro-2-iodophenol (2.22)

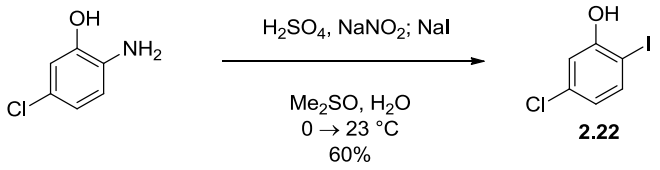

Caution: While no incident occurred, diazotation of aniline derivatives is dangerous and should be conducted with care using explosion safety equipment like a blast shield.

A round-bottom flask open to air was charged with dimethylsulfoxide (DMSO) (150 mL) and cooled in an ice-water bath so that the solvent partly solidified. Separately, concentrated sulfuric acid (45 mL) was mixed with 105 mL H_2O. The resulting 30% sulfuric acid solution was added to the DMSO at 0 ºC. To the

solution was then added 2-amino-5-chlorophenol (4.50 g, 31.3 mmol, 1.00 equiv) with vigourous stirring followed by a solution of H_2O (15 mL) containing sodium nitrite (3.24 g, 47.0 mmol, 1.50 equiv). The reaction mixture was stirred at 0 ºC for 1 hour. Sodium iodide (14.1 g, 93.9 mmol, 3.00 equiv) dissolved in H_2O (15 mL) was added dropwise over 5 minutes at 0 ºC. The ice-water bath was removed, and the reaction mixture was allowed to warm to 23 ºC and stirred for 1 hour. An additional portion of sodium iodide (14.1 g, 93.9 mmol, 3.00 equiv) dissolved in H_2O (15 mL) was added dropwise over 5 minutes. The reaction mixture was stirred at 23 ºC for 1 hour. The reaction mixture was transferred to a separatory funnel. EtOAc (800 mL) and brine (150 mL) were added to the separatory funnel, which was shaken and the organic phase collected. The organic phase was washed with brine (200 mL), 10% $NaHSO_3$ aqueous solution (300 mL), and brine (150 mL). The organic phase was dried with Na_2SO_4 and concentrated *in vacuo*. The residue was purified by chromatography on silica gel, eluting with a gradient of 10–20% EtOAc in hexanes to afford 4.75 g of the title compound as a colorless oil (60% yield).

R*f* = 0.25 (hexanes/EtOAc 9:1 (v/v)). NMR Spectroscopy: ^{1}H NMR (500 MHz, $CDCl_3$, 23 ºC, δ): 7.56 (d, *J* = 8.3 Hz, 1H), 7.01 (d, *J* = 2.5 Hz, 1H), 6.70 (dd, *J* = 8.8, 2.4 Hz, 1H), 5.32 (s, 1H). ^{13}C NMR (125 MHz, $CDCl_3$, 23 ºC, δ): 155.7, 138.8, 136.0, 122.9, 115.7, 83.2. HRMS-FIA (m/z): calcd for C_6H_5ClIO $[M + H]^+$, 254.9074; found, 254.9077.

4-Chloro-1-iodo-2-(methoxymethoxy)benzene (2.23)

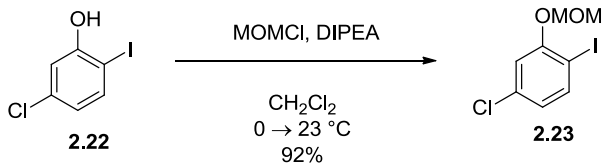

To 5-chloro-2-iodophenol (**2.22**) (2.40 g, 9.43 mmol, 1.00 equiv) in CH_2Cl_2 (10 mL) in an oven-dried round-bottom flask under a N_2 atmosphere at 0 ºC was added *N*,*N*-diisopropylethylamine (DIPEA) (1.34 g, 1.81 mL, 10.4 mmol, 1.10 equiv) followed by the dropwise addition of chloromethyl methyl ether (MOMCl) (835 mg, 0.788 mL, 10.4 mmol, 1.10 equiv). The reaction mixture was stirred at 23 ºC for 30 minutes. The reaction mixture was allowed to warm to 23 ºC and stirred for an additional 2 hours. The reaction mixture was then poured onto a saturated NH_4Cl aqueous solution (100 mL) in a separatory funnel.

The funnel was shaken and the organic phase collected. The organic phase was washed with H_2O (50 mL) and then brine (25 mL). The organic phase was dried with Na_2SO_4 and concentrated *in vacuo*. The residue was purified by chromatography on silica gel, eluting with a gradient of 5–8% EtOAc in hexanes to afford 2.59 g of the title compound as a colorless oil (92% yield).

R*f* = 0.55 (hexanes/EtOAc 9:1 (v/v)). NMR Spectroscopy: ^{1}H NMR (500 MHz, $CDCl_3$, 23 ºC, δ): 7.67 (d, *J* = 8.2 Hz, 1H), 7.09 (d, *J* = 2.3 Hz, 1H), 6.77 (dd, *J* = 8.2, 2.3 Hz, 1H), 5.23 (s, 2H), 3.51 (s, 3H). ^{13}C NMR (125 MHz, $CDCl_3$, 23 ºC, δ): 156.8, 139.9, 135.3, 123.9, 115.6, 95.2, 84.5, 56.7. HRMS-FIA (m/z): calcd for $C_8H_8ClINaO_2$ $[M + Na]^+$, 320.9155; found, 320.9185.

5-(4-Chloro-2-(methoxymethoxy)phenyl)furan-2-carbaldehyde (2.24)

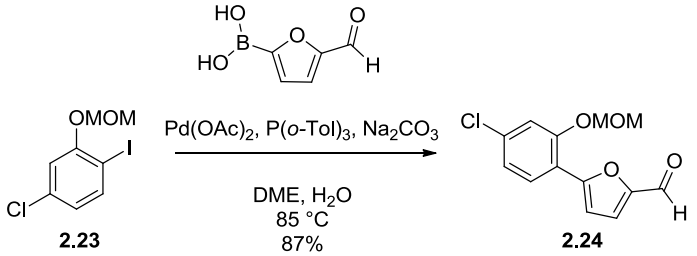

2.23 **2.24**

A Schlenk tube was charged with (5-formylfuran-2-yl)boronic acid (839 mg, 6.00 mmol, 1.50 equiv) and Na_2CO_3 (848 mg, 8.00 mmol, 2.00 equiv). A 6:1 solution of DME:H_2O (v/v) (28 mL) was added followed by 4-chloro-1-iodo-2-(methoxymethoxy)benzene (**2.23**) (1.19 g, 4.00 mmol, 1.00 equiv). The reaction mixture was degassed via two consecutive freeze/pump/thaw cycles. The Schlenk tube was then refilled with N_2. $Pd(OAc)_2$ (44.9 mg, 0.200 mmol, 0.0500 equiv) and tri-*o*-tolylphosphine (122 mg, 0.400 mmol, 0.100 equiv) were added. The reaction mixture was degassed again via two consecutive freeze/pump/thaw cycles. The Schlenk tube was then refilled with N_2 and immersed in an oil bath heated to 85 ºC for 3.25 hours. The reaction mixture was cooled and filtered through a plug consisting of a bottom layer of Celite and a top layer of $NaHCO_3$ eluting with EtOAc (100 mL). The solution was concentrated *in vacuo*, and the residue was purified by chromatography on silica gel, eluting with a gradient of 10–33% EtOAc in hexanes to afford 927 mg of the title compound as a white/beige solid (87% yield).

R*f* = 0.20 (hexanes/EtOAc 3:1 (v/v)). NMR Spectroscopy: ^{1}H NMR (500 MHz, $CDCl_3$, 23 ºC, δ): 9.65 (s,

1H), 7.95 (d, J = 8.7 Hz, 1H), 7.32 (d, J = 3.7 Hz, 1H), 7.24 (d, J = 1.8 Hz, 1H), 7.11–7.08 (m, 2H), 5.32 (s, 2H), 3.51 (s, 3H). ^{13}C NMR (125 MHz, $CDCl_3$, 23 ºC, δ): 177.3, 155.1, 154.8, 151.2, 136.2, 128.3, 123.8, 122.5, 117.4, 115.3, 112.7, 94.7, 56.7. HRMS-FIA (m/z): calcd for $C_{13}H_{11}ClNaO_4$ $[M + Na]^+$, 289.0244; found, 289.0249.

5-(2-(Methoxymethoxy)-4-(4,4,5,5-tetramethyl-1,3,2-dioxaborolan-2-yl)phenyl)furan-2-carbaldehyde (2.25)

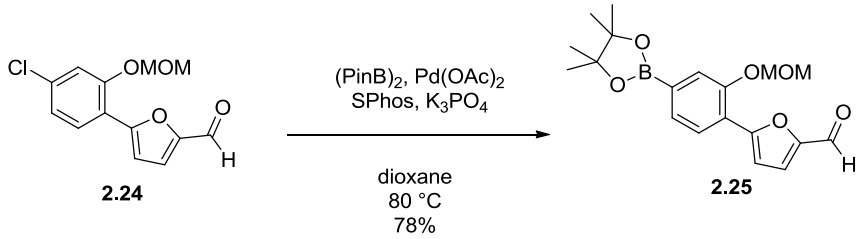

Based on a reported procedure for the conversion of aryl chlorides to aryl pinacol boronic esters:[90] An oven-dried Schlenk tube was charged with 5-(4-chloro-2-(methoxymethoxy)phenyl)furan-2-carbaldehyde (**2.24**) (600. mg, 2.25 mmol, 1.00 equiv), bis(pinacolato)diboron (1.71 g, 6.75 mmol, 3 equiv), potassium phosphate (1.43 g, 6.75 mmol, 3 equiv), $Pd(OAc)_2$ (20.2 mg, 0.0900 mmol, 0.0400 equiv), and dicyclohexyl(2',6'-dimethoxy-[1,1'-biphenyl]-2-yl)phosphine (SPhos) (92.0 mg, 0.225 mmol, 0.100 equiv). Three times, the Schlenk tube was evacuated and refilled with N_2. Dioxane (4.5 mL) was added and the reaction mixture was heated with vigorous stirring at 80 ºC for 2.75 hours. The green suspension was cooled and filtered through Celite rinsing with EtOAc (25 mL). The yellow solution was concentrated *in vacuo* and the residue was purified by chromatography on silica gel, eluting with a gradient of 10–25% EtOAc in hexanes to afford 625 mg of the title compound as a white/beige solid (78% yield).

Rf = 0.20 (hexanes/EtOAc 5:1 (v/v)). NMR Spectroscopy: ^{1}H NMR (500 MHz, $CDCl_3$, 23 ºC, δ): 9.68 (s, 1H), 8.05 (d, J = 7.3 Hz, 1H), 7.55–7.53 (m, 2H), 7.34 (d, J = 3.7 Hz, 1H), 7.22 (d, J = 3.7 Hz, 1H), 5.39 (s, 2H), 3.52 (s, 3H), 1.36 (s, 12H). ^{13}C NMR (125 MHz, $CDCl_3$, 23 ºC, δ): 177.4, 156.0, 153.7, 151.2, 128.4,

90. Billingsley, K. L.; Barder, T. E.; Buchwald, S. L. *Angew. Chem., Int. Ed.* **2007**, *46*, 5359.

126.8, 123.9, 121.1, 119.9, 113.4, 94.4, 84.2, 56.7, 25.0. HRMS-FIA (m/z): calcd for $C_{19}H_{24}BO_6$ $[M + H]^+$, 359.1666; found, 359.1666.

3-(Bis(4-methoxyphenyl)methyl)thiazolidine-2,4-dione (2.26)

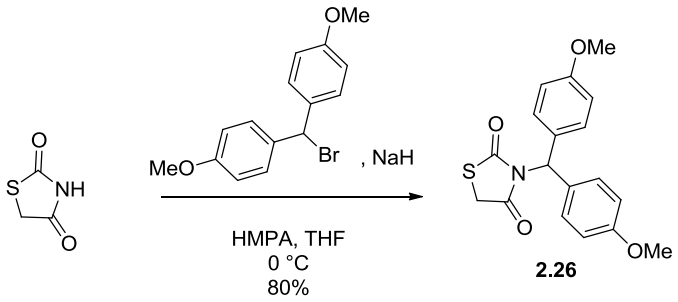

To thiazolidine-2,4-dione (250. mg, 2.13 mmol, 1.00 equiv) in an oven-dried round-bottom flask in THF (10 mL) under a N_2 atmosphere was added hexamethylphosphoramide (HMPA) (2.29 g, 2.23 mL, 12.8 mmol, 6.00 equiv). The reaction mixture was cooled to 0 ºC in an ice-water bath. Sodium hydride (128 mg (60% by weight in mineral oil), 3.2 mmol, 1.5 equiv) was added in one portion, which was accompanied by foaming. The reaction mixture was stirred for 15 minutes at 0 ºC. 4,4'-(bromomethylene)bis(methoxybenzene) (1.05 g, 3.42 mmol, 1.60 equiv) was added at 0 ºC. The reaction mixture was stirred for 2 hours at 0 ºC. Saturated aqueous NH_4Cl solution (10 mL) was then added followed by H_2O (10 mL). The reaction mixture was transferred to a separatory funnel, diluted with CH_2Cl_2 (30 mL), shaken, and partitioned. The aqueous phase was extracted from with CH_2Cl_2 (2 × 30 mL). The organic phases were combined and dried with Na_2SO_4, concentrated *in vacuo*, and the residue was purified by chromatography on silica gel, eluting with a gradient of 0–5% MeOH in CH_2Cl_2 to afford 590. mg of the title compound as a colorless solid (80% yield).

R*f* = 0.35 (hexanes/EtOAc 3:1 (v/v)). NMR Spectroscopy: ^{1}H NMR (600 MHz, $CDCl_3$, 23 ºC, δ): 7.26–7.24 (m, 4H), 6.88–6.85 (m, 4H), 6.59 (s, 1H), 3.93 (s, 2H), 3.80 (s, 6H). ^{13}C NMR (125 MHz, $CDCl_3$, 23 ºC, δ): 171.5, 171.4, 159.4, 130.0, 129.2, 113.9, 60.6, 55.4, 33.6. HRMS-FIA (m/z): calcd for $C_{18}H_{17}NNaO_4S$ $[M + Na]^+$, 366.0776; found, 366.0745.

(*Z*)-3-(Bis(4-methoxyphenyl)methyl)-5-((5-(2-(methoxymethoxy)-4-(4,4,5,5-tetramethyl-1,3,2-

dioxaborolan-2-yl)phenyl)furan-2-yl)methylene)thiazolidine-2,4-dione (S19)

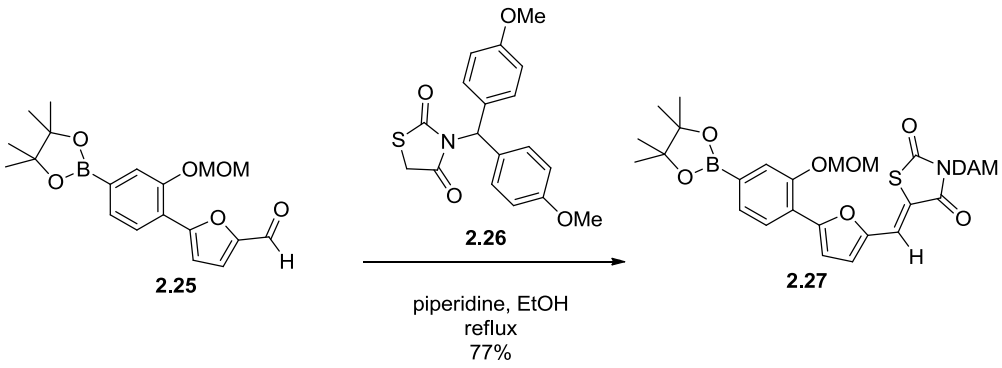

To 3-(bis(4-methoxyphenyl)methyl)thiazolidine-2,4-dione (**2.26**) (537 mg, 1.56 mmol, 1.00 equiv) suspended in ethanol (10 mL) in a round-bottom flask open to air was added 5-(2-(methoxymethoxy)-4-(4,4,5,5-tetramethyl-1,3,2-dioxaborolan-2-yl)phenyl)furan-2-carbaldehyde (**2.25**) (560. mg, 1.56 mmol, 1.00 equiv) and piperidine (106 mg, 0.124 mL, 1.25 mmol, 0.800 equiv). The round-bottom flask was fitted with a reflux condenser and submerged in an 80 ºC oil bath for 1 hour. Upon cooling, a bright yellow solid precipitated which was collected by filtration and washed with hexanes (20 mL) to afford 825 mg of the title compound as a bright yellow solid (77% yield).

R*f* = 0.30 (hexanes/EtOAc 3:1 (v/v)). NMR Spectroscopy: ^{1}H NMR (600 MHz, $CDCl_3$, 23 ºC, δ): 7.91 (d, *J* = 7.6 Hz, 1H), 7.63 (s, 1H), 7.57 (d, *J* = 7.9 Hz, 1H), 7.54 (s, 1H), 7.31–7.29 (m, 4H), 7.21 (d, *J* = 3.7, 1H), 6.90–6.86 (m, 5H), 6.75 (s, 1H), 5.39 (s, 2H), 3.81 (s, 6H), 3.51 (s, 3H), 1.35 (s, 12H). ^{13}C NMR (125 MHz, $CDCl_3$, 23 ºC, δ): 168.7, 166.1, 159.3, 154.9, 153.1, 148.6, 130.0, 129.6, 128.7, 126.1, 121.3, 120.7, 119.9, 119.4, 118.2, 114.5, 113.9, 94.4, 84.2, 60.3, 56.8, 55.4, 25.0. HRMS-FIA (m/z): calcd for $C_{37}H_{38}BNNaO_9S$ $[M + Na]^+$, 706.2258; found, 706.2253.

Palladium aryl complex 10

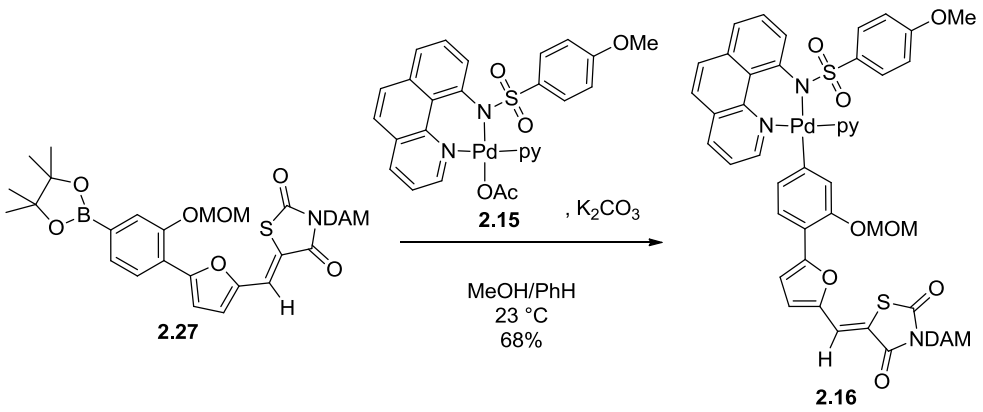

To (*Z*)-3-(bis(4-methoxyphenyl)methyl)-5-((5-(2-(methoxymethoxy)-4-(4,4,5,5-tetramethyl-1,3,2-dioxaborolan-2-yl)phenyl)furan-2-yl)methylene)thiazolidine-2,4-dione (**2.27**) (100. mg, 0.146 mmol, 1.00 equiv) in a round-bottom flask open to air in a 1:1 solution PhH:MeOH (4 mL) was added palladium acetate complex **2.15** (98.0 mg, 0.161 mmol, 1.10 equiv) and potassium carbonate (30.3 mg, 0.219 mmol, 1.50 equiv). The suspension was stirred at 23 ºC for 3.5 hours. The reaction mixture was filtered through microfiber filter paper eluting with CH_2Cl_2 (10 mL). The solution was concentrated *in vacuo* and the residue was purified by chromatography on silica gel, eluting with a gradient of 33–90% EtOAc in hexanes to afford 110. mg of the title compound as a bright yellow solid (68% yield).

R*f* = 0.25 (hexanes/EtOAc 1:5 (v/v)). NMR Spectroscopy: ^{1}H NMR (500 MHz, CD_2Cl_2, 23 ºC, δ): 9.04 (d, *J* = 4.8 Hz, 2H), 8.39 (dd, *J* = 5.4, 1.5 Hz, 1H), 8.07 (dd, *J* = 7.8, 1.4 Hz, 1H), 7.84–7.80 (m, 2H), 7.68–7.62 (m, 2H), 7.61 (dd, *J* = 6.8, 2.5 Hz, 1H), 7.55 (s, 1H), 7.47 (d, *J* = 8.8 Hz, 1H), 7.38 (dd, *J* = 6.8, 6.8 Hz, 2H), 7.34 (d, *J* = 8.3 Hz, 1H), 7.26–7.24 (m, 4H), 7.13–7.10 (m, 3H), 6.95 (d, *J* = 3.9 Hz, 1H), 6.88–6.86 (m, 5H), 6.72 (d, *J* = 5.4 Hz, 2H), 6.68 (s, 1H), 6.25–6.22 (m, 2H), 5.08 (d, *J* = 6.5 Hz, 1H), 5.02 (d, *J* = 6.5 Hz, 1H), 3.79 (s, 6H), 3.56 (s, 3H), 3.30 (s, 3H). ^{13}C NMR (125 MHz CD_2Cl_2, 23 ºC, δ): 169.1, 166.3, 162.1, 160.7, 159.6, 156.6, 154.3, 153.5, 151.5, 147.8, 144.9, 143.6, 138.3, 138.2, 136.7, 130.3, 130.2, 130.1, 130.0, 129.3, 127.9, 127.8, 127.4, 125.3, 124.5, 124.1, 123.9, 121.7, 121.5, 121.0, 119.5, 116.8, 114.7, 114.0, 112.6, 112.5, 94.6, 60.4, 56.4, 55.6, 55.5. Anal: calcd for $C_{56}H_{46}N_4O_{10}PdS_2$: C, 60.84; H, 4.19; N, 5.07; found: C, 60.59; H, 4.36; N, 4.97.

5-Bromo-2-(cyclopropylmethoxy)benzaldehyde (2.28)

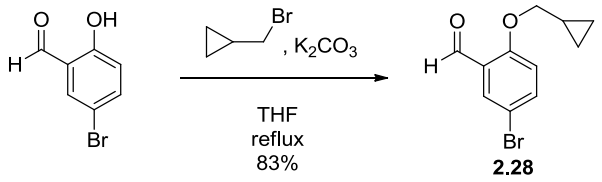

2.28

To 5-bromo-2-hydroxybenzaldehyde (1.00 g, 4.97 mmol, 1.00 equiv) and K_2CO_3 (3.44 g, 24.9 mmol, 5.00 equiv) in THF (10 mL) in an oven-dried round-bottom flask fitted with a reflux condenser under a N_2 atmosphere at 23 ºC was added (bromomethyl)cyclopropane (1.01 g, 0.724 mL, 7.46 mmol, 1.50 equiv). The reaction mixture was warmed in an oil heating bath at a temperature of 70 ºC and heated at reflux with vigorous stirring for 40 hours. The reaction mixture was cooled to 23 ºC and poured into H_2O (30 mL) in a separatory funnel. $CHCl_3$ (30 mL) was added, the funnel was shaken and the organic phase collected. The aqueous phase was then extracted with $CHCl_3$ (2 × 30 mL). The combined organic phases were washed with brine (30 mL), dried with Na_2SO_4, and concentrated *in vacuo*. The residue was purified by chromatography on silica gel, eluting with 2–7% EtOAc in hexanes (v/v) to afford 1.05 g of the title compound as a colorless solid (83% yield).

R*f* = 0.30 (hexanes/EtOAc 19:1 (v/v)). NMR Spectroscopy: ^{1}H NMR (600 MHz, $CDCl_3$, 23 ºC, δ): 10.45 (s, 1H), 7.91 (d, *J* = 2.5 Hz, 1H), 7.58 (dd, *J* = 8.9, 2.6 Hz, 1H), 6.84 (d, *J* = 8.9 Hz, 1H), 3.91 (d, *J* = 7.2 Hz, 2H), 1.32–1.26 (m, 1H), 0.71–0.63 (m, 2H), 0.41–0.34 (m, 2H). ^{13}C NMR (125 MHz, $CDCl_3$, 23 ºC, δ): 188.7, 160.5, 138.3. 130.9, 126.5, 115.0, 113.5, 73.9, 10.1, 3.4. HRMS-FIA (m/z): calcd for $C_{11}H_{11}BrNaO_2$ $[M + Na]^+$, 276.9840; found, 276.9820.

(*E*)-Ethyl 3-(5-bromo-2-(cyclopropylmethoxy)phenyl)acrylate (2.29)

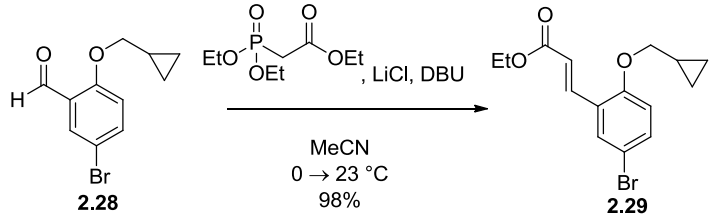

2.28 **2.29**

To 5-bromo-2-(cyclopropylmethoxy)benzaldehyde (**2.28**) (3.10 g, 12.2 mmol, 1.00 equiv) and LiCl (0.541 g, 12.8 mmol, 1.05 equiv) in MeCN (45 mL) in a round-bottom flask under a N_2 atmosphere at 0 ºC was

added triethyl phosphonoacetate (3.00 g, 2.68 mL, 13.4 mmol, 1.10 equiv) and 1,8-diazabicycloundec-7-ene (DBU) (2.04 g, 2.02 mL, 13.4 mmol, 1.10 equiv). Upon the addition of DBU, the reaction mixture turned yellow. The reaction mixture was warmed to 23 ºC and stirred for 15 hours. The reaction mixture was poured into H_2O (75 mL) in a separatory funnel. $CHCl_3$ (75 mL) was added and the funnel was shaken and the organic phase collected. The aqueous phase was extracted from with $CHCl_3$ (2 × 50 mL). All organic phases were combined and washed with brine (50 mL), dried with Na_2SO_4, and concentrated *in vacuo*. The residue was purified by chromatography on silica gel, eluting with 5–10% EtOAc in hexanes (v/v) to afford 3.89 g of the title compound as a colorless solid (98% yield).

R*f* = 0.25 (hexanes/EtOAc 19:1 (v/v)). NMR Spectroscopy: ^{1}H NMR (500 MHz, $CDCl_3$, 23 ºC, δ): 7.93 (d, *J* = 16.1 Hz, 1H), 7.60 (d, *J* = 2.4 Hz, 1H), 7.37 (dd, *J* = 8.8, 2.5 Hz, 1H), 6.74 (d, 8.8 Hz, 1H), 6.53 (d, *J* = 16.1 Hz, 1H), 4.26 (q, *J* = 6.8 Hz, 2H), 3.84 (d, *J* = 6.8 Hz, 2H), 1.34–1.25 (m, 4H), 0.70–0.61 (m, 2H), 0.40–0.31 (m, 2H). ^{13}C NMR (125 MHz, $CDCl_3$, 23 ºC, δ): 167.3, 156.9, 138.7, 133.7, 131.3, 125.9, 120.0, 114.4, 113.0, 73.9, 60.6, 14.4, 10.2, 3.4. HRMS-FIA (m/z): calcd for $C_{15}H_{18}BrO_3$ $[M + H]^+$, 325.0439; found, 325.0428.

(*E*)-3-(5-Bromo-2-(cyclopropylmethoxy)phenyl)prop-2-en-1-ol (2.30)

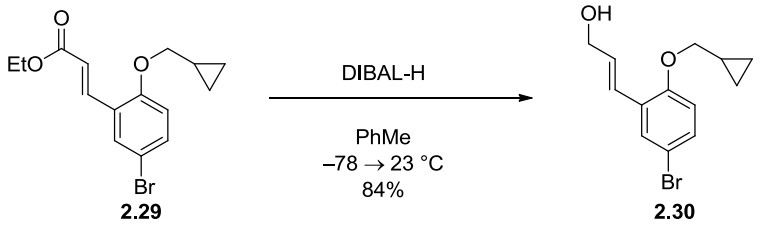

To (*E*)-ethyl 3-(5-bromo-2-(cyclopropylmethoxy)phenyl)acrylate (**2.29**) (3.78 g, 11.6 mmol, 1.00 equiv) in PhMe (30 mL) in a flame-dried round-bottom flask under a N_2 atmosphere at –78 ºC was added a 1.0 M solution of diisobutylaluminum hydride (DIBAL-H) in PhMe (26 mL, 26 mmol, 2.2 equiv) in 6 portions dropwise every 10 minutes for 1 hour. The reaction was warmed to 0 ºC over 2 hours and then warmed to 23 ºC and stirred at this temperature for 1 hour. The reaction mixture was poured onto a concentrated aqueous Rochelle's salt (potassium sodium tartrate) solution (400 mL). EtOAc (400 mL) was added and the mixture was stirred for 3 hour until two liquid phases separated cleanly. The phases were partitioned

and the aqueous phase was extracted from with EtOAc (300 mL). The organic phases were combined and washed with brine (200 mL), dried with Na_2SO_4, and concentrated *in vacuo*. The residue was purified by chromatography on silica gel, eluting with a gradient of 10–25% EtOAc in hexanes (v/v) to afford 2.77 g of the title compound as a colorless solid (84% yield).

R*f* = 0.15 (hexanes/EtOAc 6:1 (v/v)). NMR Spectroscopy: ^{1}H NMR (500 MHz, $CDCl_3$, 23 ºC, δ): 7.53 (d, *J* = 2.4 Hz, 1H), 7.26 (dd, *J* = 8.8, 2.4 Hz, 1H), 6.88 (d, *J* = 16.1 Hz, 1H), 6.69 (d, *J* = 8.8 Hz, 1H), 6.39 (dt, *J* = 16.1, 5.9 Hz, 1H), 4.33 (br dd, *J* = 4.6, 4.6 Hz, 2H), 3.79 (d, *J* = 6.8 Hz, 2H), 1.71 (br t, *J* = 5.1 Hz, 1H), 1.31–1.23 (m, 1H), 0.68–0.58 (m, 2H), 0.38–0.30 (m, 2H). ^{13}C NMR (125 MHz, $CDCl_3$, 23 ºC, δ): 155.4, 131.2, 130.5, 129.7, 128.2, 125.0, 114.2, 113.2, 73.7, 64.1, 10.3, 3.4. HRMS-FIA (m/z): calcd for $C_{13}H_{15}BrNaO_2$ $[M + Na]^+$, 305.0153; found, 305.0123.

((1*S*,2*S*)-2-(5-Bromo-2-(cyclopropylmethoxy)phenyl)cyclopropyl)methanol (2.31)

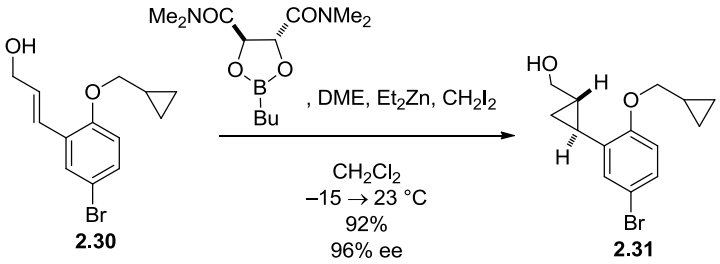

Following a published procedure for asymmetric allylic cyclopropanation:[91] To dimethoxyethane (DME) (1.39 g, 1.60 mL, 15.4 mmol, 1.90 equiv) in CH_2Cl_2 (50 mL) in a flame-dried round-bottom flask under a N_2 atmosphere cooled in an ethylene glycol/CO_2 bath at –15 ºC was added diethylzinc (2.01 g, 1.67 mL, 16.3 mmol, 2.00 equiv), while maintaining the bath temperature between –15 and –10 ºC. CH_2I_2 (8.70 g, 2.62 mL, 32.5 mmol, 4.00 equiv) was added dropwise over 20 minutes at –15 ºC. The reaction mixture was stirred at –15 ºC for 10 minutes. A solution of (4*R*,5*R*)-2-butyl-*N*,*N*,*N'*,*N'*-tetramethyl-1,3,2-dioxaborolane-4,5-dicarboxamide (2.63 g, 2.46 mL, 9.75 mmol, 1.20 equiv) in CH_2Cl_2 (10 mL) from a separate flame-dried round-bottom flask under a N_2 atmosphere was added over 5 minutes via syringe. A

91. Charette, A. B.; Juteau, H.; Lebel, H.; Molinaro, C. *J. Am. Chem. Soc.* **1998**, *120*, 11943.

solution of (*E*)-3-(5-bromo-2-(cyclopropylmethoxy)phenyl)prop-2-en-1-ol (**2.30**) (2.30 g, 8.12 mmol, 1.00 equiv) in CH_2Cl_2 (10 mL) from a separate flame-dried round-bottom flask under a N_2 atmosphere was added over 5 minutes via syringe. The reaction mixture was allowed to warm to 23 ºC and stirred for 20 hours. Saturated aqueous NH_4Cl solution (10 mL) and 1M HCl (50 mL) were added to the reaction mixture. The reaction mixture was transferred to a separatory funnel. Diethyl ether (200 mL) was added and the separatory funnel was shaken and the organic phase was separated. The aqueous phase was extracted from with diethyl ether (200 mL) and then again with diethyl ether (100 mL). The combined organic phases were transferred to an Erlenmeyer flask. 2 M NaOH solution (60 mL) and 30% H_2O_2 solution (15 mL) were added. The reaction mixture was stirred vigorously for 5 minutes. The reaction mixture was transferred into a separatory funnel and partitioned. The organic phase was washed with 1.0 M aqueous HCl (75 mL), saturated aqueous Na_2CO_3 solution (75 mL), saturated aqueous $NaHCO_3$ solution (75 mL) and brine (75 mL). The organic phase was dried with $MgSO_4$, and concentrated *in vacuo*. The residue was purified by chromatography on silica gel, eluting with a gradient of 10–30% EtOAc in hexanes (v/v) to afford 2.21 g of the title compound as a colorless oil (92% yield and 96% *ee* as determined on a Chiracel OD-H column with 5% isopropanol/hexanes eluent (see Figure 4.2). Racemic **2.31** was synthesized using the above procedures omitting the addition of (4*R*,5*R*)-2-butyl-*N*,*N*,*N'*,*N'*-tetramethyl-1,3,2-dioxaborolane-4,5-dicarboxamide. Absolute stereochemistry was assigned by analogy.[91]

R*f* = 0.20 (hexanes/EtOAc 6:1 (v/v)). NMR Spectroscopy: ^{1}H NMR (500 MHz, $CDCl_3$, 23 ºC, δ): 7.24 (dd, *J* = 8.8, 2.4 Hz, 1H), 7.09 (d, *J* = 2.4 Hz, 1H), 6.65 (d, *J* = 8.8 Hz, 1H), 3.95 (ddd, *J* = 10.7, 8.8, 4.9 Hz, 1H), 3.82 (d, *J* = 7.3 Hz, 2H), 3.19 (ddd, *J* = 10.7, 10.7, 2.0, 1H), 2.40 (dd, *J* = 8.5, 2.0 Hz, 1H), 1.86 (ddd, *J* = 8.5, 5.0, 5.0 Hz, 1H) 1.34–1.27 (m, 1H), 1.20–1.15 (m, 1H), 1.14–1.09 (m, 1H), 0.86 (ddd, *J* = 9.0, 5.0, 5.0 Hz, 1H), 0.71–0.65 (m, 2H), 0.40–0.34 (m, 2H). ^{13}C NMR (125 MHz, $CDCl_3$, 23 ºC, δ): 157.2, 132.4, 130.2, 129.9, 112.8, 112.6, 73.6, 67.3, 24.5, 17.2, 10.2, 9.9, 3.7, 3.2. HRMS-FIA (m/z): calcd for $C_{14}H_{17}BrNaO_2$ $[M + Na]^+$, 319.0310; found, 319.0327.

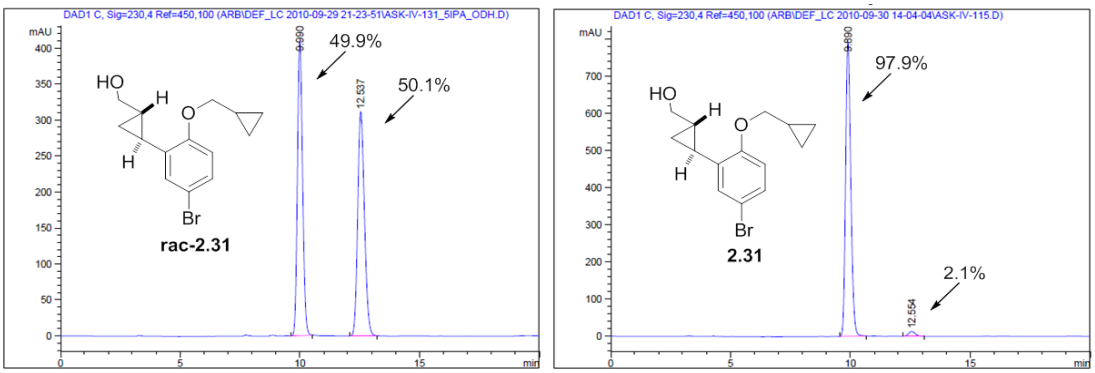

Figure 4.2. Enantiodiscriminating HPLC trace of **2.31**. HPLC method: Chiracel OD-H column with 5% isopropanol/hexanes eluent for racemic **2.31** and enantioenriched **2.31**. Percent of total integration listed for each peak.

2-((1*S*,2*S*)-2-(Azidomethyl)cyclopropyl)-4-bromo-1-(cyclopropylmethoxy)benzene (2.32)

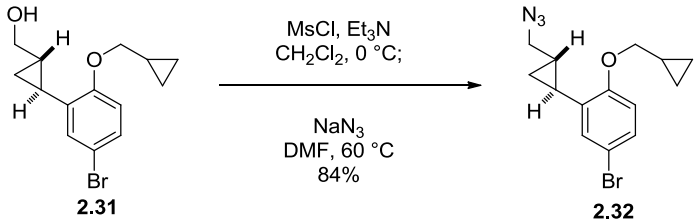

To ((1*S*,2*S*)-2-(5-bromo-2-(cyclopropylmethoxy)phenyl)cyclopropyl)methanol (**2.31**) (2.15 g, 7.23 mmol, 1.00 equiv) in CH_2Cl_2 (30 mL) in an oven-dried round-bottom flask under a N_2 atmosphere at 0 ºC was added Et_3N (2.20 g, 3.03 mL, 21.7 mmol, 3.00 equiv) and MsCl (1.66 g, 1.13 mL, 14.5 mmol, 2.00 equiv). The reaction mixture was stirred at 0 ºC for 2 hours. The reaction mixture turned yellow and a precipitate formed. The reaction mixture was poured into a separatory funnel with saturated NH_4Cl solution (40 mL). The funnel was shaken and the organic phase collected. The aqueous phase was extracted from with diethyl ether (3 × 75 mL). The organic phases were combined and washed with saturated $NaHCO_3$ (100 mL) and brine (100 mL), dried with $MgSO_4$, and concentrated *in vacuo*. The residue was dissolved in DMF (30 mL) and NaN_3 (1.88 g, 28.9 mmol, 4.00 equiv) was added. The reaction mixture was heated at 60 ºC for 1 hour. The reaction mixture was cooled and poured into 60 mL of water. The reaction mixture was extracted from with diethyl ether (3 × 75 mL). The combined organic phases were washed with brine (100 mL), dried with $MgSO_4$, and concentrated *in vacuo*. The residue was purified by chromatography on

silica gel, eluting with a gradient of 5–10% EtOAc in hexanes (v/v) to afford 1.95 g of the title compound as a colorless oil (84% yield).

R*f* = 0.60 (hexanes/EtOAc 19:1 (v/v)). NMR Spectroscopy: ^{1}H NMR (500 MHz, $CDCl_3$, 23 ºC, δ): 7.21 (dd, *J* = 8.7, 2.3 Hz, 1H), 6.96 (d, *J* = 2.3 Hz, 1H), 6.66 (d, *J* = 8.7 Hz, 1H), 3.84-3.78 (m, 2H), 3.40 (dd, *J* = 12.8, 6.4, 1H), 3.24 (dd, *J* = 12.8, 7.1 Hz, 1H), 2.11 (ddd, *J* = 8.7, 5.0, 5.0 Hz, 1H), 1.38–1.32 (m, 1H), 1.31–1.25 (m, 1H), 1.08–1.04 (m, 1H), 0.98–0.94 (m, 1H), 0.68–0.58 (m, 2H), 0.40–0.31 (m, 2H). ^{13}C NMR (125 MHz, $CDCl_3$, 23 ºC, δ): 156.9, 132.8, 129.5, 128.8, 113.4, 112.9, 73.3, 55.3, 20.8, 16.2, 12.8, 10.4, 3.3, 3.2. HRMS-FIA (m/z): calcd for $C_{14}H_{16}BrN_3NaO$ $[M + Na]^+$, 344.0374; found, 344.0363.

***t*-Butyl (((1*S*,2*S*)-2-(5-bromo-2-(cyclopropylmethoxy)phenyl)cyclopropyl)methyl) carbamate (2.33)**

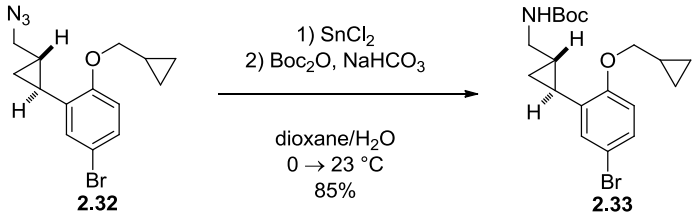

To 2-((1*S*,2*S*)-2-(azidomethyl)cyclopropyl)-4-bromo-1-(cyclopropylmethoxy)benzene (**2.32**) (1.90 g, 5.90 mmol, 1.00 equiv) in a round-bottom flask open to air in a 2:1 solution of dioxane:H_2O (45 mL) cooled to 0 ºC was added tin(II) chloride (5.59 g, 29.5 mmol, 5.00 equiv). The reaction mixture was allowed to warm to 23 ºC and stirred for 15 hours. Saturated aqueous $NaHCO_3$ solution (50 mL) was carefully added. The addition was accompanied by foaming. H_2O (15 mL) was added followed by Boc_2O (3.86 g, 4.11 mL, 17.7 mmol, 3.00 equiv). The reaction mixture was stirred for 3 hours and then transferred to a separatory funnel. The reaction mixture was extracted from with EtOAc (3 × 75 mL). The combined organic phases were washed with brine (75 mL), dried with Na_2SO_4, and concentrated *in vacuo*. The residue was purified by chromatography on silica gel, eluting with a gradient of 5–20% EtOAc in hexanes (v/v) to afford 1.96 g of the title compound as a colorless solid (85% yield). The enantioenriched product could be recrystallized by suspending the solid in hexanes (10 mL), heating the suspension to reflux to dissolve the solid, cooling the solution, and collecting the solid by filtration, affording the title compound in >99% *ee* as determined on a Chiracel OD-H column with 5% isopropanol/hexanes eluent (see Figure 4.3).

R*f* = 0.25 (hexanes/EtOAc 19:1 (v/v)). NMR Spectroscopy: ^{1}H NMR (500 MHz, $CDCl_3$, 23 ºC, δ): 7.23 (dd, *J* = 8.3, 2.4 Hz, 1H), 7.06 (br d, *J* = 2.0 Hz, 1H), 6.66 (d, *J* = 8.8 Hz, 1H), 5.27 (br, 1H), 3.97 (dd, *J* = 9.5, 7.1 Hz, 1H), 3.72–3.66 (m, 2H), 2.66 (br dd, *J* = 10.0, 10.0, 1H), 1.83 (ddd, *J* = 6.6, 6.6, 4.9 Hz, 1H), 1.43 (br, 10H), 1.06–0.99 (br m, 2H), 0.83–0.80 (br m, 1H), 0.67 (br m, 2H), 0.38 (br m, 2H). ^{13}C NMR (125 MHz, $CDCl_3$, 23 ºC, δ): 157.2, 155.9, 132.6, 130.3, 129.7, 112.8, 112.7, 79.1, 73.5, 45.7, 28.6, 21.1, 17.4, 10.6, 10.3, 3.5. HRMS-FIA (m/z): calcd for $C_{19}H_{26}BrNNaO_3$ $[M + Na]^+$, 418.0988; found, 418.0994.

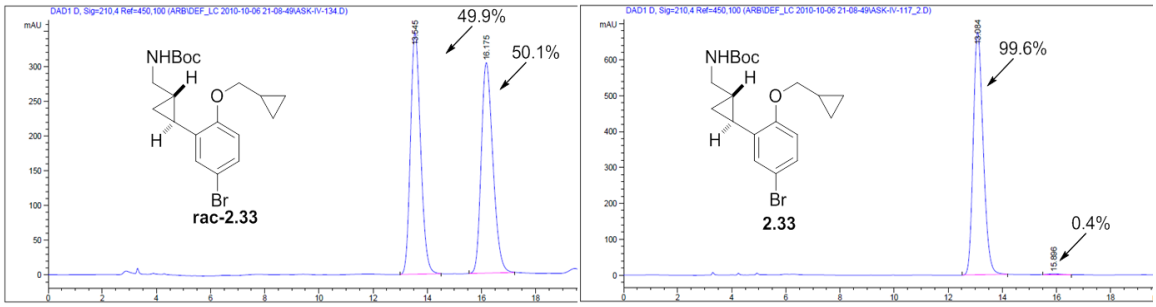

Figure 4.3. Enantiodiscriminating HPLC trace of **2.33** HPLC method: Chiracel OD-H column with 5% isopropanol/hexanes eluent for racemic **2.33** and enantioenriched **2.33**. Percent of total integration listed for each peak.

_t_-Butyl (((1*S*,2*S*)-2-(2-(cyclopropylmethoxy)-5-(4,4,5,5-tetramethyl-1,3,2-dioxaborolan-2-yl)phenyl)cyclopropyl)methyl)carbamate (2.34)

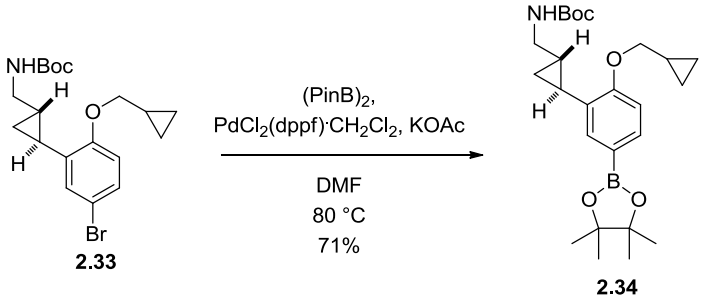

A flame-dried Schlenk tube under a N_2 atmosphere was charged with *t*-butyl (((1*S*,2*S*)-2-(5-bromo-2-(cyclopropylmethoxy)phenyl)cyclopropyl)methyl) carbamate (**2.33**) (250. mg, 0.631 mmol, 1.00 equiv), bis(pinacolato)diboron (176 mg, 0.694 mmol, 1.10 equiv), potassium acetate (186 mg, 1.89 mmol, 3.00 equiv), and $PdCl_2(dppf)\cdot CH_2Cl_2$ (15.5 mg, 18.9 umol, 0.0300 equiv). DMF (25 mL) was added via syringe. The reaction mixture was degassed via 2 consecutive freeze/pump/thaw cycles. The Schlenk tube was then

backfilled with N_2 and heated at 80 ºC for 16 hours. The reaction mixture was cooled and poured into H_2O (25 mL). The reaction mixture was extracted from with diethyl ether (4 × 30 mL). The combined organic phases were washed with brine (50 mL), dried with $MgSO_4$, and concentrated *in vacuo*. The residue was purified by chromatography on silica gel, eluting with a gradient of 5–20% EtOAc in hexanes (v/v) to afford 198 mg of the title compound as a colorless solid (71% yield).

R*f* = 0.40 (hexanes/EtOAc 4:1 (v/v)). NMR Spectroscopy: ^{1}H NMR (500 MHz, $CDCl_3$, 23 ºC, δ): 7.63 (d, *J* = 8.2 Hz, 1H), 7.42 (s, 1H), 6.80 (d, *J* = 8.2 Hz, 1H), 5.36 (br, 1H), 4.04 (dd, *J* = 9.6, 6.9 Hz, 1H), 3.77 (dd, *J* = 9.6, 7.8 Hz, 1H), 3.70 (br m, 1H), 2.63 (br dd, *J* = 10.8, 10.8 Hz, 1H), 1.82 (ddd, *J* = 6.6, 6.6, 5.5 Hz, 1H), 1.43 (br , 10H), 1.32 (br, 12H), 1.18–1.14 (m, 1H), 1.04–0.98 (br m, 1H), 0.80–0.76 (m, 1H), 0.70–0.64 (br m, 2H), 0.41–0.36 (br m, 2H). ^{13}C NMR (125 MHz, $CDCl_3$, 23 ºC, δ): 160.8, 155.9, 134.7, 134.1, 129.3, 120.1 (br), 110.3, 83.7, 79.0, 73.1, 46.0, 28.6, 25.0, 24.9, 20.5, 17.6, 10.3, 3.5, 3.5. HRMS-FIA (m/z): calcd for $C_{25}H_{38}BNNaO_5$ $[M + Na]^+$, 466.2741; found, 466.2750.

Palladium aryl complex 2.17

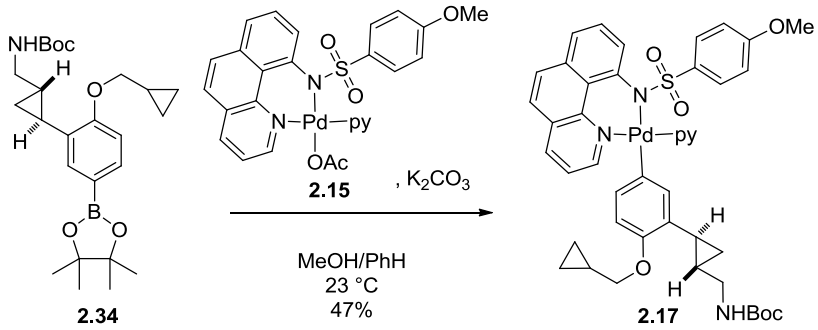

To *t*-butyl (((1*S*,2*S*)-2-(2-(cyclopropylmethoxy)-5-(4,4,5,5-tetramethyl-1,3,2-dioxaborolan-2-yl)phenyl)cyclopropyl)methyl)carbamate (**2.34**) (195 mg, 0.440 mmol, 1.00 equiv) in a round-bottom flask open to air in a 1:1 solution PhH:MeOH (8 mL) was added palladium acetate complex **2.15** (267 mg, 0.440 mmol, 1.00 equiv) and potassium carbonate (91.0 mg, 0.660 mmol, 1.50 equiv). The suspension was stirred at 23 ºC for 4 hours. The reaction was filtered through microfiber filter paper using CH_2Cl_2 (10 mL). The solution was concentrated *in vacuo* and the residue was purified by chromatography on silica gel, eluting with a gradient of 25–75% EtOAc in hexanes to afford 180 mg of the title compound as a

yellow solid (47% yield).

R*f* = 0.30 (hexanes/EtOAc 1:2 (v/v)). NMR Spectroscopy: ^{1}H NMR (500 MHz, CD_2Cl_2, 23 ºC, δ): 8.99 (dd, *J* = 5.1, 1.7 Hz, 2H), 8.33 (ddd, *J* = 9.3, 5.4, 1.5 Hz, 1H), 8.06–8.03 (m, 1H), 7.82–7.77 (m, 2H), 7.66–7.62 (m, 2H), 7.58–7.56 (m, 1H), 7.45 (dd, *J* = 8.5, 5.6 Hz, 1H), 7.35 (dd, *J* = 6.3, 6.3 Hz, 2H), 7.10–7.05 (m, 3H), 6.58 (dd, *J* = 8.3, 1.5, 0.5H), 6.53 (dd, *J* = 8.3, 1.5, 0.5H), 6.37–6.34 (m, 2H), 6.28 (s, 1H), 6.23–6.20 (m, 2H), 5.27 (br, 1H), 3.82 (br dd, *J* = 16.6, 9.8 Hz, 1H), 3.59–3.50 (m, 5H), 2.57–2.52 (br m, 0.5H), 2.58–2.46 (br m, 0.5H), 1.64 (br m, 1H), 1.42–1.29 (m, 10H), 0.84–0.76 (br m, 1H), 0.64–0.53 (m, 4H) 0.31–0.28 (m, 2H). Note: fractional hydrogen integration and broad peaks are possibly due to slow rotation about bonds as seen for similar complexes. ^{13}C NMR (125 MHz CD_2Cl_2, 23 ºC, δ): 160.6, 155.9, 155.4, 155.4, 154.5, 154.3, 153.6, 153.6, 145.1, 145.1, 144.8, 144.4, 143.9, 138.1, 138.0, 136.8, 136.7, 136.6, 132.7, 132.6, 132.5, 130.0, 129.8, 128.9, 128.6, 127.9, 127.7, 127.6, 127.5, 125.9, 125.1, 124.5, 123.7, 121.5, 121.4, 112.5, 110.5, 110.4, 78.8, 73.2, 55.5, 46.0, 28.5, 21.3, 17.6, 17.5, 10.7, 10.1, 3.4. Note: There are more ^{13}C peaks than could be expected, possibly due to slow rotation about bonds as seen for similar complexes (*18*). Anal: calcd for $C_{44}H_{46}N_4O_6PdS$: C, 61.07; H, 5.36; N, 6.47; found: C, 61.02; H, 5.22; N, 6.20.

1-(4-Bromophenyl)-3-((4-methoxyphenyl)amino)propan-1-one (2.35)

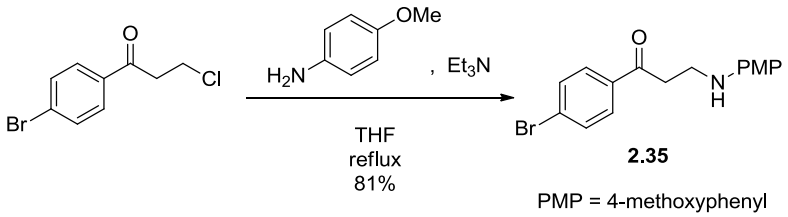

To 1-(4-bromophenyl)-3-chloropropan-1-one (43.4 g, 175 mmol, 1.00 equiv) and 4-methoxyaniline (23.8 g, 193 mmol, 1.10 equiv) in THF (250 mL) in a round-bottom flask fitted with a reflux condenser open to air was added triethylamine (21.3 g, 29.3 mL, 210 mmol, 1.20 equiv). The reaction mixture was heated at reflux for 4 hours and then cooled. The reaction mixture was poured into H_2O (400 mL). EtOAc (300 mL) was added and the organic phase was collected, washed with brine (150 mL), dried with Na_2SO_4, and concentrated *in vacuo*. The residual solid was triturated with diethyl ether (100 mL), collected by filtration,

and dried *in vacuo* to afford 47.4 g of the title compound as a light green solid (81% yield).

R*f* = 0.30 (hexanes/EtOAc 3:1 (v/v)). NMR Spectroscopy: ^{1}H NMR (500 MHz, $CDCl_3$, 23 ºC, δ): 7.82–7.79 (m, 2H), 7.61–7.59 (m, 2H), 6.80–6.77 (m, 2H), 6.63–6.60 (m, 2H), 3.83 (br s, 1H), 3.75 (s, 3H), 3.56 (t, *J* = 6.3 Hz, 2H), 3.22 (t, *J* = 6.2 Hz, 2H). ^{13}C NMR (125 MHz, $CDCl_3$, 23 ºC, δ): 198.5, 152.6, 141.9, 135.6, 132.1, 129.7, 128.7, 115.1, 114.8, 55.9, 39.9, 37.8. HRMS-FIA (m/z): calcd for $C_{16}H_{16}BrNNaO_2$ [M + Na]$^{+}$, 356.0262; found, 356.0254.

4-(4-Bromophenyl)-1-(4-methoxyphenyl)-5,6-dihydropyridin-2(1*H*)-one (2.36)

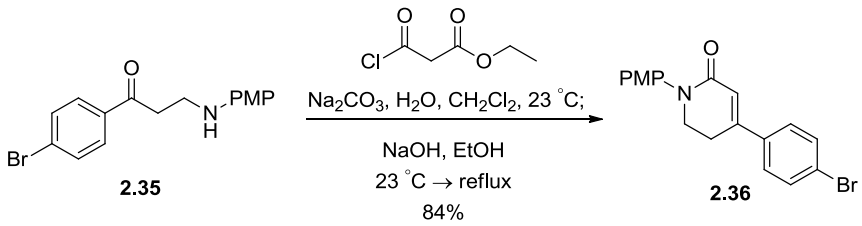

To 1-(4-bromophenyl)-3-((4-methoxyphenyl)amino)propan-1-one (**2.35**) (19.7 g, 58.8 mmol, 1.00 equiv) suspended in CH_2Cl_2 (200 mL) in a round-bottom flask open to air was added ethyl 3-chloro-3-oxopropanoate (9.32 g, 7.84 mL, 58.8 mmol, 1.00 equiv) and a saturated aqueous solution of Na_2CO_3 (100 mL). The reaction mixture was stirred at 23 ºC for 1 hour and then poured onto H_2O (100 mL) in a separatory funnel. The separatory funnel was shaken and the organic phase collected and concentrated *in vacuo*. The residue was dissolved in CH_2Cl_2 (200 mL) and ethyl 3-chloro-3-oxopropanoate (4.66 g, 3.92 mL, 29.4 mmol, 0.500 equiv) and a saturated aqueous solution of Na_2CO_3 (100 mL) were added. The reaction mixture was stirred at 23 ºC for 1 hour and then poured onto H_2O (100 mL) in a separatory funnel. The separatory funnel was shaken and the organic phase collected. The aqueous phase was extracted from with CH_2Cl_2 (100 mL). The combined organic phases were washed with brine (100 mL), dried with Na_2SO_4, and concentrated *in vacuo*. The residue was dissolved in EtOH (400 mL). NaOH (9.41 g, 235 mmol, 4.00 equiv) was added, and the reaction mixture was stirred at 23 ºC for 15 minutes and then heated at reflux for 30 minutes. The reaction mixture was cooled to 23 ºC and then poured into an Erlenmeyer flask containing H_2O (600 mL). The reaction suspension was cooled to 10 ºC in a refrigerator and the precipitate was collected on a frit. Azeotropic removal of water by suspending the solid in benzene and

concentration *in vacuo* (3 × 50 mL) afforded 17.6 g of the title compound as a beige yellow solid (84% yield).

R*f* = 0.20 (hexanes/EtOAc 2:1 (v/v)). NMR Spectroscopy: ^{1}H NMR (500 MHz, $CDCl_3$, 23 ºC, δ): 7.57–7.54 (m, 2H), 7.42–7.40 (m, 2H), 7.28–7.24 (m, 2H), 6.94–6.91 (m, 2H), 6.43 (t, *J* = 1.0 Hz, 1H), 3.93 (t, *J* = 6.8 Hz, 2H), 3.81 (s, 3H), 2.90 (dt, *J* = 6.8, 1.0 Hz, 2H). ^{13}C NMR (125 MHz, $CDCl_3$, 23 ºC, δ): 164.8, 157.9, 148.7, 136.4, 135.5, 132.2, 127.4, 126.5, 124.1, 121.1, 114.4, 55.6, 48.9, 27.1. HRMS-FIA (m/z): calcd for $C_{18}H_{17}BrNO_2[M + H]^+$, 358.0443; found, 358.0440.

(*R*)-4-(4-Bromophenyl)-1-(4-methoxyphenyl)piperidin-2-one (2.37)

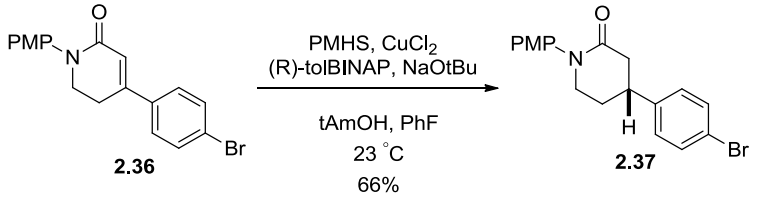

To 4-(4-bromophenyl)-1-(4-methoxyphenyl)-5,6-dihydropyridin-2(1*H*)-one (**2.36**) (28.8 g, 80.0 mmol, 1.00 equiv) suspended in PhF (224 mL) in a round-bottom flask open to air was added *t*-amyl alcohol (113 g, 141 mL, 1.29 mol, 16.0 equiv), polymethylhydrosiloxane (PMHS) (77.0 g, 76.5 mL, 1.29 mol, 16.0 equiv of [H^-], and (*R*)- 2,2'-bis(di-*p*-tolylphosphino)-1,1'-binaphthalene ((*R*)-tol-BINAP) (1.36 g, 2.01 mmol, 0.0250 equiv) and then $CuCl_2$ (0.270 g, 2.01 mmol, 0.0250 equiv) and NaO^{t}Bu (0.773 g, 8.04 mmol, 0.100 equiv). Gas evolved and the reaction mixturereturned orange and then was stirred at 23 ºC for 7 hours. The reaction mixture was poured onto a 1.0 M aqueous solution of HCl (1000 mL), and then the aqueous mixture was extracted with EtOAc (2 × 500 mL). The combined organic phases were washed with brine (300 mL), dried with Na_2SO_4, and concentrated *in vacuo*. The residual solid was triturated with diethyl ether (100 mL), collected by filtration, and dried *in vacuo* to afford 19.1 g of the title compound as a colorless solid (66% yield and 88% *ee* as determined by analysis of (3*S*,4*R*)-methyl 4-(4-bromophenyl)-1-(4-methoxyphenyl)-2-oxopiperidine-3-carboxylate (**2.38**) (see next section and Figure 4.4)). Racemic **2.37** was synthesized using the above procedures using a 1:1 mixture of (*R*)-tol-BINAP and (*S*)-tol-BINAP.

Absolute stereochemistry was assigned by analogy.[92]

R*f* = 0.20 (hexanes/EtOAc 1:1 (v/v)). NMR Spectroscopy: ^{1}H NMR (500 MHz, $CDCl_3$, 23 ºC, δ): 7.50–7.48 (m, 2H), 7.19–7.14 (m, 4H), 6.95–6.92 (m, 2H), 3.81 (s, 3H), 3.74 (ddd, *J* = 12.1, 10.1, 4.6 Hz, 1H), 3.61 (ddd, *J* = 12.4, 5.3, 3.9 Hz, 1H), 3.23 (dddd, *J* = 10.5, 10.5, 5.0, 3.2 Hz, 1H), 2.86 (ddd, *J* = 17.4, 5.3, 2.1 Hz, 1H), 2.64 (dd, *J* = 17.4, 11.0 Hz, 1H), 2.24–2.19 (m, 1H), 2.10 (dddd, *J* = 13.4, 10.7, 10.7, 5.3 Hz, 1H). ^{13}C NMR (125 MHz, $CDCl_3$, 23 ºC, δ): 169.3, 158.4, 142.5, 135.9, 132.0, 128.4, 127.5, 120.8, 114.7, 55.6, 50.9, 39.8, 38.4, 30.7. HRMS-FIA (m/z): calcd for $C_{18}H_{19}BrNO_2$ $[M + H]^+$, 360.0599; found, 360.0588.

(3*S*,4*R*)-Methyl 4-(4-bromophenyl)-1-(4-methoxyphenyl)-2-oxopiperidine-3-carboxylate (2.38)

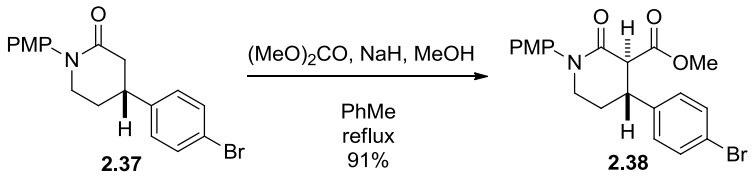

To (*R*)-4-(4-bromophenyl)-1-(4-methoxyphenyl)piperidin-2-one (**2.37**) (19.0 g, 53.7 mmol, 1.00 equiv) and NaH (12.7 g (60% by weight NaH), 320 mmol, 6.0 equiv) in a flame-dried round-bottom flask fitted with a reflux condenser was added toluene (270 mL), MeOH (5.07 g, 6.40 mL, 158 mmol, 3.00 equiv), and dimethyl carbonate (14.3 g, 13.3 mL, 158 mmol, 3.00 equiv). The reaction mixture was heated at reflux for 4 hours, cooled to 23 ºC, and poured onto H_2O (300 mL). The aqueous layer was extracted from with EtOAc (2 × 300 mL). The combined organic phases were washed with brine (300 mL), dried with Na_2SO_4, and concentrated *in vacuo*. The residual solid was triturated with hexanes/EtOAc (150 mL, 1:1 (v/v)), collected by filtration, and dried *in vacuo* to afford 20.0 g of the title compound as a colorless solid (91% yield). Enantiomeric excess (*ee*) of the product was determined to be 88% on a Chiralpak IB column with 35% isopropanol/hexanes eluent (see Figure 4.4).

R*f* = 0.40 (hexanes/EtOAc 1:1 (v/v)). NMR Spectroscopy: ^{1}H NMR (500 MHz, $CDCl_3$, 23 ºC, δ): 7.49–

92. Hughes, G.; Kimura, M.; Buchwald, S. L. *J. Am. Chem. Soc.* **2003**, *125*, 11253.

7.46 (m, 2H), 7.21–7.18 (m, 2H), 7.15–7.13 (m, 2H), 6.93–6.90 (m, 2H), 3.88–3.80 (m, 4H), 3.70 (d, J = 10.5 Hz, 1H), 3.66–3.56 (m, 5H), 2.23–2.17 (m, 2H). ^{13}C NMR (125 MHz, $CDCl_3$, 23 ºC, δ): 170.3, 165.7, 158.5, 140.6, 135.2, 132.2, 128.7, 127.3, 121.4, 114.6, 56.7, 55.6, 52.6, 50.7, 42.1, 29.9. HRMS-FIA (m/z): calcd for $C_{20}H_{21}BrNO_4[M + H]^+$, 418.0654; found, 418.0659.

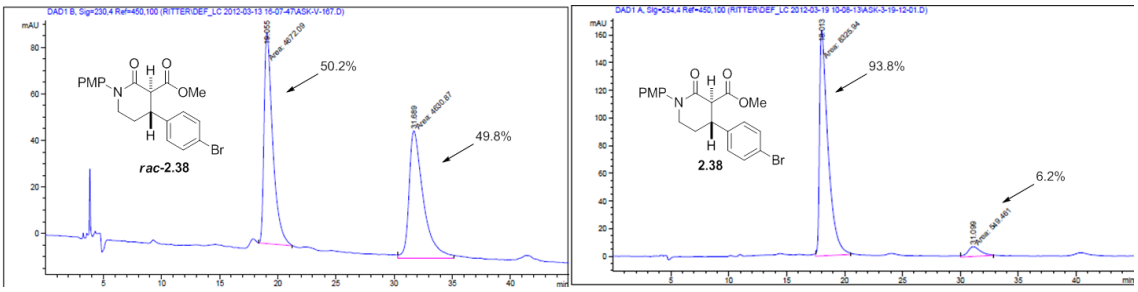

Figure 4.4. Enantiodiscriminating HPLC trace of **2.38**. HPLC method: Chiralpak IB column with 35% isopropanol/hexanes eluent for racemic **2.38** and enantioenriched **2.38**. Percent of total integration listed for each peak.

((3*S*,4*R*)-4-(4-Bromophenyl)-1-(4-methoxyphenyl)piperidin-3-yl)methanol (2.39)

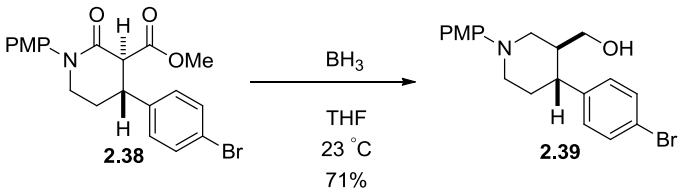

To (3*S*,4*R*)-methyl 4-(4-bromophenyl)-1-(4-methoxyphenyl)-2-oxopiperidine-3-carboxylate (**2.38**) (5.33 g, 12.7 mmol, 1.00 equiv) in a 340 mL pressure tube open to air was added BH_3 (1.0 M solution in THF, 76 mL, 76 mmol, 6.0 equiv). The pressure tube was sealed and the reaction mixture was heated at 90 ºC for 18 hours and then cooled. The reaction mixture was added dropwise over 1 minute to a 1.0 M aqueous solution of NaOH (100 mL). The reaction mixture was extracted from with EtOAc (3 × 60 mL). The combined organic phases were washed with brine (50 mL), dried with Na_2SO_4, and concentrated *in vacuo*. The residue was purified by chromatography on silica gel, eluting with a gradient of 33–50% EtOAc in hexanes (v/v). The resulting solid was then triturated with pentane/diethyl ether (50 mL, 1:1 (v/v)), collected by filtration, and dried *in vacuo* to afford 4.05 g of the title compound as a colorless solid (85% yield). The enantioenriched product could be recrystallized by suspending the solid in MeOH (30 mL),

heating the suspension to reflux to dissolve the solid, cooling the solution, and collecting the solid by filtration, affording 3.40 g (71% yield) of the title compound in >99% *ee* as determined on a Chiracel OD-H column with 10% isopropanol/hexanes eluent (see Figure 4.5).

R*f* = 0.20 (hexanes/EtOAc 2:1 (v/v)). NMR Spectroscopy: ^{1}H NMR (600 MHz, $CDCl_3$, 23 ºC, δ): 7.44–7.43 (m, 2H), 7.12–7.10 (m, 2H), 6.99–6.97 (m, 2H), 6.87–6.84 (m, 2H), 3.82 (ddd, *J* = 11.8, 3.8, 1.8 Hz, 1H), 3.78 (s, 3H), 3.61–3.58 (br m, 1H), 3.48–3.44 (br m, 1H), 3.31–3.27 (br m, 1H), 2.71 (ddd, *J* = 12.0, 12.0, 2.9 Hz, 1H), 2.59 (dd, *J* = 11.5, 11.5 Hz, 1H), 2.42 (ddd, *J* = 11.6, 11.6, 4.1 Hz, 1H), 2.15–2.09 (m, 1H), 1.95 (ddd, *J* = 25.0, 12.3, 4.1 Hz, 1H) 1.90–1.87 (m, 1H). ^{13}C NMR (125 MHz, $CDCl_3$, 23 ºC, δ): 154.1, 146.2, 143.4, 131.9, 129.4, 120.3, 119.2, 114.6, 63.9, 55.7, 55.3, 52.2, 44.2, 44.1, 34.5. HRMS-FIA (m/z): calcd for $C_{19}H_{23}BrNO_2$ $[M + H]^+$, 376.0912; found, 376.0915.

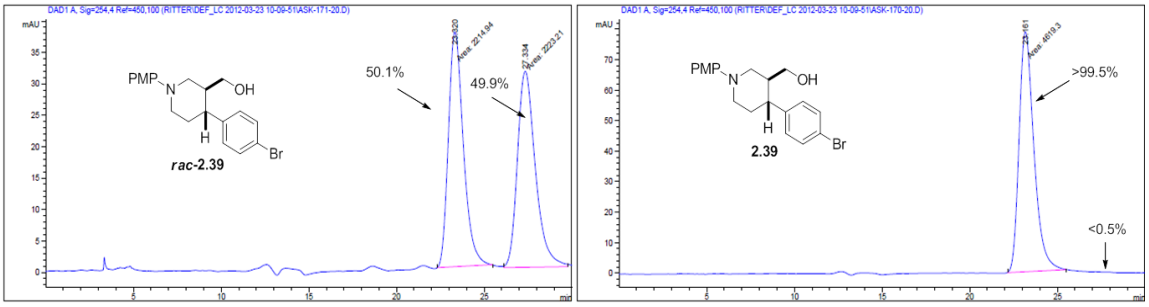

Figure 4.5. Enantiodiscriminating HPLC trace of **2.39**. HPLC method: Chiralcel OD-H column with 10% isopropanol/hexanes eluent for racemic **2.39** and enantioenriched **2.39**. Percent of total integration listed for each peak.

(3*S*,4*R*)-*t*-Butyl 4-(4-bromophenyl)-3-(hydroxymethyl)piperidine-1-carboxylate (2.40)

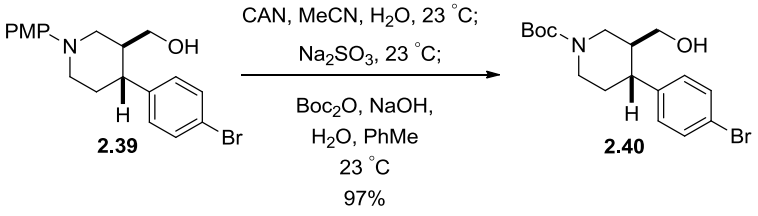

To ((3*S*,4*R*)-4-(4-bromophenyl)-1-(4-methoxyphenyl)piperidin-3-yl)methanol (**2.39**) (6.00 g, 16.0 mmol, 1.00 equiv) suspended in 3:1 solution MeCN/H_2O (320 mL) in a round-bottom flask open to air was added ceric ammonium nitrate (CAN) (35.0 g, 63.8 mmol, 4.00 equiv). The reaction mixture turned purple/red

and then red/orange upon stirring for 30 minutes at 23 ºC. Sodium sulfite (5.02 g, 39.9 mmol, 2.50 equiv) was added and the reaction mixture turned yellow upon stirring for 15 minutes at 23 ºC. The suspension was concentrated *in vacuo* to approximately 50 mL. H_2O (100 mL) and PhMe (150 mL) were added followed by a 3.0 M aqueous solution of NaOH until the reaction mixture pH was greater than 10. Boc_2O (6.96 g, 7.33 mL, 31.9 mmol, 2.00 equiv) was added and the reaction mixture was stirred at 23 ºC for 3 hours. The reaction mixture was filtered through celite. The celite was washed with EtOAc (200 mL) and combined with the reaction mixture in a separatory funnel. The funnel was shaken and the organic phase collected. The aqueous phase was extracted from with EtOAc (2 × 200 mL). The combined organic phases were washed with brine (150 mL), dried with Na_2SO_4, and concentrated *in vacuo*. The residue was purified by chromatography on silica gel, eluting with a gradient of 25–50% EtOAc in hexanes (v/v) to afford 5.70 g of the title compound as a colorless solid (97% yield).

R*f* = 0.20 (hexanes/EtOAc 3:1 (v/v)). NMR Spectroscopy: ^{1}H NMR (500 MHz, $CDCl_3$, 23 ºC, δ): 7.47–7.44 (m, 2H), 7.08–7.05 (m, 2H), 4.38 (br s, 1H), 4.22 (br s, 1H), 3.97 (dd, *J* = 10.1, 2.7 Hz, 1H), 3.81 (dd, *J* = 10.1, 6.8 Hz, 1H), 2.78–2.71 (br m, 2H) 2.53 (ddd, *J* = 11.9, 11.9, 3.8 Hz, 1H), 2.08–2.02 (m, 1H), 1.80 (dd, *J* = 13.3, 2.7 Hz, 1H), 1.66 (ddd, *J* = 25.6, 12.6, 4.4 Hz, 1H), 1.49 (s, 9H). ^{13}C NMR (125 MHz, $CDCl_3$, 23 ºC, δ): 154.7, 141.5, 132.2, 129.2, 121.1, 80.2, 69.5, 44.3, 41.0, 37.3, 34.0, 28.6. Note: The ^{13}C NMR spectrum contains one less carbon signal than is expected. HRMS-FIA (m/z): calcd for $C_{17}H_{23}BrNO_3$ [M - X]$^-$, 368.0861; found, 368.0839.

(3*S*,4*R*)-*t*-Butyl 3-((benzo[*d*][1,3]dioxol-5-yloxy)methyl)-4-(4-bromophenyl)piperidine-1-carboxylate (2.41)

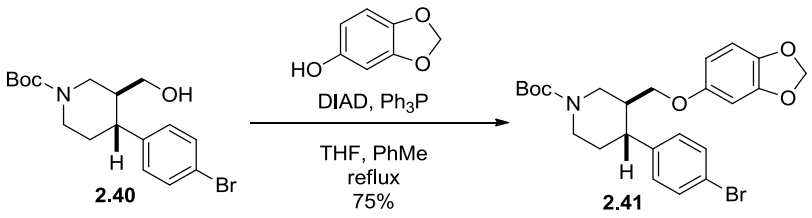

To (3*S*,4*R*)-*t*-Butyl 4-(4-bromophenyl)-3-(hydroxymethyl)piperidine-1-carboxylate (**2.40**) (1.00 g, 2.70 mmol, 1.00 equiv), sesamol (0.746 g, 5.40 mmol, 2.00 equiv), triphenyl phosphine (0.921 g, 3.51 mmol,

1.30 equiv) in a 5:1 solution THF:PhMe (18 mL) in a flame-dried round-bottom flask fitted with a reflux condenser under nitrogen was added diisopropyl azodicarboxylate (DIAD) (0.710 g, 0.691 mL, 3.51 mmol, 1.30 equiv). The reaction mixture was heated at reflux for 18 hours, cooled to 23 ºC, and then poured into a 1.0 M aqueous solution of NaOH in a separatory funnel. The reaction mixture was extracted from with diethyl ether (3 × 50 mL). The combined organic phases were washed with brine (100 mL), dried with $MgSO_4$, and concentrated *in vacuo*. The residue was purified by chromatography on silica gel, eluting with a gradient of 10–20% EtOAc in hexanes (v/v) to afford 0.987 g of the title compound as a colorless solid (75% yield).

R*f* = 0.30 (hexanes/EtOAc 5:1 (v/v)). NMR Spectroscopy: ^{1}H NMR (600 MHz, $CDCl_3$, 23 ºC, δ): 7.42–7.40 (m, 2H), 7.07–7.05 (m, 2H), 6.63 (d, *J* = 8.4 Hz, 1H), 6.35 (d, *J* = 2.5 Hz, 1H), 6.13 (dd, *J* = 8.5, 2.5 Hz, 1H), 5.88 (s, 2H), 4.43 (br s, 1H), 4.24 (br s, 1H), 3.60 (dd, *J* = 9.5, 2.8 Hz, 1H), 3.45 (dd, *J* = 9.4, 6.5 Hz, 1H), 2.82–2.78 (br m, 2H), 2.66 (br dd, *J* = 10.3, 10.3 Hz, 1H), 2.04–1.98 (br m, 1H), 1.80–1.79 (br m, 1H), 1.70 (br ddd, *J* = 25.3, 12.6, 4.1 Hz, 1H), 1.49 (s, 9H). ^{13}C NMR (125 MHz, $CDCl_3$, 23 ºC, δ): 154.9, 154.4, 148.3, 142.6, 141.8, 132.0, 129.3, 120.6, 108.0, 105.7, 101.3, 98.1, 79.9, 68.9, 44.4, 41.8, 33.9, 28.6. Note: The ^{13}C NMR spectrum contains two less carbon signals than is expected. HRMS-FIA (m/z): calcd for $C_{24}H_{29}BrNO_5$ $[M + H]^+$, 490.1229; found, 490.1207.

(3*S*,4*R*)-*t*-Butyl 3-((benzo[*d*][1,3]dioxol-5-yloxy)methyl)-4-(4-(4,4,5,5-tetramethyl-1,3,2-dioxaborolan-2-yl)phenyl)piperidine-1-carboxylate (2.42)

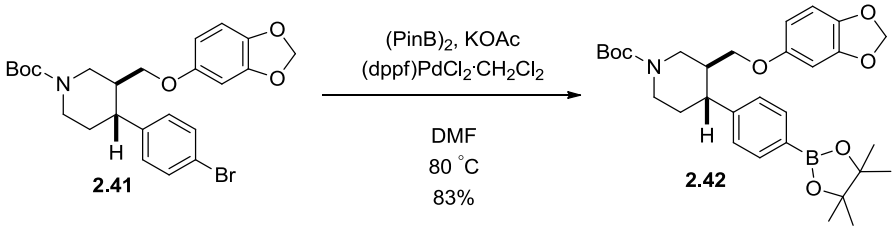

A flame-dried Schlenk tube under a N_2 atmosphere was charged with (3*S*,4*R*)-*t*-butyl 3-((benzo[*d*][1,3]dioxol-5-yloxy)methyl)-4-(4-bromophenyl)piperidine-1-carboxylate (**2.41**) (975 mg, 1.99 mmol, 1.00 equiv), bis(pinacolato)diboron (555 mg, 2.19 mmol, 1.10 equiv), potassium acetate (585 mg, 5.96 mmol, 3.00 equiv), and $PdCl_2(dppf)\cdot CH_2Cl_2$ (49.0 mg, 60.0 μmol, 0.0300 equiv). DMF (30 mL) was

added via syringe. The reaction mixture was degassed via 2 consecutive freeze/pump/thaw cycles. The Schlenk tube was then backfilled with N_2 and heated at 80 ºC for 2.5 hours. The reaction mixture was cooled and poured into H_2O (100 mL). The reaction mixture was extracted from with diethyl ether (3 × 100 mL). The combined organic phases were washed with brine (100 mL), dried with $MgSO_4$, and concentrated *in vacuo*. The residue was purified by chromatography on silica gel, eluting with a gradient of 15–25% EtOAc in hexanes (v/v) to afford 882 mg of the title compound as a colorless solid (83% yield).

R*f* = 0.25 (hexanes/EtOAc 5:1 (v/v)). NMR Spectroscopy: ^{1}H NMR (500 MHz, $CDCl_3$, 23 ºC, δ): 7.77–7.75 (m, 2H), 7.22–7.21 (m, 2H), 6.63 (d, *J* = 8.2 Hz, 1H), 6.36 (d, *J* = 2.7 Hz, 1H), 6.14 (dd, *J* = 8.5, 2.6 Hz, 1H), 5.89 (s, 2H), 4.48 (br s, 1H), 4.27 (br s, 1H), 3.62 (dd, *J* = 9.2, 2.8 Hz, 1H), 3.45 (dd, *J* = 9.6, 6.9 Hz, 1H), 2.82–2.77 (br m, 2H), 2.69 (br dd, *J* = 9.4, 9.4 Hz, 1H), 2.15–2.09 (br m, 1H), 1.84–1.72 (br m, 2H), 1.52 (s, 9H), 1.35 (s, 12H). ^{13}C NMR (125 MHz, $CDCl_3$, 23 ºC, δ): 154.9, 154.4, 148.2, 146.9, 141.7, 135.3, 127.0, 107.9, 105.7, 101.2, 98.2, 83.9, 79.7, 69.0, 45.2, 41.6, 33.8, 28.6, 25.0. Note: The ^{13}C NMR spectrum contains three less carbon signals than is expected. HRMS-FIA (m/z): calcd for $C_{30}H_{41}BNO_7$ [M + H]$^+$, 538.2976; found, 538.2991.

Palladium aryl complex 2.17

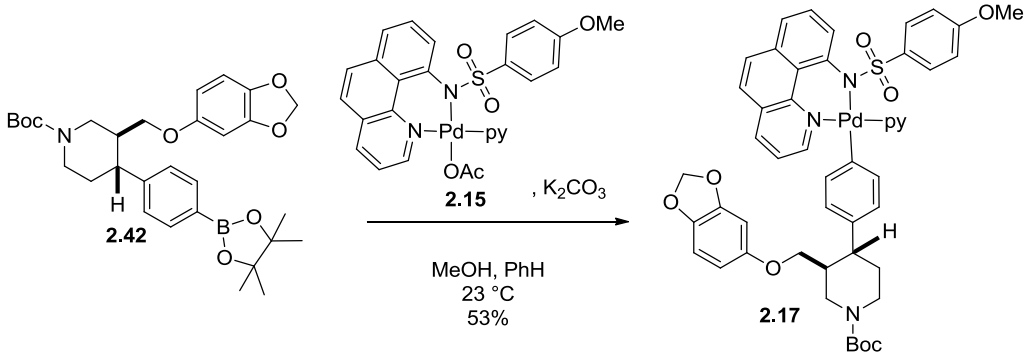

To (3*S*,4*R*)-*t*-butyl 3-((benzo[*d*][1,3]dioxol-5-yloxy)methyl)-4-(4-(4,4,5,5-tetramethyl-1,3,2-dioxaborolan-2-yl)phenyl)piperidine-1-carboxylate (**2.42**) (820 mg, 1.53 mmol, 1.00 equiv) in a round-bottom flask open to air in a 1:1 solution PhH:MeOH (30 mL) was added palladium acetate complex **2.15** (928 mg, 1.53 mmol, 1.00 equiv) and potassium carbonate (316 mg, 2.29 mmol, 1.50 equiv). The suspension was stirred

at 23 ºC for 6 hours. The reaction mixture was filtered through a frit eluting with CH_2Cl_2 (30 mL). The solution was concentrated *in vacuo* and the residue was purified by chromatography on silica gel, eluting with a gradient of 33–80% EtOAc in hexanes to afford 795 mg of the title compound as a yellow solid (54% yield).

R*f* = 0.40 (hexanes/EtOAc 1:3 (v/v)). NMR Spectroscopy: ^{1}H NMR (600 MHz, CD_2Cl_2, 23 ºC, δ): 8.99 (ddd, *J* = 5.0, 3.4, 1.6 Hz, 2H), 8.32 (ddd, *J* = 16.7, 5.4, 1.7 Hz, 1H), 8.00 (ddd, *J* = 17.9, 4.0, 1.6 Hz, 1H), 7.79–7.76 (m, 2H), 7.65–7.60 (m, 3H), 7.44 (dd, *J* = 8.8, 4.1 Hz, 1H), 7.32 (ddd, *J* = 7.6, 5.1, 1.5 Hz, 2H), 7.12–7.09 (m, 2H), 6.94 (ddd, *J* = 15.5, 7.9, 5.3 Hz, 1H), 6.85 (dd, *J* = 9.1, 8.1 Hz, 2H), 6.65–6.61 (m, 3H), 6.27 (dd, *J* = 14.0. 2.4 Hz, 1H), 6.24–6.21 (m, 2H), 6.09 (ddd, *J* = 8.5, 2.3, 2.3 Hz, 1H), 5.91 (dd, *J* = 4.5, 1.3 Hz, 1H), 5.90 (dd, *J* = 2.0, 1.4 Hz, 1H), 4.38 (br s, 1H), 4.15 (br s, 1H), 3.55 (s, 3H), 3.47 (ddd, *J* = 9.4, 9.4, 3.0 Hz, 1H), 3.33 (ddd, *J* = 19.7, 9.7, 7.8 Hz, 1H), 2.73–2.63 (br m, 2H), 2.37–2.31 (m, 1H), 2.91–1.85 (br m, 1H), 1.69–1.56 (m, 2H), 1.45 (s, 9H). ^{13}C NMR (125 MHz, CD_2Cl_2, 23 ºC, δ): 160.5, 154.9, 154.8, 154.3, 153.4, 148.5, 145.0, 143.8, 141.9, 138.5, 138.1, 138.0, 136.9, 136.6, 135.1, 130.0. 127.9, 127.7, 127.3, 126.3, 126.3, 125.1, 124.5, 123.7, 121.3, 112.5, 108.1, 106.1, 101.1, 98.1, 97.9, 79.4, 69.7, 55.5, 44.7, 42.3, 42.1, 33.9, 28.5. Note: The ^{13}C NMR spectrum contains two less carbon signals than is expected. δ):. Anal: calcd for $C_{49}H_{48}N_4O_8PdS$: C, 61.34; H, 5.04; N, 5.84; found: C, 61.09; H, 4.84; N, 5.74.

Fluorination of aryl palladium complexes

3-Benzyloxyphenyl fluoride (2.5)

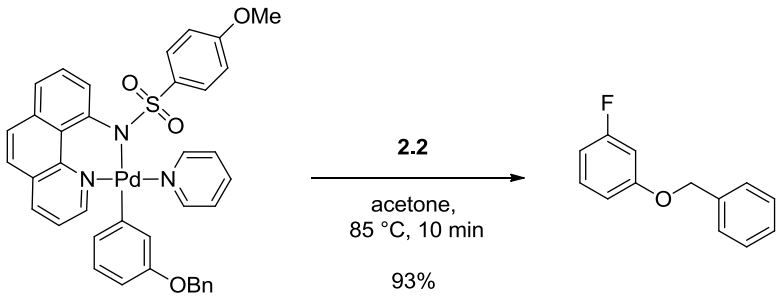

In a glove box under a N_2 atmosphere, palladium aryl complex **2.3** (100 mg, 0.140 mmol, 1.00 equiv) was dissolved in acetone (7 mL) and added to a soda lime glass bottle charged with Pd(IV)-F complex **2.2** (102 mg, 0.140 mmol, 1.00 equiv). The bottle was sealed, taken out of the glove box, and immersed in an oil bath heated at 85 ºC for 10 minutes. The reaction mixture was cooled and concentrated *in vacuo*. The residue was extracted from with diethyl ether (5 × 5 mL). The extract was concentrated *in vacuo* and the residue was purified by chromatography on silica gel eluting with hexanes/EtOAc 10:1 (v/v) to afford 25.6 mg of the title compound as a colorless oil (93% yield).

R_f = 0.55 (hexanes/EtOAc 20:1 (v/v)). NMR Spectroscopy: ^{1}H NMR (500 MHz, $CDCl_3$, 23 ºC, δ): 7.44–7.33 (m, 5H), 7.26–7.21 (m, 1H), 6.78–6.66 (m, 3H), 5.06(s, 2H). ^{13}C NMR (125 MHz, $CDCl_3$, 23 ºC, δ): 163.8 (d, J = 246 Hz), 160.3 (d, J = 11 Hz), 136.6, 130.4 (d, J = 10 Hz), 128.8, 128.3, 127.6, 110.8 (d, J = 3 Hz), 107.9 (d, J = 22 Hz), 102.8 (d, J = 25 Hz), 70.4. ^{19}F NMR (375 MHz, CD_3CN, 23 ºC, δ): –112.2 (m). These spectroscopic data correspond to previously reported data.[93]

3-Deoxy-3-fluoroestrone (2.6)

---

93. Watson, D. A.; Su, M. J.; Teverovskiy, G.; Zhang, Y.; Garcia-Fortanet, J.; Kinzel, T.; Buchwald, S. L. *Science* **2009**, *325*, 1661.

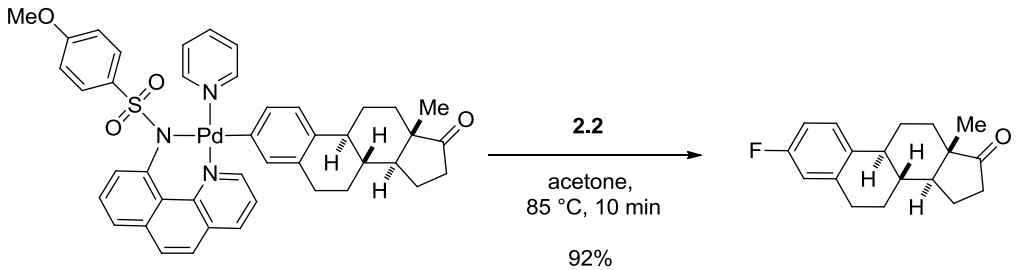

2.4 **2.6**

In a glove box under a N_2 atmosphere, palladium aryl complex **2.4** (100 mg, 0.124 mmol, 1.00 equiv) was dissolved in acetone (7 mL) and added to a soda lime glass bottle charged with Pd(IV)-F complex **2.2** (90.7 mg, 0.124 mmol 1.00 equiv). The bottle was sealed, taken out of the glove box, and immersed in an oil bath heated at 85 ºC for 10 minutes. The reaction mixture was cooled and concentrated *in vacuo*. The residue was extracted from with diethyl ether (5 × 5 mL). The extract was concentrated *in vacuo* and the residue was purified by chromatography on silica gel eluting with hexanes/EtOAc 10:1 (v/v) to afford 31.1 mg of the title compound as a colorless solid (92% yield).

R_f = 0.33 (hexanes/EtOAc 9:1 (v/v)). NMR Spectroscopy: ^{1}H NMR (500 MHz, $CDCl_3$, 23 ºC, δ): 7.23 (dd, *J* = 8.5 Hz, 3.2 Hz, 1H), 6.83 (td, *J* = 8.5 Hz, 2.1 Hz, 1H), 6.79 (dd, *J* = 9.6 Hz, 3.2 Hz, 1H), 2.91–2.89 (m, 2H), 2.54–2.48 (m, 1H), 2.42–2.38 (m, 1H), 2.29–2.23 (m, 1H), 2.18–1.94 (m, 4H), 1.67–1.41 (m, 6H,), 0.92 (s, 3H). ^{13}C NMR (125 MHz, $CDCl_3$, 23 ºC, δ): 220.8, 161.2 (d, *J* = 244 Hz), 138.8 (d, *J* = 6 Hz), 135.5 (d, *J* = 3 Hz), 126.9 (d, *J* = 8 Hz), 115.3 (d, *J* = 20 Hz), 112.6 (d, *J* = 21 Hz), 50.5, 48.1, 44.1, 38.3, 36.0, 31.7, 29.6, 26.5, 26.0, 21.7, 14.0. ^{19}F NMR (375 MHz, $CDCl_3$, 23 ºC, δ): –117.1. These spectroscopic data correspond to previously reported data.[94]

(*Z*)-3-(Bis(4-methoxyphenyl)methyl)-5-((5-(4-fluoro-2-(methoxymethoxy)phenyl)furan-2-yl)methylene)thiazolidine-2,4-dione (2.19)

94. Tang, P. P.; Furuya, T.; Ritter, T. *J. Am. Chem. Soc.* **2010**, *132*, 12150.

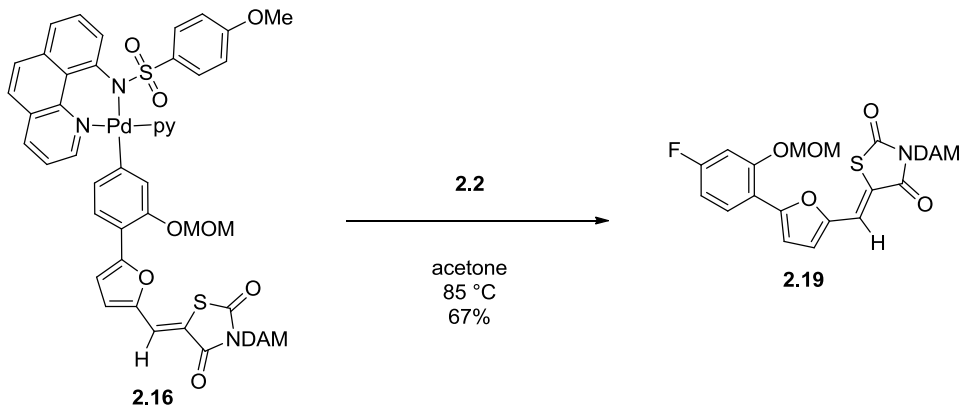

In a glove box under a N_2 atmosphere, palladium aryl complex **2.16** (90.0 mg, 81.4 umol, 1.00 equiv) was dissolved in acetone (5 mL) and added to a soda lime glass bottle charged with Pd(IV)-F complex **2.2** (62.6 mg, 85.5 umol, 1.05 equiv). The bottle was sealed, taken out of the glove box, and immersed in an oil bath heated at 85 ºC for 10 minutes. The reaction mixture was cooled and concentrated *in vacuo*. The residue was purified by chromatography on silica gel, eluting with a gradient of 10–25% EtOAc in hexanes to afford 31.5 mg of the title compound as a bright yellow solid (67% yield).

R_f = 0.20 (hexanes/EtOAc 3:1 (v/v)). NMR Spectroscopy: ^{1}H NMR (600 MHz, $CDCl_3$, 23 ºC, δ): 7.88 (dd, *J* = 7.6, 6.6 Hz, 1H), 7.61 (s, 1H), 7.31–7.29 (m, 4H), (7.06 (dd, *J* = 3.7, 1.0 Hz, 1H), 6.99 (dd, *J* = 10.6, 1.3 Hz, 1H), 6.89–6.87 (m, 5H), 6.74 (s, 1H), 5.32 (s, 2H), 3.81 (s, 6H), 3.51 (s, 3H). ^{13}C NMR (125 MHz, $CDCl_3$, 23 ºC, δ): 168.7, 166.1, 163.5 (d, *J* = 251 Hz), 159.3, 155.1 (d, *J* = 10 Hz), 154.3, 148.2, 130.1, 129.6, 128.1 (d, *J* = 10 Hz), 120.7, 119.4, 117.8, 115.4, 113.9, 112.8, 109.4 (d, *J* = 22 Hz), 102.9 (d, *J* = 26 Hz), 94.7, 60.3, 56.6, 55.4. ^{19}F NMR (375 MHz, $CDCl_3$, 23 ºC, δ): –108.4 (ddd, *J* = 11.0, 7.3, 7.3 Hz). HRMS-FIA (m/z): calcd for $C_{31}H_{26}FNNaO_7S$ $[M + Na]^+$, 598.1312; found, 598.1322.

***t*-Butyl (((1*S*,2*S*)-2-(2-(cyclopropylmethoxy)-5-fluorophenyl)cyclopropyl)methyl)carbamate (2.20)**

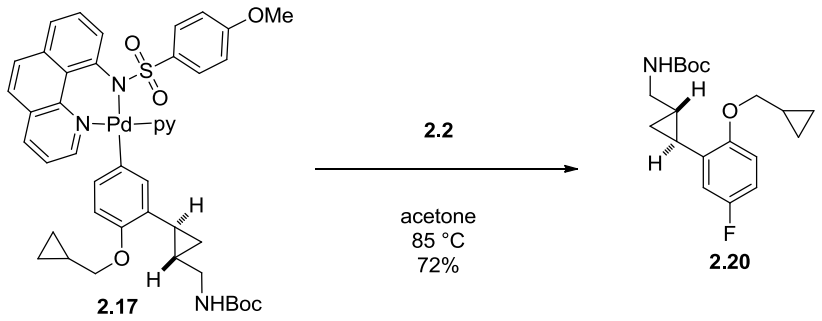

In a glove box under a N_2 atmosphere, palladium aryl complex **2.17** (25.0 mg, 29.4 umol, 1.20 equiv) was dissolved in acetone (3 mL) and added to a soda lime glass bottle charged with Pd(IV)-F complex **2.2** (18.0 mg, 24.5 umol, 1.00 equiv). The bottle was sealed, taken out of the glove box, and immersed in an oil bath heated at 85 ºC for 10 minutes. The reaction mixture was cooled and concentrated *in vacuo*. The residue was purified by chromatography on silica gel, eluting with a gradient of 10–15% EtOAc in hexanes to afford 5.9 mg of the title compound as a colorless solid (72% yield).

R_f = 0.35 (hexanes/EtOAc 85:15 (v/v)). NMR Spectroscopy: ^{1}H NMR (500 MHz, $CDCl_3$, 23 ºC, δ): 6.80 (ddd, *J* = 8.8, 8.8, 2.9 Hz, 1H), 6.72 (dd, *J* = 9.1, 4.9, Hz, 1H), 6.66 (dd, *J* = 9.3, 3.0 Hz, 1H), 5.27 (br s, 1H), 3.96 (dd, *J* = 9.8, 6.8 Hz, 1H), 3.71 (dd, *J* = 9.8, 7.8 Hz, 1H), 3.66 (br s, 1H), 2.69 (br m, 1H), 1.88 (ddd, *J* = 6.8, 6.8, 4.9 Hz, 1H), 1.43–1.38 (m, 10H), 1.05–0.99 (m, 2H), 0.85–0.80 (m, 1H), 0.72–0.62 (m, 2H), 0.42–0.32 (m, 2H). ^{13}C NMR (125 MHz, $CDCl_3$, 23 ºC, δ): 157.2 (d, *J* = 238 Hz), 155.9, 154.1, 132.3 (d, *J* = 7 Hz), 114.1 (d, *J* = 24 Hz), 112.7 (d, *J* = 23 Hz), 112.2 (d, *J* = 9 Hz), 79.1, 73.9, 45.7, 28.6, 21.3, 17.5, 10.8, 10.4, 10.2, 3.5. ^{19}F NMR (375 MHz, $CDCl_3$, 23 ºC, δ): –123.8 (dd, *J* = 12.8, 8.0 Hz). HRMS-FIA (m/z): calcd for $C_{19}H_{26}FNNaO_3$ $[M + Na]^+$, 358.1794; found, 358.1808.

(3*S*,4*R*)-*t*-Butyl 3-((benzo[*d*][1,3]dioxol-5-yloxy)methyl)-4-(4-fluorophenyl)piperidine-1-carboxylate (2.21)

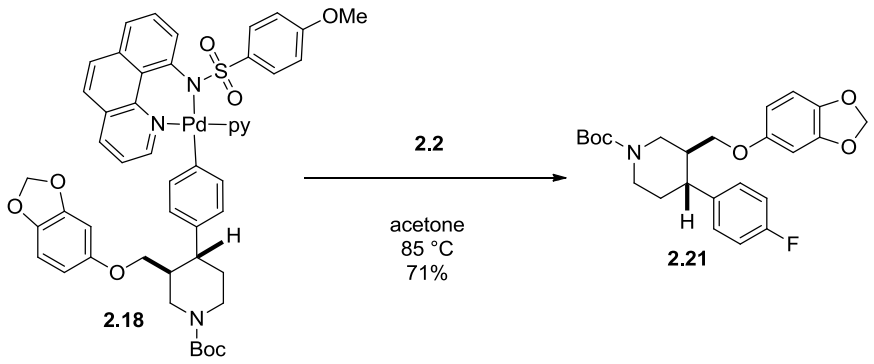

In a glove box under a N_2 atmosphere, palladium aryl complex **2.18** (135 mg, 141 μmol, 1.00 equiv) was dissolved in acetone (6 mL) and added to a soda lime glass bottle charged with Pd(IV)-F complex **2.2** (103 mg, 141 μmol, 1.00 equiv). The bottle was sealed, taken out of the glove box, and immersed in an oil bath heated at 85 ºC for 10 minutes. The reaction mixture was cooled and concentrated *in vacuo*. The residue was purified by chromatography on silica gel, eluting with a gradient of 10–20% EtOAc in hexanes to afford 42.7 mg of the title compound as a colorless solid (71% yield). The enantiomeric excess of the title compound remained >99% *ee* as determined on a Chiracel OD-H column with 3% isopropanol/hexanes eluent. The absolute configuration was identical to a sample of the title compound prepared from commercially available paroxetine (see Figure 4.6).

R_f = 0.25 (hexanes/EtOAc 6:1 (v/v)). NMR Spectroscopy: ^{1}H NMR (500 MHz, $CDCl_3$, 23 ºC, δ): 7.15–7.11 (m, 2H), 6.99–6.96 (m, 2H), 6.62 (d, J = 8.3 Hz, 1H), 6.34 (d, J = 2.4 Hz, 1H), 6.13 (dd, J = 8.8, 2.4 Hz, 1H), 5.88 (s, 2H), 4.43 (br s, 1H), 4.24 (br s, 1H), 3.60 (dd, J = 9.7, 2.9 Hz, 1H), 3.44 (dd, J = 9.5, 6.5 Hz, 1H), 2.82–2.77 (br m, 2H), 2.67 (br ddd, J = 11.5, 11.5, 2.7 Hz, 1H), 2.04–1.99 (br m, 1H), 1.81–1.78 (br m, 1H), 1.70 (br ddd, J = 24.9, 12.7, 4.4 Hz, 1H), 1.50 (s, 9H). ^{13}C NMR (125 MHz, $CDCl_3$, 23 ºC, δ): 161.7 (d, J = 244 Hz), 155.0, 154.4, 148.3, 141.8, 139.3 (d, J = 3 Hz), 128.9 (d, J = 7 Hz), 115.6 (d, J = 19 Hz), 108.0, 105.7, 101.2, 98.1, 79.8, 69.0, 44.2, 42.1, 34.1, 28.6. Note: The ^{13}C NMR spectrum contains two less carbon signals than is expected. ^{19}F NMR (375 MHz, $CDCl_3$, 23 ºC, δ): –116.0– –116.1 (m). HRMS-FIA (m/z): calcd for $C_{24}H_{29}FNO_5$ $[M + H]^+$, 430.2030; found, 430.1998.

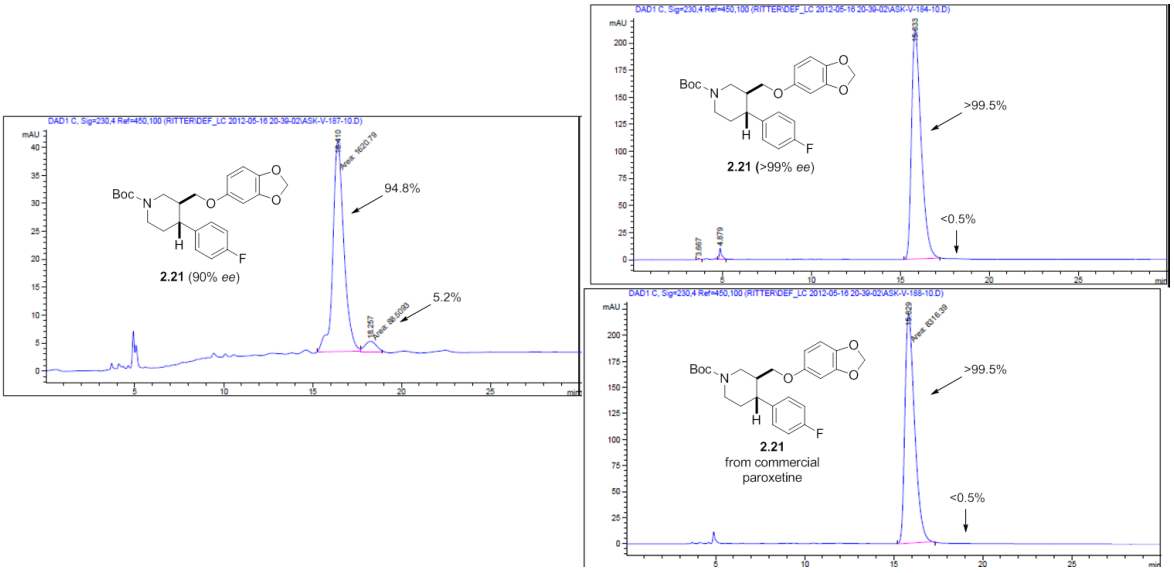

Figure 4.6. Enantiodiscriminating HPLC trace of **2.21**. HPLC method: Chiralcel OD-H column with 3% isopropanol/hexanes eluent for 90% ee **2.21** and for >99% ee **2.21** and **2.21** synthesized from commercially available paroxetine. Percent of total integration listed for each peak.

Deprotection of aryl fluorides

((1*S*,2*S*)-2-(2-(Cyclopropylmethoxy)-5-fluorophenyl)cyclopropyl)methanaminium 2,2,2-trifluoroacetate (2.43)

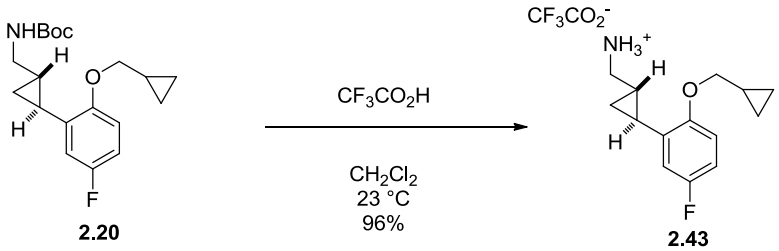

t-butyl(((1S,2S)-2-(2-(cyclopropylmethoxy)-5-fluorophenyl)cyclopropyl)methyl)carbamate (**2.20**) (65.0 mg, 0.194 mmol, 1.00 equiv) was dissolved in a 1:1 solution CH_2Cl_2:CF_3CO_2H (2 mL). The solution was stirred at 23 ºC for 10 minutes. The solution was then dripped into saturated aqueous $NaHCO_3$ solution (20 mL). The aqueous layer was extracted with EtOAc (3 × 10 mL). The combined organic phases were washed with brine (15 mL), dried with Na_2SO_4, and concentrated *in vacuo*. The residue was purified by chromatography on silica gel that had been washed with Et_3N, eluting with 0–10% MeOH in CH_2Cl_2 (v/v)

to afford the amine base. The title compound was isolated by adding a 10% CF_3CO_2H in CH_2Cl_2 solution (1 mL) to the amine base. The solution was concentrated *in vacuo* and heated *in vacuo* at 50 ºC to provide 65.5 mg of the title compound (96% yield).

NMR Spectroscopy: ^{1}H NMR (500 MHz, D_2O, 23 ºC, δ): 6.99 (dd, *J* = 9.0, 5.0 Hz, 1H), 6.95 (ddd, *J* = 9.0, 9.0, 3.0 Hz, 1H), 6.78 (dd, *J* = 10.0, 3.0 Hz, 1H), 3.95 (dd, *J* = 10.0, 7.0, 1H), 3.87 (dd, *J* = 10.0, 2.5 Hz, 1H), 3.16 (dd, *J* = 12.0, 7.0 Hz, 1H), 3.02 (dd, *J* = 13.0, 8.0 Hz, 1H), 2.16 (ddd, *J* = 7.0, 7.0, 5.0 Hz, 1H), 1.38–1.27 (m, 2H), 1.16 (ddd, *J* = 5.5, 5.3, 5.3 Hz, 1H), 1.07 (ddd, *J* = 7.3, 7.3, 5.5 Hz, 1H), 0.65–0.62 (m, 2H), 0.37–0.34 (m, 2H). ^{19}F NMR (375 MHz, D_2O, 23 ºC, δ): -76.1 (s, 3F), -123.9 (ddd, *J* = 7.2, 7.2, 6.0, 1F). ^{13}C NMR (125 MHz, D_2O, 23 ºC, δ): 157.7 (d, *J* = 237 Hz), 153.4 (d, *J* = 2 Hz), 132.4 (d, *J* = 7 Hz), 115.4 (d, *J* = 9 Hz), 113.4 (d, *J* = 23 Hz), 113.1 (d, *J* = 24 Hz), 75.8, 43.9, 18.7, 16.7, 12.6, 9.9, 2.9, 2.6. HRMS-FIA (m/z): $[C_{14}H_{19}FNO + Na]^+$ calcd for $C_{14}H_{19}FNNaO$, 258.1270; found, 258.1274.

(3*S*,4*R*)-3-((Benzo[*d*][1,3]dioxol-5-yloxy)methyl)-4-(4-fluorophenyl)piperidine (2.44)

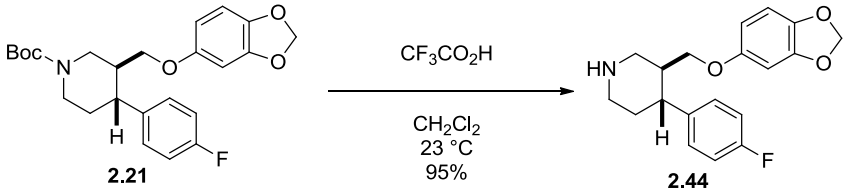

(3*S*,4*R*)-*t*-butyl 3-((benzo[*d*][1,3]dioxol-5-yloxy)methyl)-4-(4-fluorophenyl)piperidine-1-carboxylate (**2.21**) (35.0 mg, 81.5 μmol, 1.00 equiv) was dissolved in a 7:1 solution CH_2Cl_2:CF_3CO_2H (2 mL). The solution was stirred at 23 ºC for 15 minutes. The solution was then dripped into saturated aqueous $NaHCO_3$ solution (10 mL). The aqueous layer was extracted with CH_2Cl_2 (3 × 10 mL). The combined organic phases were washed with brine (15 mL), dried with Na_2SO_4, and concentrated *in vacuo*. The residue was purified by chromatography on silica gel that had been washed with Et_3N, eluting with 0–10% MeOH in CH_2Cl_2 (v/v) to afford 25.6 mg of the title compound as a colorless oil (95% yield).

R_f = 0.35 (CH_2Cl_2/MeOH 19:1 (v/v) (Et_3N washed silica)). NMR Spectroscopy: ^{1}H NMR (600 MHz, $CDCl_3$, 23 ºC, δ): 7.18–7.16 (m, 2H), 6.98–6.96 (m, 2H), 6.61 (d, *J* = 8.5 Hz, 1H), 6.33 (d, *J* = 2.3 Hz, 1H), 6.13 (dd, *J* = 8.5, 2.5 Hz, 1H), 5.86 (s, 2H), 4.65 (br s, 1H), 3.56 (dd, *J* = 9.4, 2.6 Hz, 1H), 3.56 (dd, *J* = 9.4,

2.6 Hz, 1H), 3.48 (dd, J = 12.4, 3.6 Hz, 1H), 3.44 (dd, J = 9.2, 6.7 Hz, 1H), 3.28 (d, J = 12.2 Hz, 1H), 2.83–2.76 (m, 2H), 2.65 (ddd, J = 11.0, 11.0, 5.7 Hz, 1H), 2.22–2.17 (m, 1H), 1.91–1.84 (m, 2H). ^{13}C NMR (125 MHz, $CDCl_3$, 23 ºC, δ): 161.7 (d, J = 244 Hz), 154.3, 148.3, 141.8, 139.4 (d, J = 3 Hz), 128.9 (d, J = 8 Hz), 115.6 (d, J = 21 Hz), 107.9, 105.6, 101.2, 98.0, 69.1, 49.6, 46.5, 44.0, 42.2, 34.2. ^{19}F NMR (375 MHz, $CDCl_3$, 23 ºC, δ): -116.0 (tt, J = 8.6, 5.5 Hz). HRMS-FIA (m/z): calcd for $C_{19}H_{21}FNO_3$ $[M + H]^+$, 330.1505; found, 330.1497.

4.3 Radiochemistry General Methods

No-carrier-added [^{18}F]fluoride was produced from water 97% enriched in ^{18}O (Sigma-Aldrich®) by the nuclear reaction $^{18}O(p,n)^{18}F$ using a Siemens Eclipse HP cyclotron and a silver-bodied target at MGH Athinoula A. Martinos Center for Biomedical Imaging. The produced [^{18}F]fluoride in water was transferred from the cyclotron target by helium push. Liquid chromatographic analysis (LC) was performed with Agilent 1100 series HPLCs connected to a Carol and Ramsey Associates Model 105-S radioactivity detector. An Agilent Eclipse XDB-C18, 5 μm, 4.6 x 150 mm HPLC column was used for analytical analysis and a Macherey-Nagel VP 250/10 Nucleosil 100-5 C18 Nautilus column was used for preparative HPLC. In the analysis of the ^{18}F-labeled compounds, isotopically unmodified reference substances were used for identification. Radioactivity was measured in a Capintec, Inc. CRC-25PET ion chamber. *Solvents and reagents for radiochemical experiments:* Acetone (HPLC grade) was distilled over B_2O_3 and subsequently redistilled before use. 2-Butanone was distilled over B_2O_3. Acetonitrile was distilled over P_2O_5. Water was obtained from a Millipore Milli-Q Integral Water Purification System. 18-crown-6 was sublimed. Potassium bicarbonate (≥99.99%) and JandaJel™-polypyridine (100-200 mesh, extent of labeling: ~8.0 mmol/g loading, 1% cross-linked) were purchased from Sigma-Aldrich® and dried at 23 °C for 24 hours under dynamic vacuum (10^{-4} Torr) before use. Cotton was washed with acetone and water and dried at 150°C.

4.4 Radiosynthesis of ^{18}F-labeled Molecules

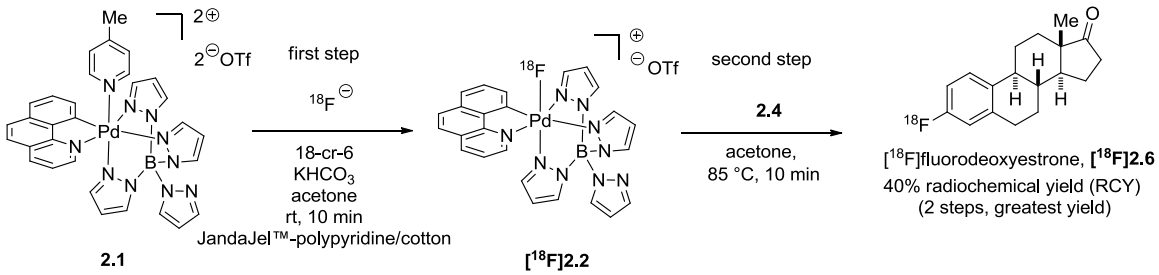

[^{18}F]Fluoride solution obtained from a cyclotron was loaded onto a Macherey-Nagel SPE Chromafix 30-PS-HCO3 cartridge that had been previously washed with 2.0 mL of 5.0 mg/mL $KHCO_3$ in Millipore Milli-Q water and then 20 mL of Millipore Milli-Q water. After loading, the cartridge was washed with 2 mL of Millipore Milli-Q water. [^{18}F]Fluoride was eluted with 2.0 mL of a 5.0 mg/mL $KHCO_3$ in Millipore Milli-Q water solution. The solution was diluted with 8.0 mL of acetonitrile providing 10. mL of 4:1 MeCN:H_2O solution containing 1.0 mg/mL $KHCO_3$. 1.0 mL of this solution was then put in a magnetic-stir-bar-containing conical vial that had been washed with acetone, deionized water, sodium hydroxide/ethanol solution, and deionized water, and dried at 150 °C prior to use. 0.50 mL of a stock solution containing 18-crown-6 (26.2 mg/mL MeCN) was then added. The solution was evaporated at 108 °C with a constant nitrogen gas stream. At dryness, 0.5 mL of acetonitrile was added and evaporated at 108 °C with a constant nitrogen gas stream. Another 0.5 mL of acetonitrile was added and evaporated at 108 °C with a constant nitrogen gas stream to leave a white precipitate around the bottom and sides of the vial. 0.5 mL of acetone was added and evaporated to dryness at 108 °C with a constant nitrogen gas stream to leave a glassy film on the bottom and sides of the vial. The vial was cooled in a water bath, purged with nitrogen, and sealed with a cap fitted with a septum.

First step: 10. mg of Pd(IV) complex **2.1** dissolved in 0.5 mL of acetone was added via the septum to the vial. The vial was sonicated and then the reaction mixure was allowed to stir at 23 °C for 10 minutes. During this time, the orange/brown clear solution became opaque. At the end of 10 minutes, the vial was opened and the suspension was loaded with a glass pipette into another glass pipette containing 10 mg of cotton and 25 mg of JandaJel™-polypyridine that had been suspended in 0.3 mL of acetone for 15 minutes (to swell the JandaJel™-polypyridine) and then drained prior to loading the reaction suspension. The

conical vial was washed with 0.5 mL of acetone and the acetone wash was added onto the JandaJel™-polypyridine in the glass pipette. At this point the combined reaction suspension and acetone wash were fully pushed through the JandaJel™-polypyridine and cotton with air into a new 1 dram vial equipped with a magnetic stir bar. An additional 0.5 mL of acetone was used to wash the conical vial. The acetone wash was added onto the JandaJel™-polypyridine in the glass pipette and pushed through with air into the 1 dram vial.

Second step: To the 1.5 mL acetone solution was added 10. mg of the Pd(II) aryl complex. The vial was capped securely, and the mixture heated at 85 °C. After 10 minutes the solution was cooled. A capillary tube was used to spot the solution on a silica gel TLC plate. The TLC plate was emerged in an appropriate organic solvent mixture. The TLC plate was scanned with a Bioscan AR-2000 Radio TLC Imaging Scanner.

Measurement of radiochemical yield:

Radiochemical yield was determined by multiplying the percentage of radioactivity in the final solution and the relative peak integrations of a radio TLC scan. First, the radioactivity of the 1.5 mL solution collected after filtration was measured in an ion chamber, followed by the amount of radioactivity on the JandaJel™-polypyridine/cotton pipette and the amount of radioactivity left on the walls of the initial conical vial. These measurements determined the fraction of radioactivity that entered the second step (typically 55–75%). After the second step was complete the solution was transferred to a second 1 dram vial using an additional 0.5 mL acetone wash and the amount of radioactivity in this solution was measured. The amount of radioactivity on the original 1 dram vial was then measured to determine the percentage of radioactivity of the solution that spotted onto the TLC plate (typically 90%). After radio TLC quantification, the radiochemical yield was determined by multiplying the product quantified during TLC by the fraction of radioactivity in solution over two steps (typically 50–70%).

For example, Entry 1 of Radiochemical Yield Data section:

Measured radioactivity in 1.5 mL acetone solution after first step: 256 μCi
Measured radioactivity of pipette containing JandaJel™-polypyridine and cotton: 30 μCi
Measured radioactivity of conical vial from first step: 26 μCi
Radioactivity percentage that entered second step: 82% ((256 + 30 + 26) / 256 * 100)
Measured radioactivity of acetone solution after second step: 215 μCi
Measured radioactivity of dram vial from second step:16 μCi
Radioactivity percentage from second step that was spotted on to TLC plate: 93% ((215 + 16) / 215 * 100)
Percent ^{18}F in solution: 76% (0.82 * 0.93 * 100)
Radio TLC yield (RTLC yield): 43%
Radiochemical yield (RCY): **33%** (0.76 * 0.43 * 100)

Table 4.1. Radiochemical yield data

Entry	Molecule	RTLC yield	% ^{18}F in solution	RCY	Average RCY
1	**[^{18}F]2.6**	43	76%	33	
2	**[[^{18}F]2.6**	51	68%	35	
3	**[^{18}F]2.6**	36	76%	27	
4	**[^{18}F]2.6**	43	69%	30	
5	**[^{18}F]2.6**	58	68%	40	
6	**[^{18}F]2.6**	57	66%	38	
7	**[^{18}F]2.6**	49	57%	28	
8	**[^{18}F]2.6**	44	66%	29	**33**
9	**[^{18}F]2.19**	21	54%	11	
10	**[^{18}F]2.19**	21	55%	11	
11	**[^{18}F]2.19**	16	50%	8	
12	**[^{18}F]2.19**	25	46%	11	
13	**[^{18}F]2.19**	19	46%	9	
14	**[^{18}F]2.19**	17	65%	11	
15	**[^{18}F]2.19**	19	58%	11	**10**
16	**[^{18}F]2.20**	45	51%	23	
17	**[^{18}F]2.20**	30	59%	18	
18	**[^{18}F]2.20**	27	60%	16	
19	**[^{18}F]2.20**	27	61%	16	
20	**[^{18}F]2.20**	30	58%	17	
21	**[^{18}F]2.20**	31	54%	17	
22	**[^{18}F]2.20**	30	53%	16	
23	**[^{18}F]2.20**	29	61%	18	**18**
24	**[^{18}F]2.21**	52	51%	26	
25	**[^{18}F]2.21**	27	67%	18	**22**

Example radio TLC scans:

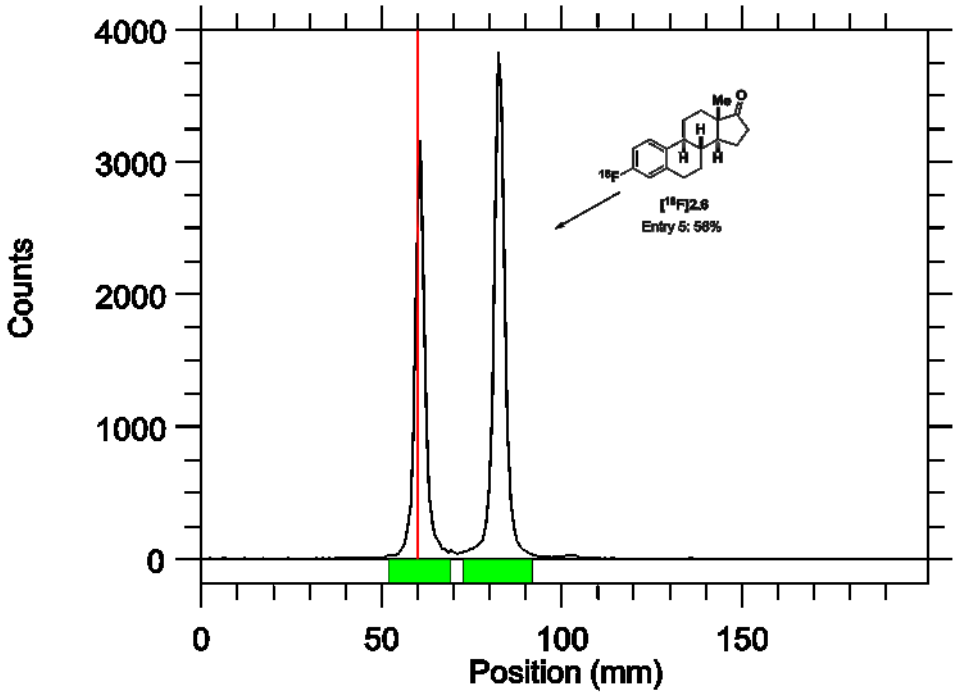

Figure 4.7. Example crude radio TLC scan of **[^{18}F]2.6**. Entry 5 of Table 4.1. Percent of total integration listed for **[^{18}F]2.6**.

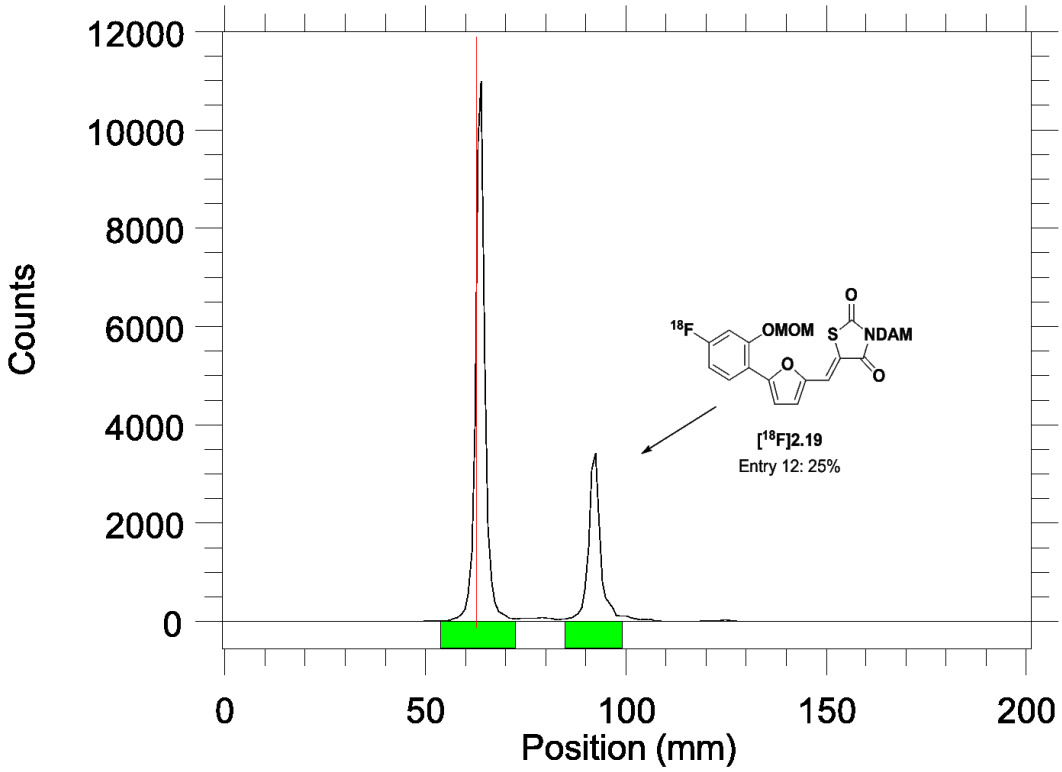

Figure 4.8. Example crude radio TLC scan of **[^{18}F]2.19**. Entry 12 of Table 4.1. Percent of total integration listed for **[^{18}F]2.19**.

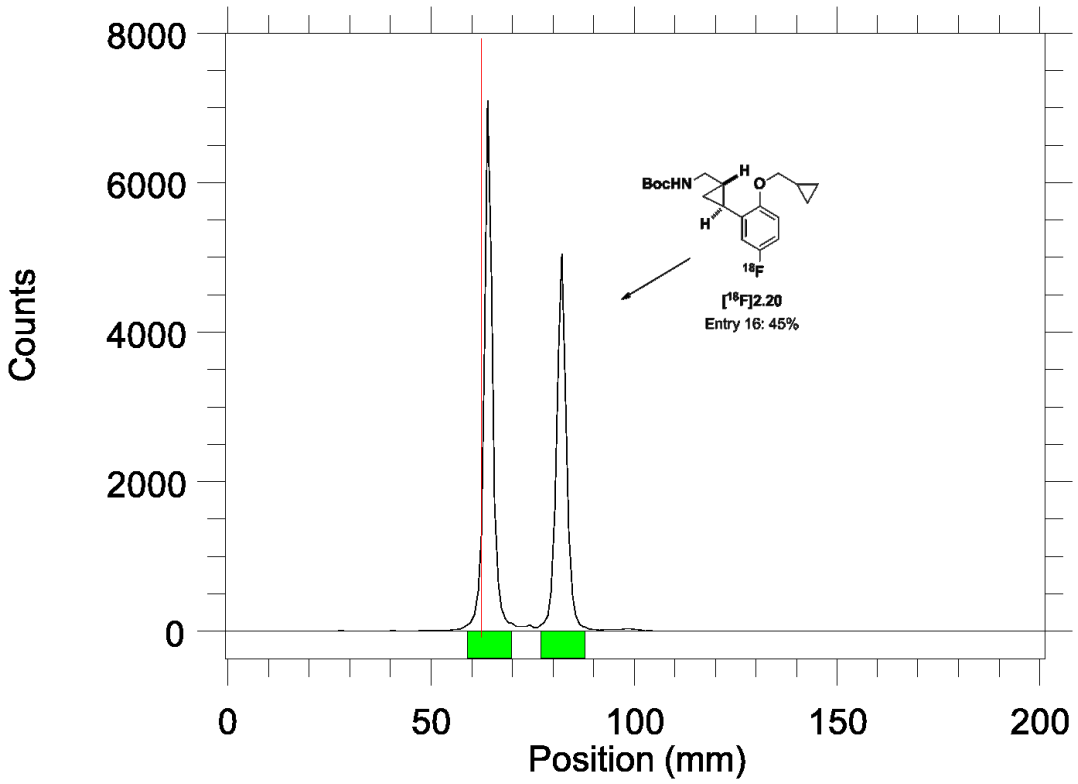

Figure 4.9. Example crude radio TLC scan of **[^{18}F]2.20**. Entry 16 of Table 4.1. Percent of total integration listed for **^{18}F]2.20**.

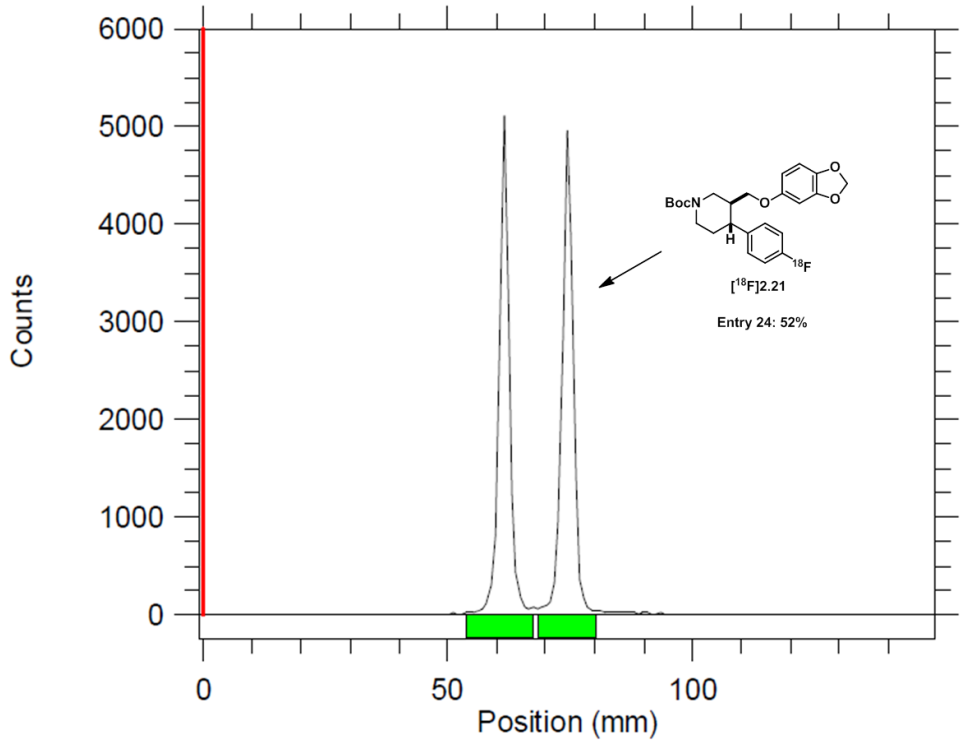

Figure 4.10. Example crude radio TLC scan of **[^{18}F]2.21**. Entry 24 of Table 4.1. Percent of total integration listed for **[^{18}F]2.21**.

Characterization of ^{18}F-labeled molecules

All ^{18}F-labeled molecules were characterized by comparing the radioactivity HPLC trace of the crude reaction mixture to the HPLC UV trace of authentic reference sample. An Agilent Eclipse XDB-C18, 5 μm, 4.6 x 150 mm HPLC column was used for analytical HPLC analysis. Note: radioactivity chromatographs have been offset (–0.125 min) to account for the delay volume (time) between the diode array detector and the radioactivity detector.

In addition ^{18}F-labeled molecules were characterized by comparing the TLC R_f of radioactive products from a radio TLC scan to the R_f of authentic reference sample in two different TLC solvent mixtures.

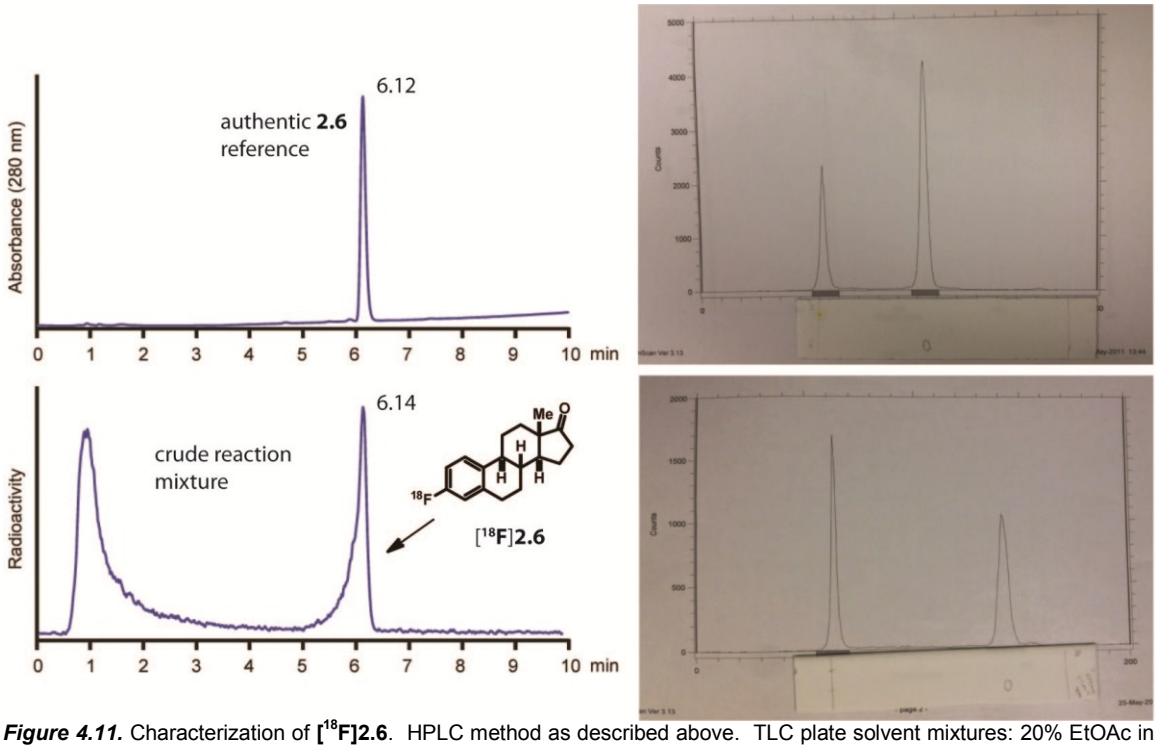

Figure 4.11. Characterization of **[^{18}F]2.6**. HPLC method as described above. TLC plate solvent mixtures: 20% EtOAc in hexanes (right top); 1% MeOH in CH_2Cl_2 (right bottom). A sample of **2.6** was spotted to the right of the crude radiochemistry reaction mixture, identified by UV visualization, and circled on the TLC plate.

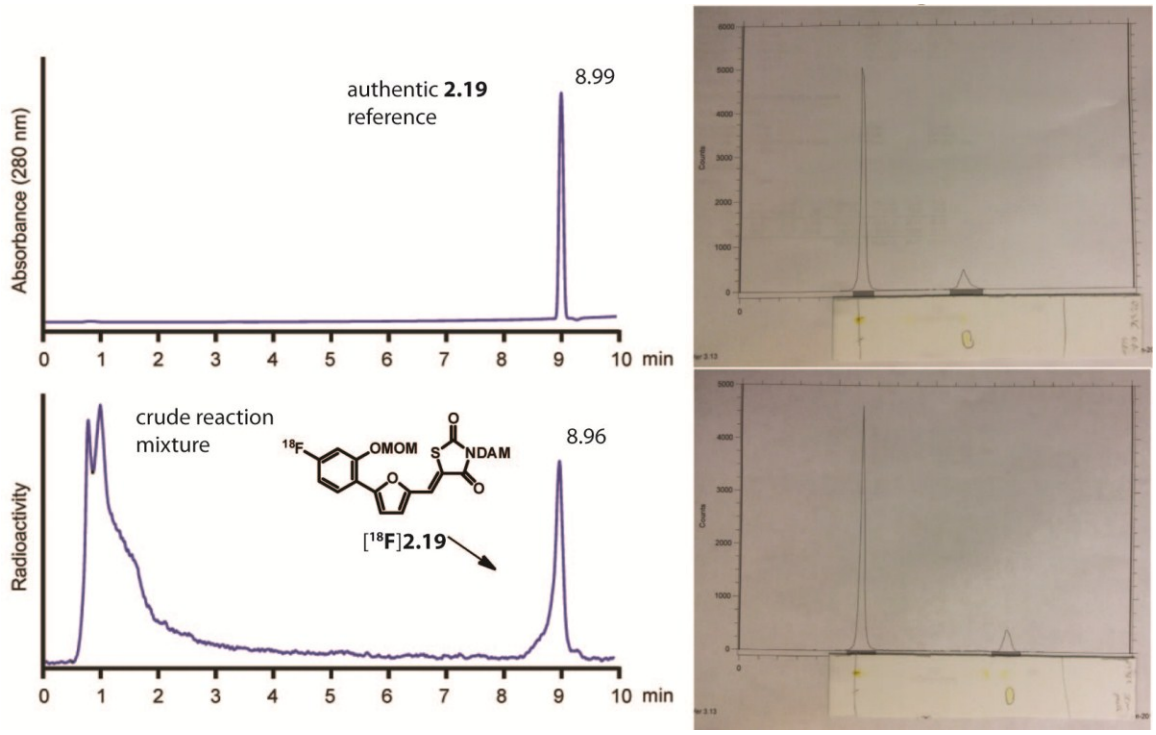

Figure 4.12. Characterization of **[^{18}F]2.19**. HPLC method as described above. TLC plate solvent mixtures: 40% EtOAc in hexanes (right top); 0.5% MeOH in CH_2Cl_2 (right bottom). A sample of **2.19** was spotted to the right of the crude radiochemistry reaction mixture, identified by UV visualization, and circled on the TLC plate.

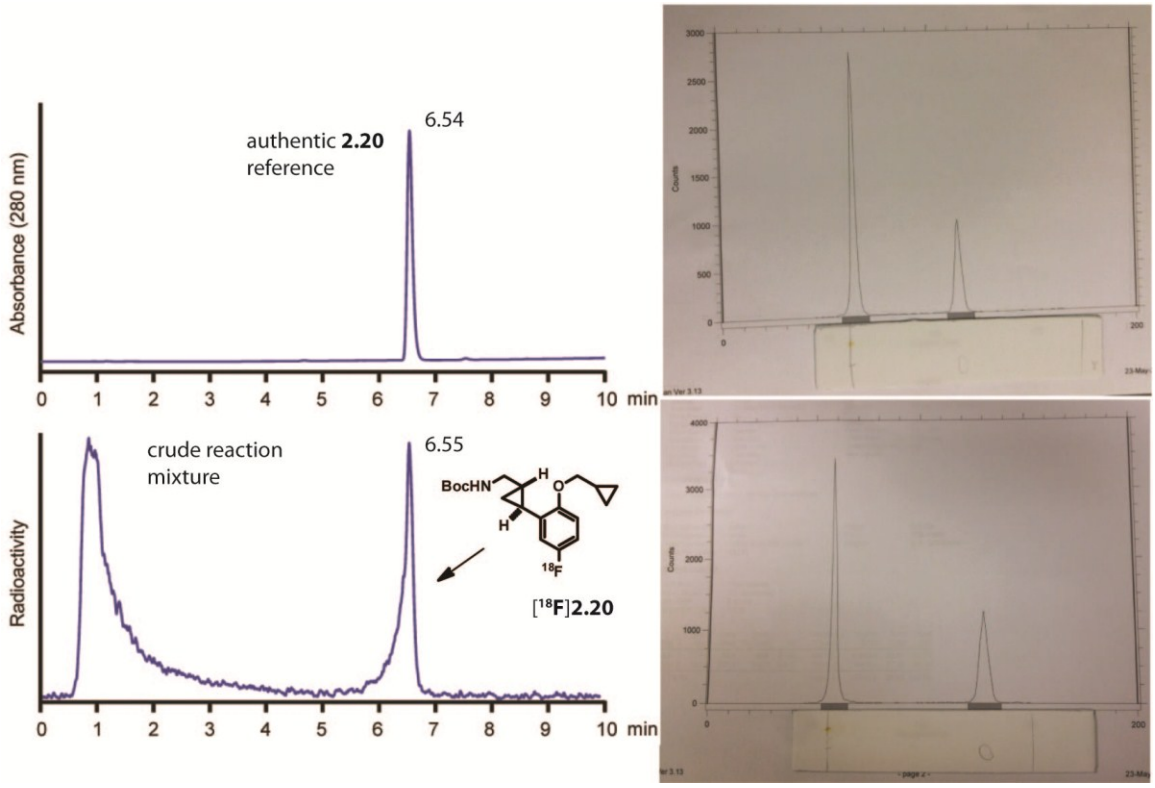

Figure 4.13. Characterization of **[^{18}F]2.20**. HPLC method as described above. TLC plate solvent mixtures: 20% EtOAc in hexanes (right top); 1% MeOH in CH_2Cl_2 (right bottom). A sample of **2.20** was spotted to the right of the crude radiochemistry reaction mixture, identified by UV visualization, and circled on the TLC plate.

Evidence for formation of [^{18}F]2.2 during radiochemical experiments

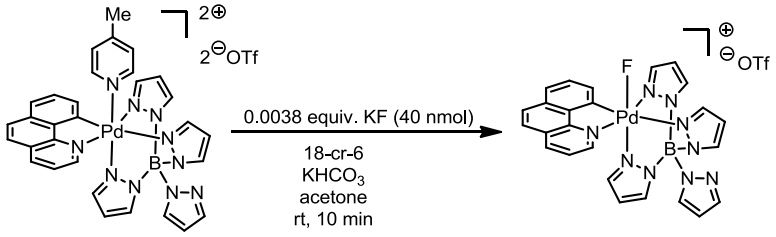

2.1 **2.2**

To provide evidence for the formation of **[^{18}F]2.2** during radiochemical experiments, PET conditions were mimicked using only [^{19}F]fluoride in order to observe **2.2** directly by NMR spectroscopy. Typical specific radioactivity of [^{18}F]fluoride from the nuclear reaction $^{18}O(p,n)^{18}F$ is 5 Ci/μmol so that 1 Ci of ^{18}F contains 200 nmol of total fluoride (0.6 nmol of [^{18}F]fluoride).[95] Based on this assumption, we used 40 nmol of KF, to mimic a 200 mCi sample at 5 Ci/μmol. Complex **2.2** was identified during the experiment by ^{19}F NMR spectroscopy (Figure 4.14). The direct observation of **2.2** shows that the complex is stable relative to other reagents such as 18-cr-6, $KHCO_3$, **2.1** as well as H_2O in reaction conditions used for the described radiochemistry.

Experimental: 1.0 mL of a 4:1 MeCN:H_2O solution containing 1.0 mg $KHCO_3$ was transferred to a conical vial that contained KF (0.0023 mg, from a solution that contained 1.0 mg of KF per 1.0 mL of H_2O) and a magnetic stir bar. 0.50 mL of a stock solution containing 18-crown-6 (26.2 mg/mL MeCN) was then added. The solution was evaporated at 108 °C with a constant nitrogen gas stream. At dryness 0.5 mL of acetonitrile was added and evaporated at 108 °C with a constant nitrogen gas stream. Another 0.5 mL of acetronitrile was added and evaporated at 108 °C with a constant nitrogen gas stream to leave a white precipitate around the bottom and sides of the vial. 0.5 mL of acetone was added and evaporated to dryness at 108 °C with a constant nitrogen gas stream to leave a glassy film on the bottom and sides of the vial.

---

95. Ting, R.; Adam, M. J.; Ruth, T. J.; Perrin, D. M. *J. Am. Chem. Soc.* **2005**, *127*, 13094.

The vial was cooled in a water bath, purged with nitrogen, and sealed with a cap fitted with a septum. 10 mg of **1** dissolved in 0.6 mL of d_6-acetone was added via the septum. The vial was sonicated for 20 seconds and then allowed to stir at 23 °C for 10 minutes. During this time, the orange/brown clear solution became opaque. At the end of 10 minutes, the solution was transferred to a NMR tube and analyzed by ^{19}F NMR spectroscopy (Figure 4.14).

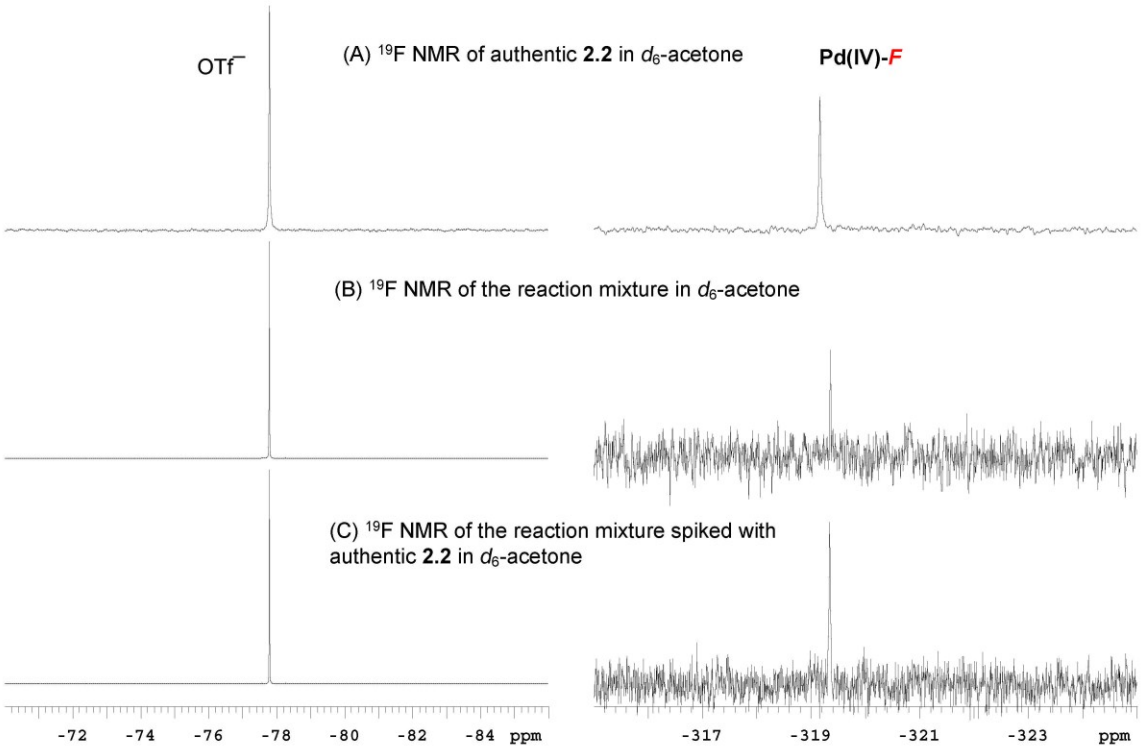

Figure 4.14. ^{19}F NMR spectra of **2.2**.

Automated syntheses of [^{18}F]2.43 and [^{18}F]2.44 using high specific activity [^{18}F]Fluoride

Automated syntheses were accomplished using Eckert and Ziegler automated synthesis modules and Modular-Lab in a hot cell. Reaction procedures were identical to the described "by hand" method (see beginning of Section 4.4), with the following exceptions: 1) The initial azeotrope contained 0.8 mL MeCN and 0.2 mL H_2O instead of 1.3 mL MeCN and 0.2 mL H_2O, 2) the first step of the reaction was stopped after 7.5 minutes instead of 10 minutes, and 3) 1.0 mL of 2-butanone was used to wash the vial and JandaJel™-polypyridine, so that the second step of the reaction proceeded in a 1.5 mL solution of 2:1 2-butanone:acetone. After the reaction, the solution was filtered through preconditioned SepPak® Plus Waters Accell™ Plus QMA cartridge (to capture leftover [^{18}F]fluoride. The second vial and anion exchange cartridge were washed with 1 mL acetone. The combined organic solutions were taken out of the hot cell. The reaction mixture was concentrated and the residue was suspended in a solution of EtOAc:hexanes (1.0 mL, 1:1 (v/v)) and filtered through a small plug of silica gel using an addition 2.0 mL as eluent. The reaction mixture was concentrated to dryness and the residue was dissolved in a solution of trifluoroacetic acid:CH_2Cl_2 (1.0 mL, 1:1 (v/v)). The solution was immediately concentrated to dryness and the residue was dissolved in a solution of MeCN:H_2O (0.10 mL, 1:3 (v/v)). The sample was then purified by preparative HPLC on a Macherey-Nagel VP 250/10 Nucleosil 100-5 C18 Nautilus column. (For **[^{18}F]2.43:** Method: 32% MeCN/H_2O with 0.1% CF_3CO_2H, 5 mL/min, elution time: 10.7–11.7 min (see Figure 4.15); For **[^{18}F]2.44:** Method: 29% MeCN/H_2O with 0.1% CF_3CO_2H, 5 mL/min, elution time: 13.5–14.5 min, (see Figure 4.16)) The purified product in HPLC solvent was diluted to 25 mL using a basic aqueous buffer (0.1 M K_2CO_3, 0.1 M $KHCO_3$) was loaded on to a Grace Extract-Clean™ SPE 50mg/1.5mL column. The column was washed with H_2O (10 mL). The product was eluted from the column using EtOH (0.5 mL), diluted with pH 5 0.1 M NaOAc solution (1 mL) and sterile saline solution (3.5–8.5 mL), and finally filtered through a sterile filter (Millex® Syringe-Driven Filter Unit LG 0.2 μm 25mm). For analytical HPLC of final products compared to authentic reference samples, see Figure 4.17 for **[^{18}F]2.43** and Figure 4.18 for **[^{18}F]2.44.**

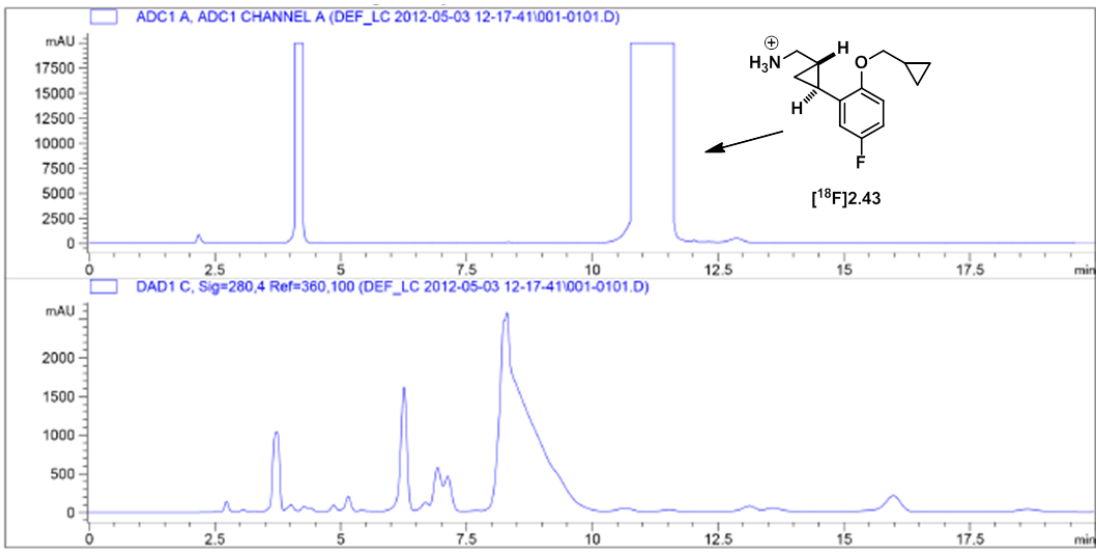

Figure 4.15. Preparatory HPLC chromatograph (280 nm and radioactivity trace) for synthesis of **[^{18}F]2.43**.

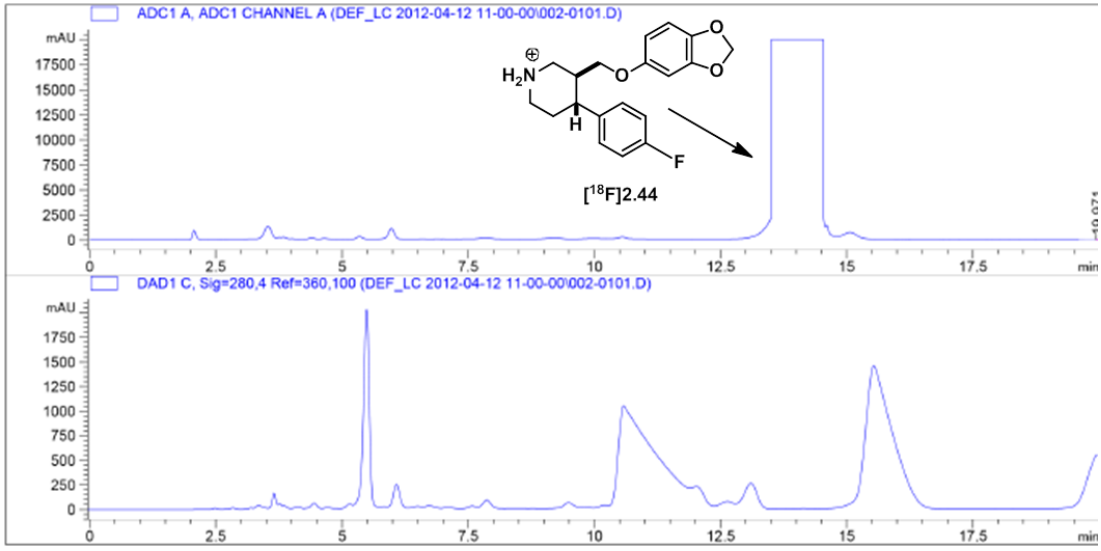

Figure 4.16. Preparatory HPLC chromatograph (280 nm and radioactivity trace) for synthesis of **[^{18}F]2.44**.

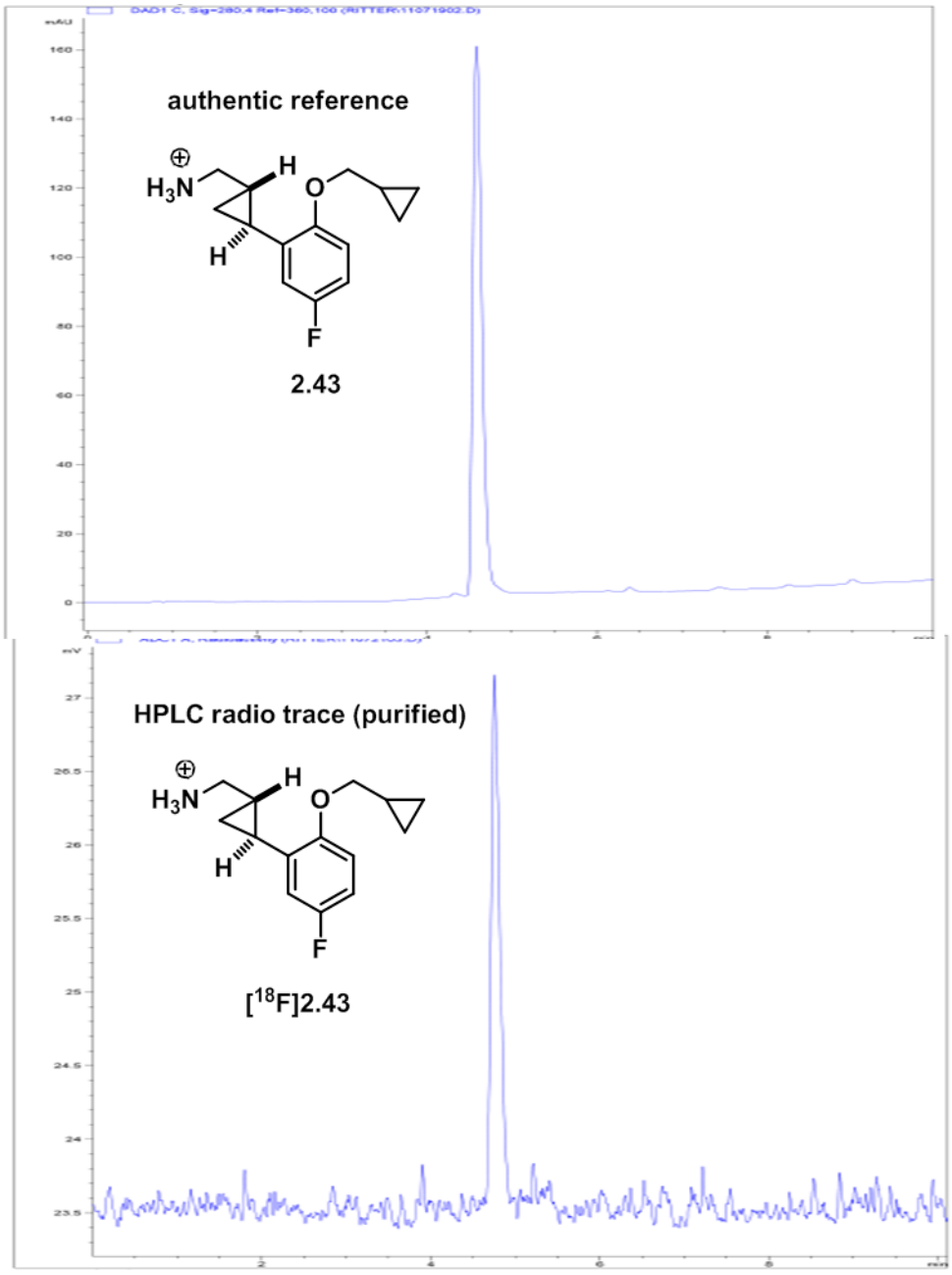

Figure 4.17. Characterization of purified **[^{18}F]2.43**. Note: radioactivity chromatographs have been *not* been offset (–0.125 min) to account for the delay volume (time) between the diode array detector and the radioactivity detector.

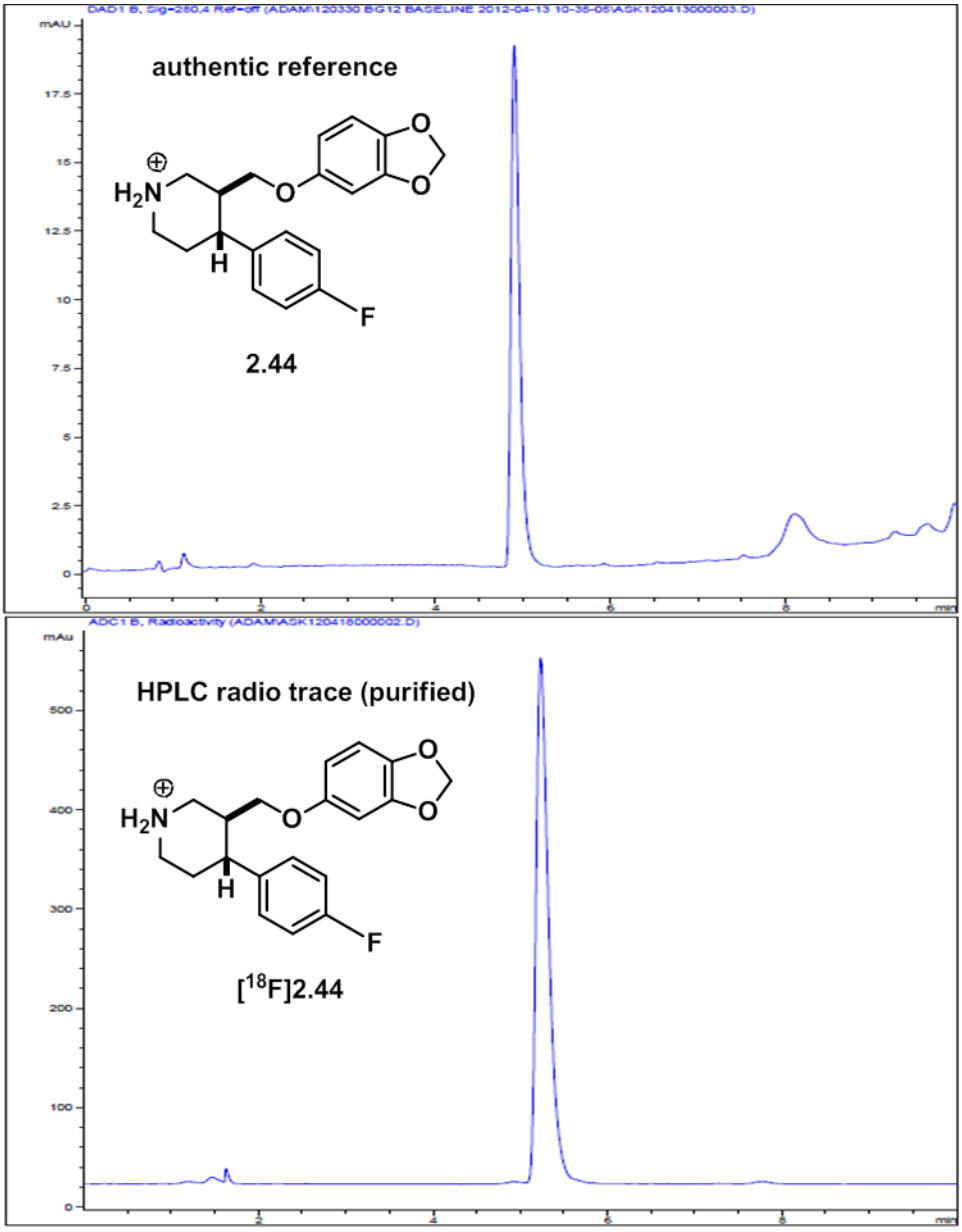

Figure 4.18. Characterization of purified **[^{18}F]2.44**. Note: radioactivity chromatographs have been *not* been offset (–0.125 min) to account for the delay volume (time) between the diode array detector and the radioactivity detector.

Specific activity of **[^{18}F]2.43** and **[^{18}F]2.44** were determined by measuring the UV absorbance of a known amount of radioactivity and comparing to a standard curve of UV absorbance vs amount of unlabeled **2.43** and **2.44.** For 122 µCi of **[^{18}F]2.43** a UV absorbance of 5.1 was measured corresponding to 120 pmol for a specific activity of 1.0 Ci/µmol at time of injection (TOI). For 89 µCi of **[^{18}F]2.44** a UV absorbance could note be detected. The smallest amount that has been detected corresponded to 7 pmol for a specific activity of at least 13 Ci/µmol at time of injection (TOI). The standard curves were generated by integration of the UV absorbance signal (at 280 nm) of at least 5 different known amounts of **2.43** and **2.44** in triplicate (see Tables 4.2 and 4.3 Figure 4.19 and 4.20).

Table 4.2. Data for standard curve of UV absorbance vs amount of **2.43**.

pmol **2.43**	UV Absorbance
29	0.93
72	1.8
286	8.4
716	27.3
2863	128.1

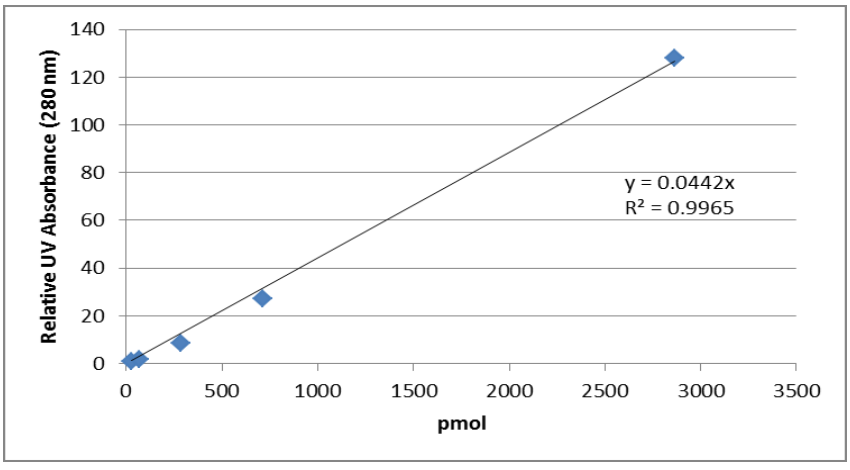

Figure 4.19. Standard curve of UV absorbance vs amount of **2.43**.

Table 4.3. Data for standard curve of UV absorbance vs amount of **2.44**.

pmol **2.44**	UV Absorbance
7	2.0
26	8.0
65	25.7
260	133.0
651	341.6
2603	1439.2

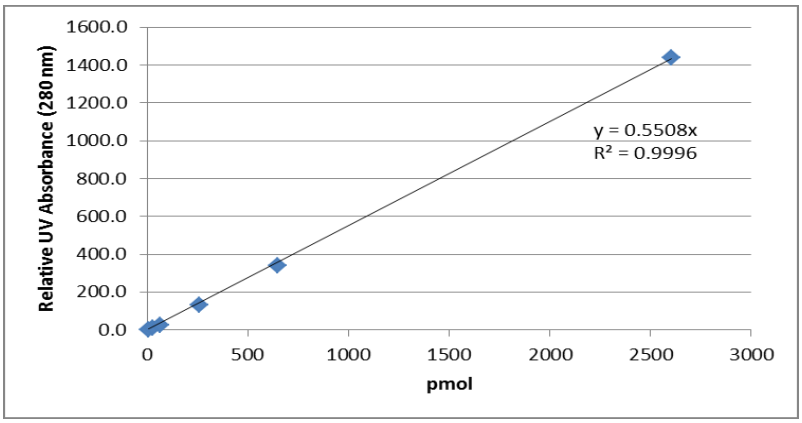

Figure 4.20. Standard curve of UV absorbance vs amount of **2.44**.

Purification of ^{18}F-labeled Molecules and Determination of Palladium Content

At the end of the synthesis and reformulation of **[^{18}F]2.43**, A portion of the sample was analyzed using an Agilent 7500a ICP-MS to determine palladium content. An average of 2 samples (HPLC fraction:ICP diluent 1:99 (m/m)) were compared to a standard curve of relative ion count versus palladium concentration. The standard curve was generated by creating a dilution series of known palladium concentrations (from 0.020 ppb to 50.0 ppb) and an internal lutetium control (see Table 4.4 and Figure 4.21). The samples averaged less than 0.02 ppb palladium. The final palladium content of the reformulated sample was 2 ppb palladium.

Table 4.4. ICP/MS data for standard curve and reformulated samples

ppb Pd	Pd-105 cps	Lu cps	Pd-105/Lu
0.02	204.44	1337281	0.000152877
0.1	801.67	1338268	0.000599035
0.5	4074.44	1346762	0.00302536
2	14839.44	1333299	0.011129867
10	77070.56	1322516	0.058275711
50	290764.3	1326804	0.219146385
sample 1	62.22	1324434	4.69786E-05
sample 2	69.44	1293053	5.37024E-05

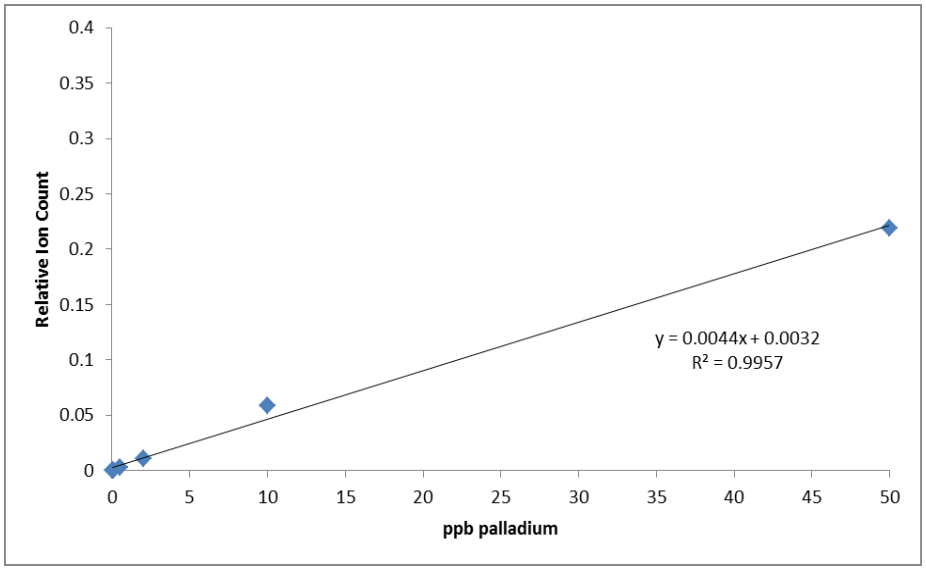

Figure 4.21. Standard curve of relative ion Count vs palladium concentration.

5. DEVELOPMENT OF REACTIVITY-DEPENDENT PCR

Note: The following chapters represent a research endeavor that was a collaboration between the Liu and Ritter Groups that is separate from the project described in the previous sections. Dr. David Gorin and I collaborated on this project. Dr. David Gorin contributed the experiments described in Figures 5.3, 5.5, and 5.7, and partially to Figure 5.4. I obtained the initial results that demonsrated RDPCR was viable as an *in vitro* selection method and contributed the experiments described in Figure 5.6 and partially to Figure 5.4.

In vitro selection is a key component of efforts to discover functional nucleic acids and small molecules from libraries of DNA, RNA, and DNA-encoded small molecules.[96] When the desired activity is binding affinity, as is the case for aptamer evolution[97] or for the discovery of DNA-linked small molecules that bind to protein targets,[98] a direct selection is possible; the library is typically incubated with immobilized target molecules, and bound library members are washed and eluted before being subjected to PCR amplification (Figure 5.1a).

In vitro selections have also been applied to evolve RNA and DNA catalysts,[99] and more recently to discover new reactions from DNA-encoded libraries of potential substrates.[100] For these applications, desired library members undergo bond formation or bond cleavage. Selections

---

96. Seminal reports: (a) Tuerk, C.; Gold, L. *Science* **1990**, *249*, 505; (b) Ellington, A. D.; Szostak, J. W. *Nature* **1990**, *346*, 818; (c) Robertson, D. L.; Joyce, G. F. *Nature* **1990**, *344*, 467; (d) Wilson, D. S.; Szostak, J. W. *Annu. Rev. Biochem.* **1999**, *68*, 611.

97. Recent reviews of evolved DNA/RNA aptamers: (a) Shamah, S. M.; Healy, J. M.; Cload, S. T. *Acc. Chem. Res.* **2008**, *41*, 130; (b) Gopinath, S. C. B. *Anal. Bioanal. Chem.* **2007**, *387*, 171.

98. *In Vitro* selections of DNA-linked small molecules: (a) Wrenn, S. J.; Weisinger, R. M.; Halpin, D. R.; Harbury, P. B. *J. Am. Chem. Soc.* **2007**, *129*, 13137; (b) Melkko, S.; Zhang, Y.; Dumelin, C. E.; Scheuermann, J.; Neri, D. *Angew. Chem., Int. Ed.* **2007**, *46*, 4671. Mock selections: (c) Doyon, J. B.; Snyder, T. M.; Liu, D. R. *J. Am. Chem. Soc.* **2003**, *125*, 12372; (d) Gartner, Z. J.; Tse, B. N.; Grubina, R.; Doyon, J. B.; Snyder, T. M.; Liu, D. R. *Science* **2004**, *305*, 1601.

99. (a) Silverman, S. K. *Chem. Commun.* **2008**, 3467; (b) Joyce, G. F. *Annu. Rev. Biochem.* **2004**, *73*, 791.

100. (a) Kanan, M. W.; Rozenman, M. M.; Sakurai, K.; Snyder, T. M.; Liu, D. R. *Nature* **2004**, *431*, 545; (b) Rozenman, M. M.; Liu, D. R. *ChemBioChem* **2006**, *7*, 253; (c) Rozenman, M. M.; Kanan, M. W.; Liu, D. R. *J. Am. Chem. Soc.* **2007**, *129*, 14933.

for reactivity are significantly more complicated than selections for binding affinity. Typically, libraries are incubated with biotinylated substrates or potential reaction partners. Bond formation results in the attachment of biotin to a library member, which in turn enables its capture by immobilized avidin (Figure 5.1b).[101] For bond cleavage, an inverse approach is commonly used in which immobilized, biotinylated library members liberate themselves upon bond scission.[102] While effective, such selections for reactivity are indirect, require the synthesis of biotin-linked substrates, and involve multiple solution-phase and solid-phase manipulations.

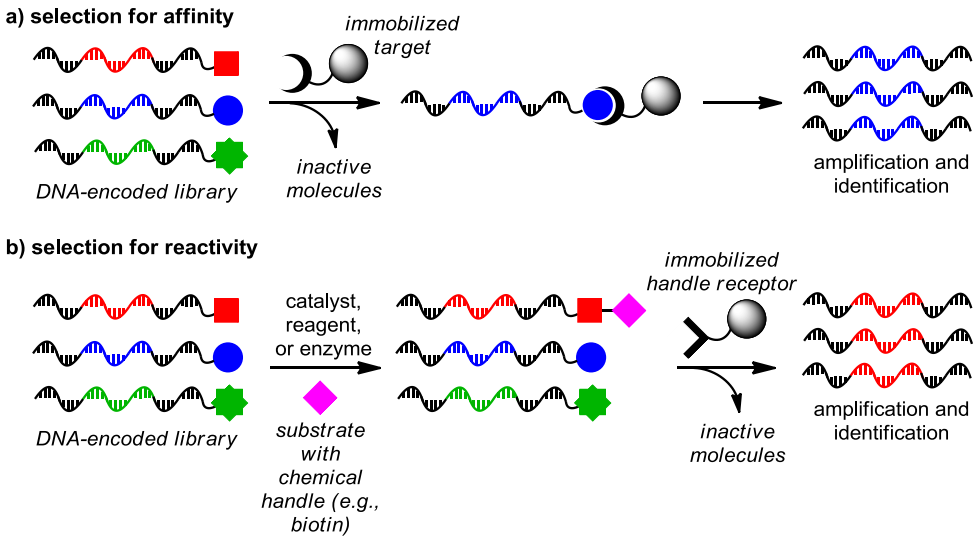

Figure 5.1. Traditional approaches to *in vitro* selection.

Motivated by our ongoing interest in applying *in vitro* selection to discovery problems that involve chemical reactivity,[103] we sought to develop a new method that more directly links

---

101. (a) Tarasow, T. M.; Tarasow, S. L.; Eaton, B. E. *Nature* **1997**, *389*, 54; (b) Seelig, B.; Jaschke, A. *Chem. Biol.* **1999**, *6*, 167. Other tags may be used. For selected examples, see: (c) Chandra, M.; Silverman, S. K. *J. Am. Chem. Soc.* **2008**, *130*, 2936; (d) Pradeepkumar, P. I.; Hobartner, C.; Baum, D. A.; Silverman, S. K. *Angew. Chem., Int. Ed.* **2008**, *47*, 1753; (e) Johnston, W. K.; Unrau, P. J.; Lawrence, M. S.; Glasner, M. E.; Bartel, D. P. *Science* **2001**, *292*, 1319.

102. (a) Breaker, R. R.; Joyce, G. F. *Chem. Biol.* **1994**, *1*, 223; (b) Sheppard, T. L.; Ordoukhanian, P.; Joyce, G. F. *Proc. Natl. Acad. Sci. U. S. A.* **2000**, *97*, 7802; (c) Hobartner, C.; Pradeepkumar, P. I.; Silverman, S. K. *Chem. Commun.* **2007**, 2255.

103. (a) Rozenman, M. M.; McNaughton, B. R.; Liu, D. R. *Curr. Opin.Chem. Biol.* **2007**, *11*, 259; (b) Wrenn, S. J.; Harbury, P. B. In *Annu. Rev. Biochem.* 2007; Vol. 76, p 331.

bond formation or bond cleavage with the amplification of desired sequences,[104] and that obviates the need for solid-phase capture, washing, and elution steps. Here we report the development and validation of such a method, reactivity-dependent PCR (RDPCR).

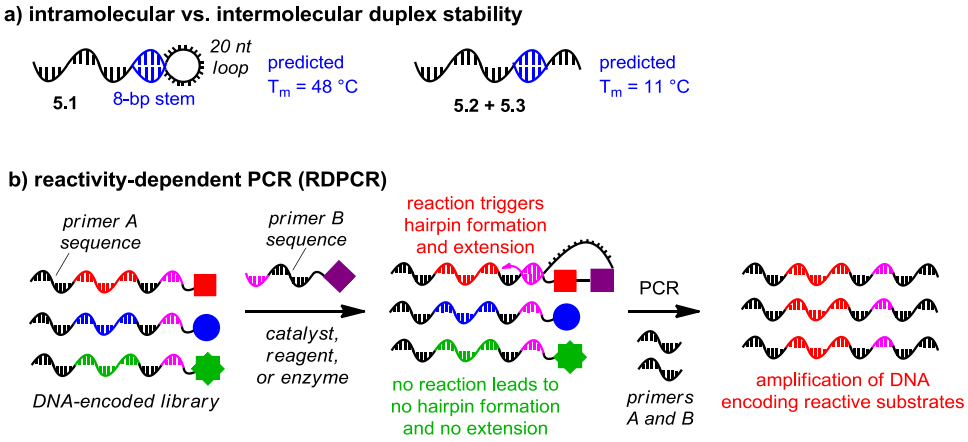

Figure 5.2. Principles underlying reactivity-dependent PCR (RDPCR). Conditions in (a): 10 nM DNA, 2 mM Mg^{2+}, 100 mM NaCl.

RDPCR is based on the well-established observation that the melting temperature (Tm) of double-stranded nucleic acids is substantially higher when hybridization occurs intramolecularly as opposed to intermolecularly.[105] For example, the DNA hairpin 5.1 with an 8 bp stem is predicted[106] to exhibit a T_m of 48 °C, while the intermolecular hybridization of two DNA strands of the same sequence (5.2 and 5.3) is predicted to be far less favorable, with a Tm of only 11 °C (Figure 5.2). We hypothesized that the significant difference in intramolecular versus intermolecular duplex stability could enable a new type of *in vitro* selection, wherein bond formation or bond cleavage is transduced into the formation of a self-priming DNA hairpin. This

---

104. Note that in contrast with a conventional selection in which unfit library members are discarded and sequences encoding surviving members are replicated in a subsequent step, RDPCR achieves the selective replication of only those sequences encoding desired library members.

105. Ogawa, A.; Maeda, M. *Bioorg. Med. Chem. Lett.* **2007**, *17*, 3156.

106. Computation carried out using the Oligonucleotide Modeling Platform (OMP, DNA Software, Inc.).

hairpin enables the selective PCR amplification of those DNA sequences that encode the reactive species (Figure 5.2b).[107]

We first assessed the ability of intramolecular self-priming to result in preferential DNA amplification. We synthesized a series of oligonucleotide pairs (**5.4a**+**5.5**), each predicted to hybridize intermolecularly at their 3' ends to form a short duplex region of 8 or 10 bp (Figure 5.3). The 5' end of each DNA oligonucleotide in the pair contained a sequence identical to either primer **5.6** or primer **5.7**. PCR amplification cannot occur until after DNA hybridization and 3' extension take place to generate a single-stranded DNA molecule containing both primer **5.6** and a sequence complementary to primer **5.7**. This 3'-extended species can then hybridize with primer **5.7** and initiate PCR amplification.

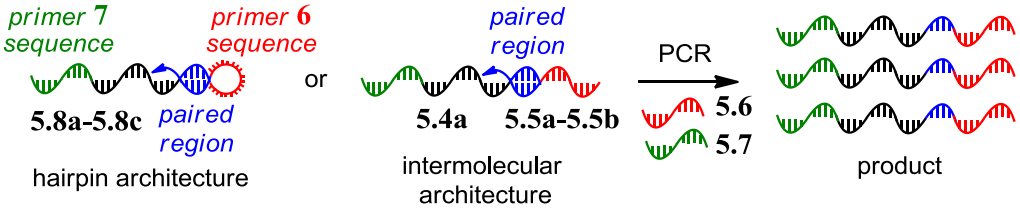

architecture	overlap (bp)	threshold cycle (C_T)
5.8a	10	16
5.8b	8	18
5.8c	6	21
5.4a	0	34
5.4a+5.5a	10	29
5.4a+5.5b	8	33

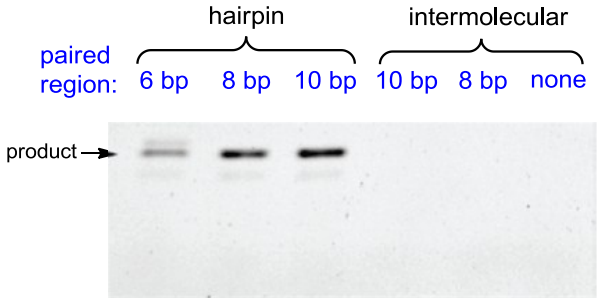

Figure 5.3. Comparison of PCR efficiency of intramolecularly primed versus intermolecularly primed DNA templates. PCR conditions for PAGE samples: 19 fmol **5.8** or 19 fmol **5.4a**+**5.5** in 30 μL, 25 cycles.

We also prepared an analogous series of DNA oligonucleotides capable of hybridizing

---

107 For examples of phosphodiester bond formation-dependent PCR, see: (a) Bartel, D. P.; Szostak, J. W. *Science* **1993**, *261*, 1411; (b) Makrigiorgos, G. M. *Human Mutation* **2004**, *23*, 406; (c) Troutt, A. B.; McHeyzerwilliams, M. G.; Pulendran, B.; Nossal, G. J. V. *Proc. Natl. Acad. Sci. U. S. A.* **1992**, *89*, 9823.

intramolecularly to form hairpin structures with 10-, 8-, or 6-bp stems (**5.8a**-**5.8c**). As with the intermolecularly hybridizing oligonucleotides, PCR amplification must be initiated by primer extension of the 3' end. Quantitative, real-time PCR (qPCR)[108] was used to compare the ability of these oligonucleotides to undergo PCR amplification.

Consistent with our initial hypothesis, under identical PCR conditions and with equal starting concentrations of DNA, the intramolecularly hybridizing templates were amplified much more efficiently than their intermolecular counterparts (**5.8a** vs. **5.4a**+**5.5a**, **5.8b** vs. **5.4a**+**5.5b**). The intramolecularly hybridizing templates reached a threshold level of amplified product 13 to 15 PCR cycles (C_T) earlier than the intermolecular templates, corresponding to a > 213-fold (> 8,000-fold) difference in effective initial template abundance. These qPCR results were corroborated by PAGE analysis; after 25 cycles of PCR, amplified product was only detected in reactions containing hairpin DNA. Collectively, these findings demonstrate that intramolecularly hybridizing templates can be amplified to abundant levels under conditions that fail to appreciably amplify the corresponding intermolecularly hybridizing templates. Subsequent experiments in this work were carried out with an 8-base stem, which was found to optimally balance robust intramolecular priming and poor intermolecular priming.

In order to use RDPCR in a general selection for bond formation, the covalently linked functional groups in the hairpin loop must not interfere with the required hybridization and 3'-extension events. To test the compatibility of non-natural linkers with the preferential amplification of self-priming templates, we repeated the qPCR experiment in Figure 5.3 with a series of non-natural linker structures, including ether, disulfide, and amide hairpin linkers. In all cases tested, DNA templates containing non-natural linkers (**5.9a**-**5.9c**) were far more efficiently

---

108. For a general review, see: Kubista, M.; Andrade, J. M.; Bengtsson, M.; Forootan, A.; Jonak, J.; Lind, K.; Sindelka, R.; Sjoback, R.; Sjogreen, B.; Strombom, L.; Stahlberg, A.; ZoriC, N. *Mol. Aspects Med.* **2006**, *27*, 95.

amplified than the analogous intermolecularly hybridizing templates (**5.4**+**5.10**) (Figure 5.4).

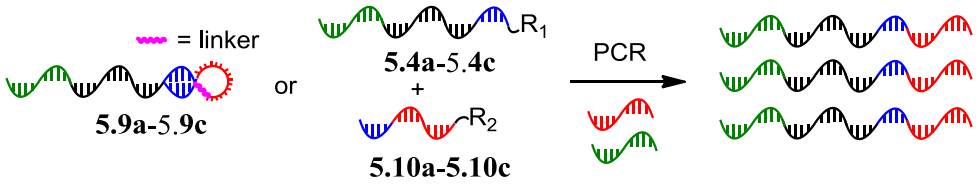

linker	R_1	R_2	architecture	C_T
ethylene glycol	3'-OH	5'-OH	**5.9a**	18
			5.4a+**5.10a**	33
disulfide	3'-SSR	5'-SSR	**5.9b**	16
			5.4b+**5.10b**	29
amide	3'-NH_2	5'-CO_2H	**5.9c**	18
			5.4c+**5.10c**	29

Figure 5.4. Non-natural hairpin linkers support self-priming PCR. R = $(CH_2)_6OH$.

Since RDPCR will ultimately be applied to mixtures of both active (resulting in DNA hairpins) and inactive (resulting in separate linear oligonucleotides) library members, we next tested the ability of hairpin templates to undergo preferential amplification in the presence of large excesses of corresponding linear molecules (Figure 5.5). For these library-format experiments, the hairpin (**5.11**) and linear (**5.12**) template sequences vary only by a single base, such that DNA amplified from the hairpin contains a cleavage site for the restriction enzyme HindIII, while DNA arising from **5.12** does not.

The quantity of **5.11** spiked into an equimolar mixture of **5.12** and **5.13** was varied to determine the selectivity of RDPCR in a library format. As little as 1 attomole of **5.11** (600,000 molecules) could be selectively amplified in the presence of a 10,000-fold excess of **5.12** and **5.13**. The use of larger quantities of hairpin (corresponding to a 10- to 1,000-fold excess of **5.12** and **5.13**) overwhelmingly provided the desired product. These results demonstrate the ability of hairpin templates to be preferentially amplified even in the presence of large excesses of linear

templates, and indicate that RDPCR can be applied to library-format selections.[109]

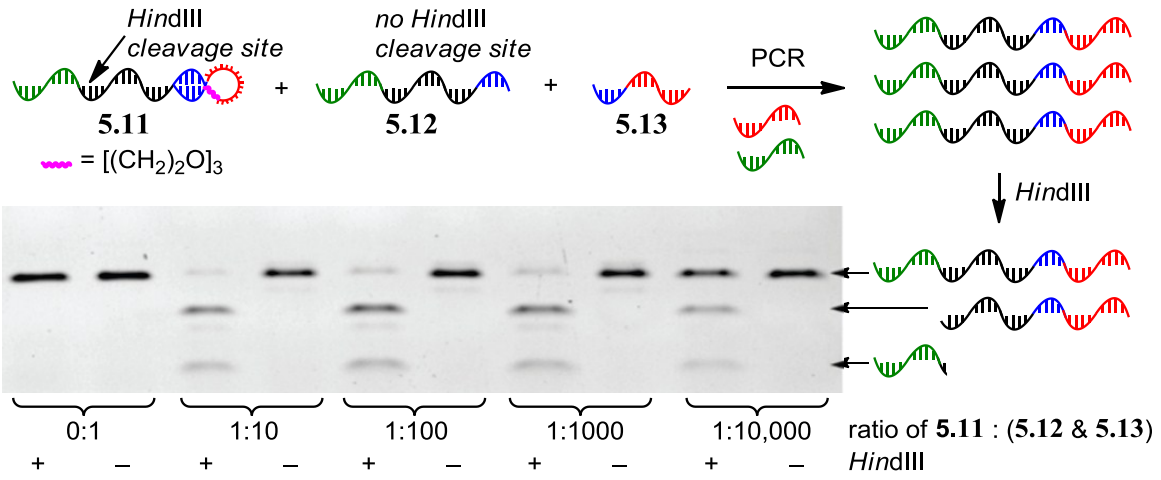

Figure 5.5. Selectivity of RDPCR in a library-format mock selection. PCR conditions: 19 fmol of **5.12** and **5.13** in 60 µL, 25-35 cycles.

Following these foundational studies, RDPCR was applied to two model *in vitro* selections. First, RDPCR was validated as a bond-formation selection for DNA-encoded reaction discovery. Previously, DNA-encoded reaction discovery required the capture, washing, and elution of active library members on avidin-linked beads (Figure 5.1b).[100] In a RDPCR version of reaction discovery, pairs of functional groups are attached to encoding DNA strands (Figure 5.6). A disulfide linker temporarily joins each substrate pair (**5.9b**, **5.9d**). Exposure to a set of reaction conditions and subsequent cleavage of the disulfide bond provides one of two possible outcomes. If a new covalent bond has formed between the functional groups, the hairpin-forming nucleotides remain tethered together through the reaction product, leaving a self-priming DNA hairpin (**5.14**). If no bond has formed, then only intermolecular hybridization is possible (**5.15**+**5.16**), resulting in inefficient PCR amplification. In contrast with previous reaction discovery selections, the RDPCR version requires no solid-phase steps and minimal

109. Gartner, Z. J.; Liu, D. R. *J. Am. Chem. Soc.* **2001**, *123*, 6961.

manipulation.

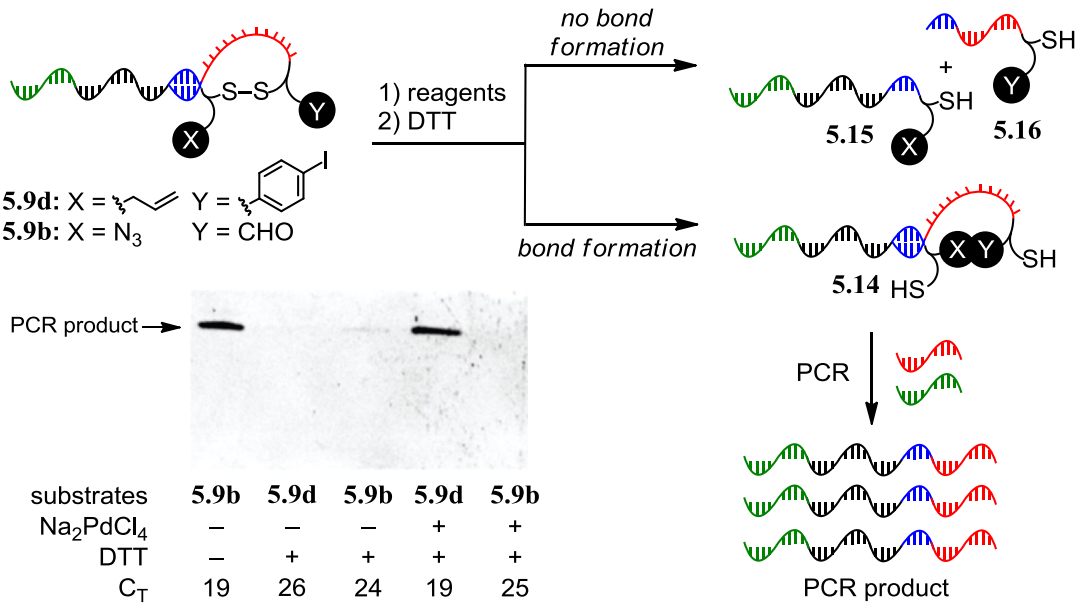

Figure 5.6. RDPCR-based DNA-encoded reaction discovery selection. PCR conditions for PAGE samples: 1 fmol of **5.9** in 20 μL, 23 cycles.

To test the ability of RDPCR to support reaction discovery, we synthesized a disulfide-linked substrate (**5.9d**) with pendant alkene and aryl iodide groups, which should undergo a Pd-mediated Heck-type reaction (Figure 5.6).[110] An unreactive control substrate (**5.9b**) containing an azide and an aldehyde was similarly generated. Each substrate was treated with 1 mM Na_2PdCl_4 (which is reduced to Pd(0) *in situ*) in aqueous pH 7.5 buffer for 30 min at 65 °C, followed by DTT to cleave the disulfide bond. The resulting material was subjected to PCR. The DNA attached to the alkene-aryl iodide pair (**5.9d**) amplified efficiently (Figure 5.6). Omission of Na_2PdCl_4 resulted in much less efficient amplification. Likewise, the unreactive substrate pair **5.9b** did not undergo PCR amplification after identical treatment. Omission of DTT, however, enabled the disulfide-linked starting substrate to amplify efficiently. Collectively, these results

110. Heck, R. F. *Org. Reactions* **1982**, *27*, 345.

indicate that RDPCR can selectively and efficiently amplify DNA templates that have undergone bond formation, and that amplification is dependent on the intramolecularity of the resulting template-primer species.[111] These experiments were corroborated using an azide/alkyne substrate that undergoes Cu(I)-catalyzed cycloaddition reaction.

In principle, RDPCR can also enable an efficient selection for bond cleavage, which has yet to be studied in a DNA-encoded context. To explore this possibility, we evaluated the ability of DNA-linked peptides to undergo cleavage mediated by a protease (Figure 5.7). We anticipated that protease-mediated cleavage of a DNA-peptide conjugate would expose a primary amine group, which would then undergo DNA-templated amide bond formation to generate a hairpin template for efficient PCR.[112] In contrast, the absence of proteolysis should result in no amide formation and thus inefficient PCR amplification.

A DNA–N-acetyl-pentapeptide conjugate (**5.17**), synthesized by solid phase co-synthesis, was exposed to subtilisin A. The peptide sequence (Ac-N-AFGPA) was designed to include cleavage sites for subtilisin A.[113] The enzyme-treated DNA was combined with a carboxylic acid-linked DNA primer (**5.10c**) under conditions (DMT-MM or sNHS+EDC) that support DNA-templated amide bond formation.[114]

---

111. As little as 10 fmol of **5.9d** and **5.9b** could be carried through the process with similar results, suggesting that selections can be performed on a very small scale.

112. For approaches to protease substrate profiling by derivitization of free R-amines, see: (a) Mahrus, S.; Trinidad, J. C.; Barkan, D. T.; Sali, A.; Burlingame, A. L.; Wells, J. A. *Cell* **2008**, *134*, 866; (b) McDonald, L.; Robertson, D. H. L.; Hurst, J. L.; Beynon, R. J. *Nat. Methods* **2005**, *2*, 955; (c) Gevaert, K.; Goethals, M.; Martens, L.; Van Damme, J.; Staes, A.; Thomas, G. R.; Vandekerckhove, J. *Nat. Biotechnol.* **2003**, *21*, 566.

113. Substrate designed in consultation with Sigma-Aldrich Protease finder (http://sigma-aldrich.com/proteasefinder).

114. DNA-templated amide bond formation with DMT-MM: (a) Li, X. Y.; Gartner, Z. J.; Tse, B. N.; Liu, D. R. *J. Am. Chem. Soc.* **2004**, *126*, 5090. With EDC/sNHS: (b) Gartner, Z. J.; Kanan, M. W.; Liu, D. R. *Angew. Chem., Int. Ed.* **2002**, *41*, 1796. For a review of DTS, see: (c) Li, X. Y.; Liu, D. R. *Angew. Chem., Int. Ed.* **2004**, *43*, 4848.

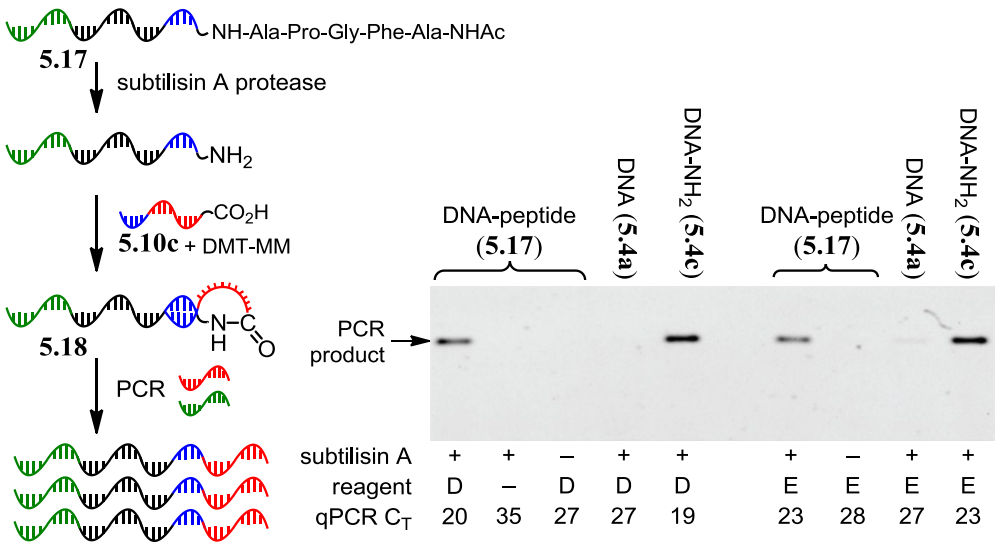

Figure 5.7. RDPCR-based protease-mediated peptide cleavage selection. PCR conditions for PAGE samples: 19 fmol DNA in 30 µL, 23 cycles (lanes 1-5) or 25 cycles (lanes 6-9). D = DMT-MM; E = EDC + sNHS.

Addition of the protease-digested and carboxylate-ligated DNA-peptide conjugate (**5.18**) to a PCR reaction resulted in efficient PCR amplification. In contrast, no PCR product was detected by PAGE when unfunctionalized DNA (**5.4a**) was used in place of the pentapeptide, or when subtilisin A was omitted. Likewise, omission of the amide formation reagents also resulted in inefficient PCR amplification, consistent with the necessity of intramolecular primer hybridization for rapid amplification. These findings together demonstrate the ability of RDPCR to rapidly detect DNA-linked peptide substrates of protease enzymes.

In conclusion, we have developed and validated RDPCR as a new, entirely solution-phase method for the selective amplification of DNA sequences encoding molecules that undergo bond formation or bond cleavage. By obviating the need to perform solid-phase capture, washing, and elution steps, RDPCR can greatly streamline the selection process for applications such as DNA-encoded reaction discovery and protease activity profiling. Compared with the performance characteristics of previous *in vitro* selection methods, the data above suggests that RDPCR may also offer superior enrichment factors (signal:background ratios). In addition,

RDPCR may be applicable to the evolution of ribozymes and DNAzymes that catalyze bond-forming or bond-cleaving reactions including those that do not generate nucleic acid-like products.

6. EXPERIMENTAL FOR CHAPTER 5[115]

115. I thank Dr. David Gorin for performing experiments in the following chapter (see note at the beginning of Chapter 5).

General Methods. DNA oligonucleotides were synthesized using standard automated solid-phase phosphoramidite coupling methods on a PerSeptive Biosystems Expedite 8909 DNA synthesizer or purchased from Integrated DNA Technologies. All reagents and phosphoramidites for DNA synthesis were purchased from Glen Research. Oligonucleotides were purified by reverse-phase high-pressure liquid chromatography (HPLC) using a C18 stationary phase and an acetonitrile/100 mM triethyl ammonium acetate gradient or by Oligonucleotide Purification Cartridge (Applied Biosystems). Oligonucleotide concentrations were quantitated by UV spectroscopy on a Nanodrop ND1000 Spectrophotometer. Non-commercial, modified oligonucleotides were characterized by LCMS on Waters Aquity UPLC equipped with a Waters Aquity UPLC BEH C18 column using an aqueous 6 mM tetraethyl ammonium bicarbonate/MeOH mobile phase. Electrospray mass spectrometry was carried out on a Waters Q-TOF premier instrument. All DNA sequences are written in the 5' to 3' orientation.

Gels stained with ethidium bromide were visualized on an Alpha Innotech AlphaImager HP. Fluorescence images were acquired on a GE Typhoon Trio variable mode imager. Solid phase peptide synthesis was carried out on an Applied Biosystems 433A peptide synthesizer using standard Fmoc chemistry. Water was purified with a Milli-Q purification system. All chemical reagents were purchased from Sigma-Aldrich, unless otherwise noted. DMT-MM was synthesized according to the method of Kunishima *et al.*[116] Subtilisin A was purchased from Sigma-Aldrich. *Hin*dIII and *Pvu*II-HF were purchased from New England Biolabs.

General Method for PCR. All PCR reactions were carried out with AmpliTaq Gold DNA Polymerase (0.1 μL/20 μL reaction volume, Applied Biosystems) in the provided buffer. PCR reactions included Mg^{2+} (3 mM), dNTPs (200 μM each, BioRad), and primers (500 nM each). Templates were amplified from a standard initial concentration of 625 pM, unless otherwise noted. The thermal cycling sequence was as follows: 95 °C for 10 minutes, then iterated cycles of 95 °C for 30 seconds, 58 °C for 30 seconds, and 72 °C for 30 seconds. In preparative PCR reactions, upon completion of the iterated cycles, a final incubation at 72 °C for 2 minutes was performed. For qPCR, conditions were identical to those above, except that Sybr Green I Nucleic Acid gel stain (0.5x final concentration from a 10,000x stock solution, Invitrogen) was added to the reaction mixture. Quantitative PCR experiments were performed in triplicate on a BioRad CFX96 Real-Time PCR Detection System.

Oligonucleotide Modeling Program (OMP) Calculation (Figure 5.2a):

Sequence for Hairpin Architecture (Complementary Region in Bold)

---

116. Kunishima, M.; Kawachi, C.; Iwasaki, F.; Terao, K.; Tani, S. *Tetrahedron Lett.* **1999**, *40*, 5327.

5.1: GCA GTA CCA ACC CTG TAC ACC ATC TCA A**GT TCT ATG** TCT GAC TAC AGA GTG GGA TG**C ATA GAA C**

Sequences for Intermolecular Architecture

5.2: GCA GTA CCA ACC CTG TAC ACC ATC TCA A**GT TCT ATG**

5.3: TCT GAC TAC AGA GTG GGA TG**C ATA GAA C**

OMP calculation was performed using the following parameters: assay temperature: 37 °C. Mg^{2+}: 2 mM. Monovalent cations: 0.1 M. DNA concentration: 10 nM.

Hairpin vs. Intermolecular Architecture Comparison (Figure 5.3):

Primer Sequences

5.6: GCT GAC TAC AGA GTG GGA TG

5.7: GCA GTA CCA ACC CTG TAC AC

Sequences for Intermolecular Architecture

5.4a: GCA GTA CCA ACC CTG TAC ACC ATC TCA A**GT TCT ATG**

5.5a: GCT GAC TAC AGA GTG GGA TG**C ATA GAA CTT** (10 bp duplex)

5.5b: GCT GAC TAC AGA GTG GGA TG**C ATA GAA C** (8 bp duplex)

Sequences for Intramolecular Architecture

5.8a: GCA GTA CCA ACC CTG TAC ACC ATC TC**A AGT TCT ATG** GCT GAC TAC AGA GTG GGA TG**C ATA GAA CTT** (10 bp duplex)

5.8b: GCA GTA CCA ACC CTG TAC ACC ATC TCA A**GT TCT ATG** GCT GAC TAC AGA GTG GGA TG**C ATA GAA C** (8 bp duplex)

5.8c: GCA GTA CCA ACC CTG TAC ACC ATC TCA AGT **TCT ATG** GCT GAC TAC AGA GTG GGA TG**C ATA GA** (6 bp duplex)

qPCR: The appropriate hairpin **5.8** (625 pM) or a 1:1 mixture of **5.4a** and **5.5** for the intermolecular cases (625 pM each) were subjected to qPCR under the standard conditions.

PAGE: The appropriate hairpin **5.8** or a 1:1 mixture of **5.4a** and **5.5** for the intermolecular cases were subjected to 25 cycles of PCR under the standard conditions. The reactions were analyzed by PAGE (10% TBE gel, 200 V, 20 minutes).

Non-Natural Linker Experiments: Oligo-Ethylene Glycol (Figure 5.4)

Primer Sequences

6.1: GCA GTA CCA ACC CTG TAC AC

6.2: CCT GAC TAC AGA GTG GGA TG

Sequences for Intermolecular Architecture

5.4a: GCA GTA CCA ACC CTG TAC ACC ATC TCA A**GT TCT ATG**

5.10a: CCT GAC TAC AGA GTG GGA TG**C ATA GAA C** (8 bp duplex)

6.3: CCT GAC TAC AGA GTG GGA TG**C ATA GAA TT** (10 bp duplex)

Sequences for Hairpin Architecture (s9 = Spacer Phosphoramidite 9, Glen Research)

6.4: GCA GTA CCA ACC CTG TAC ACC ATC TC**A AGT TCT ATG** s9 CCT GAC TAC AGA GTG GGA TG**C ATA GAA CTT** (10 bp hairpin)

5.9a: GCA GTA CCA ACC CTG TAC ACC ATC TCA A**GT TCT ATG** s9 CCT GAC TAC AGA GTG GGA TG**C ATA GAA C** (8 bp hairpin)

6.5: GCA GTA CCA ACC CTG TAC ACC ATC TCA AGT **TCT ATG** s9 CCT GAC TAC AGA GTG GGA TG**C ATA GA (**6 bp hairpin)

Optimization of Stem Length

The appropriate hairpin was subjected to qPCR under the standard conditions. The substrates with 10- and 8-bp stems were amplified to threshold detection levels in 17-18 cycles, while the 6-bp stem was far less efficient in initiating PCR (Figure 6.1).

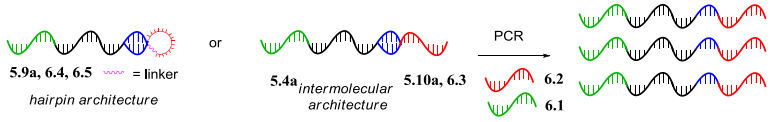

architecture	overlap (bp)	threshold cycle (C_T)
6.4	10	17
5.9a	8	18
6.5	6	28
5.4a	0	32
5.4a+6.3	10	26
5.a+6.10a	8	28

Figure 6.1. Optimization of stem length.

qPCR Standard Curve

To verify that the hairpin structures were well-behaved PCR templates over a range of concentrations, we generated a standard curve by qPCR. Five different concentrations of hairpin **5.9a** (625 pM, 31 pM, 1.6 pM, 80 aM, 4 aM) were subjected to qPCR under the standard conditions, except that a 64 °C annealing step was used instead of 58 °C. The log of starting copy number was plotted vs. threshold cycle, and a linear function was fit to the data (Figure 6.2).

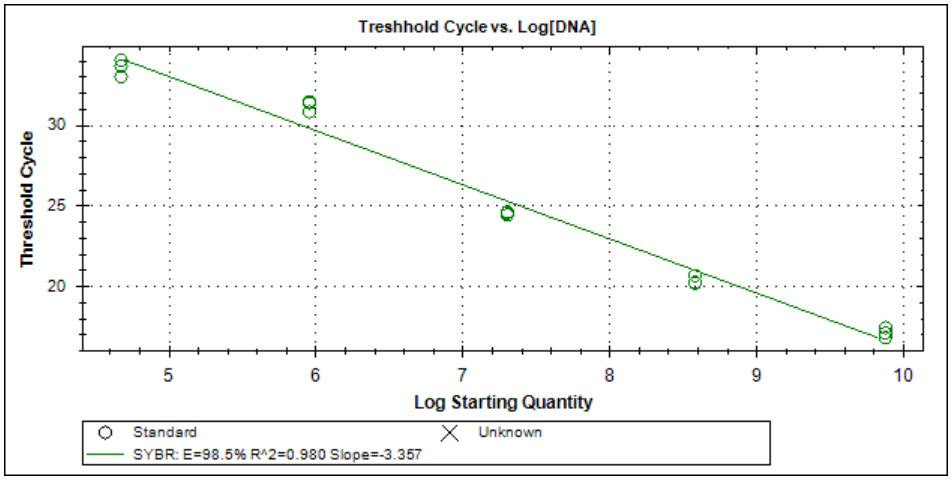

Figure 6.2. C_T is linearly correlated to initial log[**5.9a**].

Non-Natural Linker Experiments: Disulfide (Figure 5.4)

Sequences

amine = Amino-Modifier Serinol Phosphoramidite; 3'thiol = 3'-Thiol-Modifier C6 S-S CPG; 5'thiol = Thiol-Modifier C6 S-S

6.6: GAG CTC GTT GAT ATC CGC AGA CAT GAG CCC CAC TA**C ACA CAC C** (amine)(3' thiol)

6.7: (5'thiol)(amine)ACC TAA AGC TAG CAG CTG GCC GTG ATC AGC TT**G GTG TGT G**

*Synthesis of **5.9b***

The disulfide **5.9b** was synthesized using the route shown in Figure 6.3. **6.6** and **6.7** were first functionalized with small-molecule carboxylic acid derivatives, providing **5.4b** and **5.10b**. A mixed disulfide was then generated from **5.10b**, which was reacted with the free thiol analog of **5.4b** to yield **5.9b**.

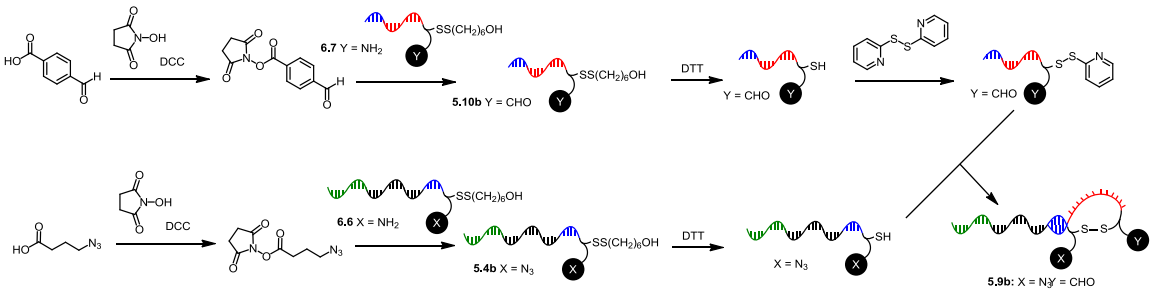

Figure 6.3. Synthesis of **5.9b**.

*Acylation of **6.6** and **6.7***

The appropriate carboxylic acid (0.1 mmol) and *N*-hydroxyl-succinimide (0.1 mmol) were dissolved in 0.1 mL DMF in a 1.5 mL eppendorf tube. *N*,*N*'-dicyclohexylcarbodiimide (DCC) (0.1 mmol) was added, and the resulting mixture was agitated at room temperature for 30 minutes. During this time, a white precipitate formed. The reaction was briefly centrifuged, and 0.05 mL of the supernatant was added to a solution of **6.6** or **6.7** (10 nmol) in 0.1 mL of 0.2 M phosphate buffer (pH 8) in a separate eppendorf tube. The resulting solution was vigorously agitated for 6 hours, and then diluted (0.5 mL total volume) prior to purification by Nap5 column. The recovered DNA was further purified by HPLC, typically yielding 1-2 nmol of the desired product (**5.10b** or **5.4b**).

4-azidobutyric acid[117] was coupled to **6.6** to give **5.4b**.

4-formylbenzoic acid was coupled to **6.7** to give **5.10b**.

*Ligation of **5.4b** and **5.10b***

A solution of **5.4b** (500 pmol) and DL-dithiothreitol (DTT, 0.3 M) in 0.1 mL of HEPES buffer (0.1 M, pH 8.5) was agitated for 30 minutes in a 1.5 mL eppendorf tube. A second solution with **5.10b** (instead of **5.4b**) was treated equivalently. The deprotected, thiol-containing DNA was precipitated with ethanol from each reaction. The residue containing **5.10b** was taken up in 0.1 mL of 9:1 50 mM TrisHCl (pH 7.5):ethanol containing 10 mM 2,2'-dipyridyl disulfide. The resulting suspension was agitated for 1 hour, and the DNA was then recovered by ethanol precipitation. The activated residue containing **5.10b** and the residue containing **5.4b** were separately dissolved in 10 μL of 50 mM TrisHCl (pH 7.5), and the concentration of DNA in each solution was determined. An equimolar quantity of the **5.4b** solution was added to the solution of **5.10b** (the total volume did not exceed 20 μL), and the resulting solution was agitated at 4 ºC for 12 hours. The DNA was precipitated with ethanol, and the desired product (**5.9b**) was isolated by gel purification (3% Ambion Agarose-HR gel). Typically, 100 pmol of disulfide **5.9b** was obtained.

qPCR Analysis

Primer Sequences

6.8: GAG CTC GTT GAT ATC CGC AG

---

117. Kanan, M. W.; Rozenman, M. M.; Sakurai, K.; Snyder, T. M.; Liu, D. R. *Nature* **2004**, *431*, 545.

6.9: ACC TAA AGC TAG CAG CTG GC

The hairpin **5.9b** (500 pM) or a 1:1 mixture of **5.4b** and **5.10b** (500 pM each) for the intermolecular case was subjected to qPCR under the standard conditions.

PAGE analysis: The appropriate hairpin **5.9b** (500 pM) or a 1:1 mixture of **5.4b** and **5.10b** for the intermolecular case was subjected to 20 cycles of PCR under the standard conditions. The reactions were analyzed by PAGE (10% TBE gel, 200 V, 20 minutes) (Figure 6.4).

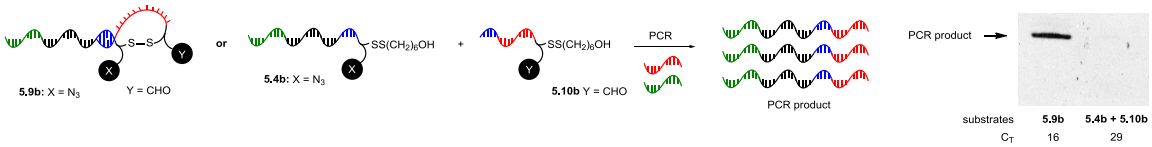

Figure 6.4. Disulfide-linked hairpin supports self-priming PCR. PCR conditions: 500 pM **5.9b** or 500 pM **5.4b** and 500 pM **5.10b**, 20 cycles.

Non-Natural Linker Experiments: Amide (Figure 5.4)

Sequences

NH_2 = 3'amino modifier C7 CPG, CO_2H = 5' carboxy modifier C10

5.4c. GCA GTA CCA ACC CTG TAC ACC ATC TCA A**GT TCT ATG-**NH_2

5.10c. CO_2H-CTG AGC TCG TTG ATA TCC GCA G**CA TAG AAC**

*Formation of **5.9c** from **5.4c** and **5.10c***

To a 45 µL solution of **5.4c** (2.5 pmol) and **5.10c** (3.75 pmol) in 8:1 MOPS buffer (100 mM MOPS, 1 M NaCl, pH 7.5):CH_3CN was added 5 µL of a 0.14 mg/µL solution of DMT-MM in MOPS buffer. The resulting solution (50 µL total volume, 9:1 MOPS:CH_3CN) was briefly vortexed and then left at 4 °C for 14 hours. The reaction was allowed to warm to room temperature and diluted with 50 µL of 0.1M aqueous NaCl. The DNA was precipitated with ethanol prior to subsequent analysis. Control experiments were performed analogously, but with omission of DMT-MM or with substitution of the amine-terminated DNA (**5.4c**) for hydroxyl-terminated DNA (**5.4a**).

qPCR Analysis

Primer sequences

6.1: GCA GTA CCA ACC CTG TAC AC

6.10: CTG AGC TCG TTG ATA TCC GCA G

DNA from the acylation reaction (**5.9c**) was subjected to qPCR under the standard conditions. DNA from

control reactions was identically treated. A dramatic dependence of C_T upon addition of DMT-MM was observed, consistent with acylation and subsequent intramolecular priming through the amide linker (Figure 6.5). Upon replacement of amine-modified DNA **4c** with unmodified, 3'-OH **4a**, DMT-MM did not influence PCR efficiency (Figure 6.5).

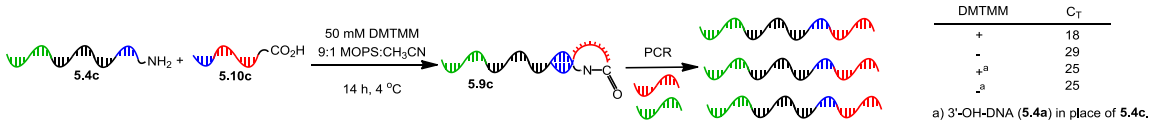

DMTMM	C_T
+	18
-	29
+[a]	25
-[a]	25

a) 3'-OH-DNA (**5.4a**) in place of **5.4c**.

Figure 6.5. Amide formation-dependent PCR.

Optimization of DNA-Templated Amide Bond Formation.

Experiments with fluorescently-tagged, amine-modified DNA enabled direct determination of conversion from amine-DNA to carboxylate-ligated DNA.

Sequences

Cy3 = Cy3 Phosphoramidite (Glen Research)

6.11: Cy3-GCA GTA CCA ACC CTG TAC ACC ATC TCA A**GT TCT ATC**-NH_2

6.12: CO_2H-CCT GAC TAC AGA GTG GGA TG**C ATA GAA C**

6.13: CO_2H- CCT GAC TAC AGA GTG GGA TG**T TGA CCG T**

*DMT-MM-Mediated Coupling of **6.11** and **6.12***

To a 90 µL solution of **6.11** (5.0 pmol) and **6.12** (7.5 pmol) in 8:1 MOPS buffer (100 mM MOPS, 1 M NaCl, pH 7.5):CH_3CN was added 10 µL of a 0.14 mg/µL solution of DMT-MM in MOPS buffer. The resulting solution (100 µL total volume, 9:1 MOPS:CH_3CN) was briefly vortexed and then left at the appropriate temperature (see conditions, Figure 6.6) for 14 hours. The DNA was precipitated with ethanol prior to subsequent analysis.

*sNHS/EDC-Mediated Coupling of **6.11** and **6.12***

A 90 µL solution of **6.11** (5.0 pmol) and **6.12** (7.5 pmol) in 8:1 MES buffer (100 mM MES, 1 M NaCl, pH 6.0):CH_3CN was added to 0.3 mg of sNHS in a 1.5 mL eppendorf tube. 10 µL of a 0.04 mg/µL solution of EDC in MES buffer was then added. The resulting solution (100 µL total volume, 9:1 MES:CH_3CN) was briefly vortexed and then left at the appropriate temperature for 14 hours. The DNA was precipitated with ethanol prior to subsequent analysis.

PAGE Analysis of Acylation Reactions

Denaturing PAGE (15% TBE-urea gel, 300 V, 25 minutes) and subsequent fluorescence quantitation was used to monitor the acylation reactions. Regardless of the acylation reagent employed, amide-bond formation was markedly more efficient at 4 °C compared with the room temperature reactions (Figure S6, lanes 1 vs. 2, 5 vs. 6). This result was consistent with our expectation that the melting temperature of the 8 bp intermolecular duplex is ~10 °C, and therefore lower temperature provides higher reactivity by stabilizing the duplex intermediate. Furthermore, an experiment with a mismatched stem sequence (**6.11**+**6.13**), such that no intermolecular hybridization is possible, resulted in no amide product, demonstrating that DNA hybridization is essential to the reaction under our experimental conditions (Figure S6, lane 4).

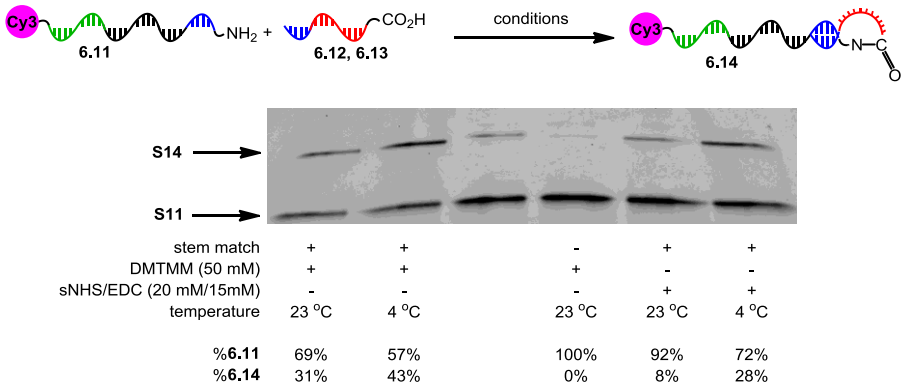

Figure 6.6. Fluorescence quantitation of the DNA-templated acylation reaction.

Library-Format Experiments (Figure 5.5)

Sequences:

Stem-forming nucleotides are in bold, point mutations are italicized, and the *Hin*dIII recognition site is underlined.

5.6: GCT GAC TAC AGA GTG GGA TG

6.10: CTG AGC TCG TTG ATA TCC GCA G

Sequences for Intermolecular Architecture

5.12: GCT GAC TAC AGA GTG GGA TGA A*T*C TTC ATC TCA A**GT TCT ATG**

5.13: CTG AGC TCG TTG ATA TCC GCA G**CA TAG AAC**

Sequences for Intramolecular Architecture

5.11: GCT GAC TAC AGA GTG GGA TGA A*G*C TTC ATC TCA A**GT TCT ATG**-spacer9-CTG AGC

TCG TTG ATA TCC GCA G**CA TAG AAC**

Restriction Digestion Experiments

PCR reactions (60 μL total volume) were performed with constant concentrations of **5.12** and **5.13** (625 pM) but varying concentrations of **5.11** (62.5 pM, 6.25 pM, 0.625 pM, 0.0625 pM). The appropriate cycle number for each reaction was determined by prior qPCR evaluation, such that each reaction proceeded while exponential amplification was occurring, but not beyond, in order to minimize dynamic compression. Following PCR, each reaction was split into two aliquots (40 and 20 μL, respectively). To the larger aliquot was added 1 μL of *Hin*dIII in glycerol (10,000 units/mL). The resulting solution was incubated at 37 °C for 1 h, and then heated to 65 °C for 20 minutes to deactivate the enzyme. The other aliquot was treated equivalently, but with omission of *Hin*dIII. The resulting samples were analyzed by PAGE (10% TBE, 175 V, 25 minutes).

Library-Format *Pvu*II Experiments

A parallel set of experiments were carried out to corroborate the *Hin*dIII digestion results. All sequences and procedures were identical to the *Hin*dIII experiments, except for those noted below. A double point mutation was used to distinguish the intermolecular and intramolecular substrates to take into account the lower sequence fidelity of *Pvu*II.

Sequences

Sequences for Intermolecular Architecture

6.15: GCT GAC TAC AGA GTG GGA TGC A*AG* TGC ATC TCA A**GT TCT ATG**

Sequences for Intramolecular Architecture

6.16: GCT GAC TAC AGA GTG GGA TGC A*GC* TGC ATC TCA A**GT TCT ATG**-spacer9-CTG AGC TCG TTG ATA TCC GCA G**CA TAG AAC**

Restriction digestion of the PCR reactions was carried out with 1 μL of *Pvu*II-HF (10,000 units/mL stock in glycerol). Heat inactivation was achieved by incubation at 80 °C for 20 minutes following the 1 h incubation at 37 °C. Reactions were analyzed as described above (Figure 6.7).

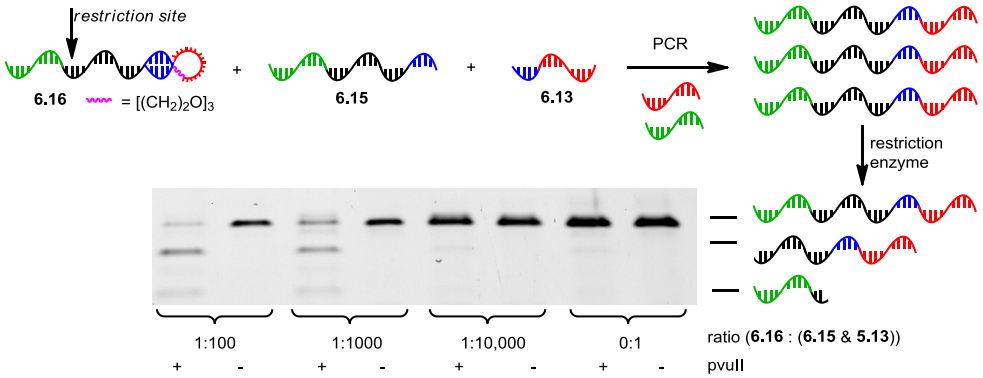

Figure 6.7. Library-format experiment with *Pvu*II.

Reaction Discovery Model System (Figure 5.6)

Sequences

Amine = Amino-Modifier Serinol Phosphoramidite; 3'thiol = 3'-Thiol-Modifier C6 S-S CPG; 5'thiol = Thiol-Modifier C6 S-S

6.17: GAG CTC GTT GAT ATC CGC AGA GCG TTA TGG TCC GA**C ACA CAC C** (amine)(3'thiol)

6.18: (5'thiol)(amine)ACC TAA AGC TAG CAG CTG GCG AGG TTC CAG AT**G GTG TGT G**

6.19: (5'thiol)(amine)ACC TAA AGC TAG CAG CTG GCC GCA CAC TTT CT**G GTG TGT G**

The free amine of each substrate above was coupled to a small-molecule carboxylic acid derivative as described earlier. For the reactions with 6-heptenoic acid and 10-undecynoic acid, the active ester was formed in 0.15 mL DMF, and 0.1 mL of the resulting soluble fraction was added to the DNA-NH_2, giving a total volume of 0.2 mL. This modification led to increased yields, presumably due to greater solubility of the hydrophobic carboxylic acids in DMF.

6-heptenoic acid was coupled to **6.17** to give **6.20**.

4-iodophenylacetic acid was coupled to **6.18** to give **6.21**.

10-undecynoic acid was coupled to **S19** to give **S22**.

Three substrates were made by formation of a disulfide bond:

5.4b was coupled to **5.10b** to give **5.9b**.

6.20 was coupled to **6.21** to give **5.9d**.

5.4b was coupled to **6.22** to give **6.23**.

Reaction of Disulfide-Linked DNA with Pd

5 pmol of the substrate oligo (**5.9b** or **5.9d**) was added to 0.1 mL of a 1 mM disodium tetrachloropalladate solution in MOPS buffer (50 mM MOPS, 0.5 M NaCl, pH 7.5). The resulting solution was heated at 65 ºC for 30 minutes. The DNA was recovered by ethanol precipitation, and then taken up in 0.1 mL of a 0.3 M DTT solution in HEPES buffer (0.1 M HEPES, pH 8.5). The reaction was left for 1 hour at 65 ºC to ensure full cleavage of the disulfide bond, and the DNA was then recovered by ethanol precipitation.

qPCR of Pd-treated DNA

Primer Sequences

6.8: GAG CTC GTT GAT ATC CGC AG

6.9: ACC TAA AGC TAG CAG CTG GC

DNA recovered from the Pd reactions and various controls was subjected to qPCR under slightly modified conditions. The starting concentration of DNA was 50 pM.

PAGE Analysis

DNA recovered from the Pd reactions and various controls was subjected to 23 cycles of PCR under slightly modified conditions. The starting concentration of DNA was 50 pM. The reactions were analyzed by PAGE (10% TBE gel, 200 V, 20 minutes).

Detection of Cu(I)-Catalyzed Huisgen Cycloaddition.[118]

1 pmol of the substrate oligo (**5.9b** or **6.23)** was added to 0.1 mL of a 9:1 H_2O:CH_3CN solution containing 2 mM Cu(I)Cl. After 30 minutes at room temperature, the reactions were subjected to ethanol precipitation. The DNA pellet was taken up in 0.1 mL of 0.3 M DTT in HEPES buffer (0.1 M HEPES, pH 8.5) and heated for 1 hour at 65 ºC to ensure full cleavage of the disulfide bond. The DNA was then recovered by ethanol precipitation.

qPCR of Cu-Treated DNA

Primer Sequences

---

118. Himo, F.; Loveli, T.; Hilgraf, R.; Rostovtsev, V. V.; Noodleman, L.; Sharpless, K. B.; Fokin, V. V. *J. Am. Chem. Soc.* **2005**, *127*, 210.

6.8: GAG CTC GTT GAT ATC CGC AG

6.9: ACC TAA AGC TAG CAG CTG GC

DNA recovered from the Cu reactions and various controls was subjected to qPCR under slightly modified conditions. The starting concentration of DNA was 5 pM.

PAGE Analysis

DNA recovered from the Cu reactions and various controls was subjected to 24 cycles of PCR under slightly modified conditions. The starting concentration of DNA was 5 pM. The reactions were analyzed by PAGE (10% TBE gel, 200 V, 20 minutes).

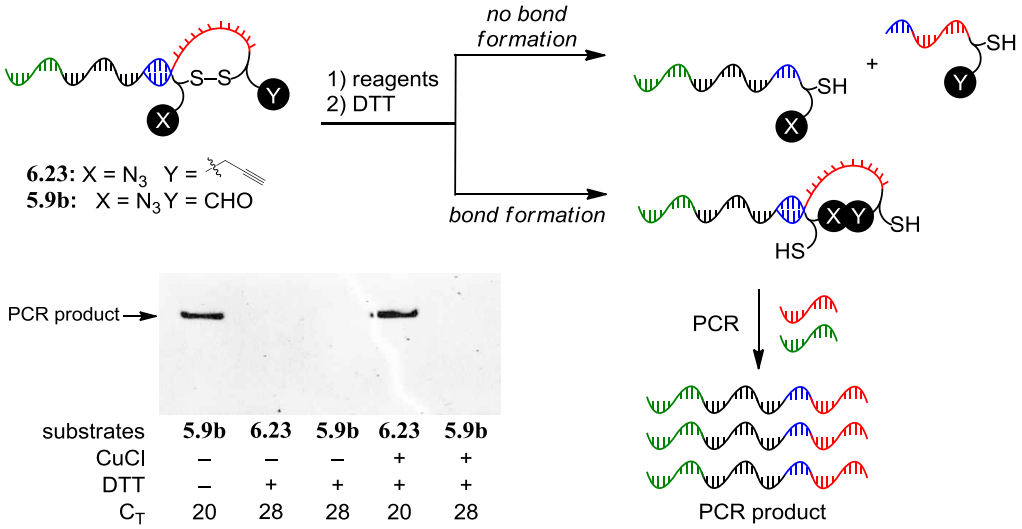

Figure 6.8. RDPCR-based DNA-encoded reaction discovery selection validation using Cu-catalyzed Huisgen cycloaddition. PCR conditions: 5 pM template, 24 cycles.

Protease Activity Detection Model System (Figure 5.7)

Primers

6.1: GCA GTA CCA ACC CTG TAC AC

6.10: CTG AGC TCG TTG ATA TCC GCA G

Sequences

3a = 3'amino modifer C7 CPG

DNA-peptide **5.17**. GCA GTA CCA ACC CTG TAC ACC ATC TCA A**GT TCT ATG**-3a-Ala-Pro-Gly-Phe-Ala-NHAc

Carboxylate **5.10c**: CO_2H- CTG AGC TCG TTG ATA TCC GCA G**CA TAG AAC**

*Synthesis of DNA-Peptide Conjugate **5.17***

Compound **5.17** was synthesized by solid-phase co-synthesis. 0.2 μmol of 3' amino modifier C7 CPG was subjected to solid-phase peptide synthesis to install the pentapeptide on the Fmoc-amine group. The peptide synthesis comprised iterated rounds of Fmoc deprotection (20% pipiridine/NMP), coupling (Fmoc-amino acid/HATU/DIPEA/NMP), and capping (5% acetic anhydride and 6% 2,6-lutidine in NMP).

The CPG was then subjected to standard solid-phase DNA synthesis to install the oligonucleotide at the site of the DMT-protected hydroxyl group. The substrate was cleaved from the resin by standard methods (NH_4OH/methylamine). The 5'-DMT-protected DNA was then purified by HPLC. Following lyophilization and deprotection of the DMT group by standard methods (3% TFA), the DNA was repurified by HPLC to yield **5.17** (26.6 nmols).

Detection of Bond Cleavage by Subtilisin A

DNA-peptide **5.17** (2.6 pmol/uL) was treated with subtilisin A (65 ng/uL) in PBS buffer.[119] After incubation at 37 °C for 90 minutes, the DNA and enzyme were separated by phenol/chloroform extraction. The DNA was recovered by ethanol precipitation, and taken up in the appropriate buffer (MOPS or MES) for acylation with **5.10c** under the conditions described earlier. Quantitative PCR and PCR/PAGE analysis were performed as described earlier.

Table 6.1. LCMS characterization of functionalized oligonucleotides.

Compound	**observed ion's charge**	**Expected m/z**	**Observed m/z**
5.9c (3'-NH2)	–6	1854.504	1854.484
5.10c (5'-CO2H)	–5	1899.930	1899.963
5.17 (DNA-peptide)	–7	1658.732	1658.683
5.4b (3'SSR)	–6	2290.563	2290.628
5.10b (5'SSR)	–6	2174.367	2174.353
6.20	–6	2307.401	2307.337
6.21	–5	2641.629	2641.669
6.22	–6	2166.382	2166.339

119. Subsequent experiments demonstrated that lower concentrations (to 650 pg/uL) of subtilisin A were sufficient to affect bond cleavage under otherwise identical conditions.